Phenotypic evolution of the marine gastropod *Littorina obtusata* across an environmental gradient at high latitudes

André Carvalho Pires
Mestrado em Bioinformática e Biologia Computacional
Departamento de Biologia
2022

Supervisor
Rui Miguel Macieira de Faria, Investigador Associado, Centro de Investigação em Biodiversidade e Recursos Genéticos (CIBIO)

Co-supervisor
Ana Rita Pires Gaio, Professora Auxiliar, Faculdade de Ciências da Universidade do Porto (FCUP)

Co-supervisor
Miguel Jorge Pinto Carneiro, Investigador Principal, Centro de Investigação em Biodiversidade e Recursos Genéticos (CIBIO)


U.PORTO
FACULDADE DE CIÊNCIAS
UNIVERSIDADE DO PORTO

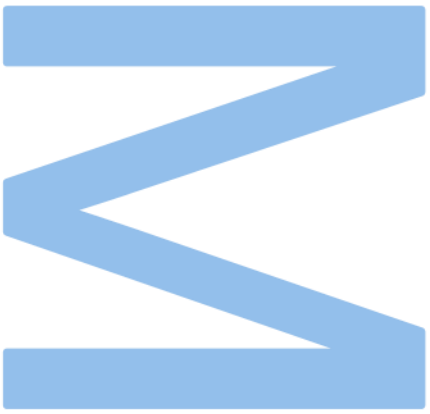

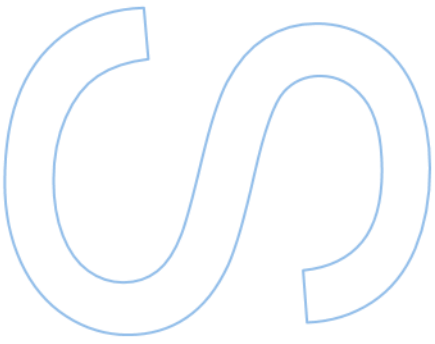

Declaração de Honra

Eu, André Carvalho Pires, inscrito no Mestrado em Bioinformática e Biologia Computacional da Faculdade de Ciências da Universidade do Porto declaro, nos termos do disposto na alínea a) do artigo 14.º do Código Ético de Conduta Académica da U.Porto, que o conteúdo da presente dissertação de projeto reflete as perspetivas, o trabalho de investigação e as minhas interpretações no momento da sua entrega.

Ao entregar esta dissertação de projeto, declaro, ainda, que a mesma é resultado do meu próprio trabalho de investigação e contém contributos que não foram utilizados previamente noutros trabalhos apresentados a esta ou outra instituição.

Mais declaro que todas as referências a outros autores respeitam escrupulosamente as regras da atribuição, encontrando-se devidamente citadas no corpo do texto e identificadas na secção de referências bibliográficas. Não são divulgados na presente dissertação de projeto quaisquer conteúdos cuja reprodução esteja vedada por direitos de autor.

Tenho consciência de que a prática de plágio e auto-plágio constitui um ilícito académico.

André Carvalho Pires

Porto, 14/12/2022

Agradecimentos

O meu primeiro agradecimento não poderia deixar de ser dirigido ao Professor Doutor Rui Faria, por todo o conhecimento e orientação ao longo desta jornada, pela forma como me expôs e incluiu no desenvolvimento da investigação científica da área, pela dedicação e rigor e por todas as oportunidades que me proporcionou. Sobretudo pela forma como conseguiu disputar em mim interesse, dedicação, persistência e resiliência, que foram fundamentais no desenvolvimento desta dissertação.

À Professora Doutora Rita Gaio, agradeço toda a compreensão, empatia, prontidão, energia positiva e a paixão que demonstra pela estatística e matemática. Com a Professora ficou mais fácil aprender e implementar novas estratégias.

Ao Professor Doutor Miguel Carneiro por todos os ensinamentos, sugestões e indicações que me proporcionaram uma visão mais clara e objetiva de certas etapas.

Um enorme obrigado também a todo o grupo de investigação EVOLGEN do CIBIO, aprendi muito com todo o grupo e foi um prazer estar sempre ocorrente de novos projetos e inovações científicas ao nível da evolução genética. Um agradecimento especial à Cristiana Marques e ao Pedro Andrade, por toda a paciência, ajuda diária e pelos conhecimentos que me transmitiram. Ultrapassei muitos obstáculos com a vossa ajuda! Agradeço também a todos os elementos do CIBIO que de uma forma ou de outra me orientaram na direção certa, em particular à Maria João e Sofia Mourão.

Queria agradecer também o apoio do Fundo de Relações Bilaterais do Mecanismo Financeiro do Espaço Económico Europeu através de uma EEA Grant (FBR_OC1_68 Adaptchange) que financiou a amostragem e a minha participação num curso em genómica populacional organizado na Nord University, Noruega.

Aos meus amigos de sempre, obrigado por todas as vezes que fizeram um esforço por me "tirar de casa" e ajudaram-me a alivar da ansiedade e da pressão com gargalhadas e bons momentos! Por todos os desabafos, todos os incentivos, e sobretudo pela forma como confiaram em mim. Fico mesmo muito feliz por saber que posso contar com vocês todos! Assim como aos meus companheiros de estudo.

O meu maior e final agradecimento é dirigido à minha família por tudo o que me proporcionaram ao longo destes cinco anos de percurso académico. Eternamente agradecido, Mãe, Pai e Mana por toda a compreensão, suporte, confiança, incentivo e por nunca me deixarem duvidar das minhas capacidades. São um exemplo diário de força e coragem. Sem vocês não era quem sou hoje, esta dissertação também é vossa!

Resumo

O meio intertidal, onde os organismos enfrentam fortes pressões seletivas divergentes associadas à variação das marés, é um laboratório natural para estudar adaptação e especiação. Várias espécies apresentam uma elevada diversidade fenotípica associada às fortes pressões seletivas nesses habitats, entre as quais se encontra o gastrópode marinho *Littorina obtusata*, a espécie-alvo deste estudo.

Duas variedades foram descritas para esta espécie, *retusa* e *palliata* (com espiral reduzida e elevada, respetivamente). Enquanto a segunda se encontra distribuída pelas costas europeias a Norte das Ilhas Lofoten (Noruega) e no Norte da Islândia, a primeira variedade ocorre a Sul dessas ilhas e na costa Sul da Islândia. Estudos anteriores nas populações Atlânticas ocidentais de *L. obtusata* mostraram que o caranguejo verde Europeu (*Carcinus maenas*), juntamente com a temperatura, impõem importantes pressões seletivas sobre várias características das conchas, resultando em indivíduos com conchas mais espessas e com uma espiral mais baixa. Embora os mesmos fatores pudessem explicar a variação fenotípica latitudinal entre as duas variedades nas costas europeias, uma caracterização detalhada destes fenótipos, assim como dos fatores que podem influenciar a sua distribuição, a sua base genética e os mecanismos evolutivos envolvidos (seleção natural e/ou plasticidade), não foram ainda estudados em detalhe.

A fim de preencher esta lacuna, neste estudo efetuaram-se análises fenotípicas, genéticas e de parâmetros ambientais das populações de *L. obtusata* distribuídas ao longo gradiente latitudinal que abrange a zona de transição geográfica entre as duas variedades (norte da Noruega) com os objetivos de: I) quantificar as principais diferenças fenotípicas entre os gradientes ambientais em altas latitudes, II) identificar regiões genómicas envolvidas em diferenças fenotípicas, e III) contribuir para a nossa compreensão das principais forças e fatores ambientais que impulsionam a evolução destas variedades.

A caracterização fenotípica (peso, espessura da concha, altura, altura da espiral, razão altura da espiral/altura total, ângulo da espiral, força e forma) dos indivíduos de *L. obtusata,* de cinco populações distribuídas ao longo de um gradiente ambiental que varia com a latitude, revelou um aumento das médias dos valores para todas estas características, exceto para a razão altura da espiral/altura total e forma, do Norte para o Sul. Este padrão é concordante com as diferenças na espessura da concha e da altura da espiral anteriormente reportadas para as variedades *retusa* e *palliata*,

respetivamente. Uma tendência semelhante foi observada em termos da temperatura do ar e da água do mar, da salinidade e da ocorrência de caranguejos, revelando uma associação entre estes fatores abióticos e bióticos e os fenótipos estudados. Embora os diferentes fatores variem de forma semelhante com a latitude e a sua contribuição individual, bem como o principal fator causal (caso exista) para a variação dos fenótipos através da latitude seja difícil de determinar, a influência da temperatura da água e da salinidade para esta variação é notável.

As populações de Breivika e Tromsø, localizadas a latitudes intermédias na nossa região de estudo, mostram valores intermédios ou assemelham-se com as populações do Norte versus Sul, dependendo da característica. Estes padrões sugerem que a região de transição entre os dois principais fenótipos associados às duas variedades, pode localizar-se mais a Norte do que anteriormente descrito (Ilhas Lofoten, Noruega). Estes resultados sugerem que este sistema tem um elevado potencial para compreender como as alterações climáticas afetam as dinâmicas eco-evolutivas da biodiversidade nas zonas costeiras marinhas.

A implementação de uma abordagem de *pool-seq* para caracterizar os dois extremos fenotípicos em termos de resistência da concha dentro da mesma população (Breivika) revelou a existência de várias regiões genómicas candidatas que podem estar envolvidas na variação desta característica. No entanto, são necessários estudos adicionais para validar estas regiões candidatas e avaliar o seu papel funcional, a fim de compreender os processos que governam a evolução da concha neste sistema.

Palavras-chave: Adaptação; *Carcinus maenas*; Fenótipo; Genómica populacional; *Littorina obtusata*

Abstract

The marine rocky intertidal, where organisms experience strong selective pressures associated with the tidal range, is a natural laboratory to study local adaptation and speciation. Various species present high phenotypic diversity associated with divergent selective pressures in this ecosystem, including the marine gastropod *Littorina obtusata*, the focal taxon of this study.

Two varieties were described for *L. obtusata*, *retusa* and *palliata* (with lower and higher spire, respectively), the latter being distributed across the European shores northern of the Lofoten Islands (Norway) and in the north of Iceland, while the former variety occurs southwards. Previous studies in the western Atlantic populations of *L. obtusata* showed that the European green crab (*Carcinus maenas*), together with temperature, imposed important selective pressures on various shell traits, resulting in individuals with thicker and low-spired shells. Although the same factors could explain the phenotypic variation in latitude between the two varieties in the European shores, a detailed characterization of the phenotypes and their genetic basis, the factors that could influence their distribution and the evolutionary mechanisms involved (natural selection and/or plasticity) remains to be done.

In order to fill this gap, here we combined phenotypic, genetic and environmental analyses of *L. obtusata* populations across a latitudinal gradient encompassing the geographic transition between the two varieties (northern Norway) with the goals of: I) quantifying the main phenotypic differences across the environmental gradients at high latitudes, II) characterising the genomic regions involved in phenotypic differences, and III) gain insights about the main forces and environmental factors driving the evolution of these different varieties.

The phenotypic characterization (weight, shell thickness, height, spire height, spire height/height ratio, spire angle, shell strength and shape) of *L. obtusata* individuals from five different populations across an environmental gradient across latitude revealed an increase in the mean value of all these traits from northern to southern populations except for spire height/height ratio and shell shape. This pattern agrees with the differences in shell thickness and spire height previously reported for the *retusa* and *palliata* varieties, respectively. A similar trend was observed in terms of air and sea water temperature, salinity, and the occurrence of crabs, revealing an association between these abiotic and biotic factors and the studied phenotypes. Although the different factors vary similarly with latitude, making it difficult to evaluate their individual contribution for

the variation in phenotypes across latitude, the contribution of sea surface temperature and sea salinity with this variation was notable.

The populations Breivika and Tromsø, located in intermediate latitudes of our study transect, show intermediate values or cluster with the northern vs southern populations, depending on the trait. These patterns suggest that the transition between the two main different phenotypes associated with the two varieties is currently northern than previously described (Lofoten Islands, Norway). This offers this region-system a strong potential to study how climate change affects the eco-evolutionary dynamics of biodiversity in marine coastal areas.

The implementation of a pool-seq approach to characterize the two phenotypic extremes in terms of shell strength within a population (Breivika) revealed several candidate regions influencing variation in this trait. However, future studies are needed to validate these candidates, as well as to understand their functional role in order to understand the processes governing shell evolution in this system.

Keywords: Adaptation; *Carcinus maenas*; *Littorina obtusata*; Phenotype; Population genomics.

Table of Contents

List of Tables

List of Figures

1. Introduction

1.1. Marine rocky intertidal

The marine rocky intertidal is at the interface between marine and terrestrial environments. Given the dynamic nature of these marine ecosystems, organisms inhabiting the intertidal have to withstand extreme environmental fluctuations (Benson, 2002).

The Intertidal realm can be divided into high, mid, and low intertidal zones, which are inhabited by different communities (Figure 1). Organisms that can be found in the high intertidal must withstand long periods of extreme temperatures and have physiological mechanisms to resist desiccation, since these regions are only immersed in sea water during high tides. The opposite applies to the organisms living in the low intertidal zone, which spend most of their time immersed and do not have to deal with water loss caused by evaporation but are usually rather more exposed to the physical action of waves. Middle tidal zones are often immersed in two occasions every 24 hours (h), facing the widest range of environmental conditions (Knox, 2001).

The main selective pressures in these habitats are thus related to abiotic factors such as temperature, dehydration, sunlight variation, salinity stress and wave force, but also to biotic factors such as predators and competitors, whose distribution are also influenced by the abiotic factors (Dayton, 1971). Because abiotic factors often vary clinally across the intertidal gradient, organisms living in the different parts of the intertidal must cope with local selective pressures, which change periodically with the tidal cycles. For example, aerobic animals that obtain oxygen from sea water slow down their metabolism to reduce oxygen consumption in low tide situations (Hand, 2007). Ectothermic animals increase the production of heat shock or antifreeze proteins in response to high or low temperatures, respectively (Feder, 1999). Photosynthetic organisms, when exposed to large amounts of sun radiation dissipate the excess absorbed through thermal energy (Erickson *et al*., 2015). Osmoconformers produce organic osmolytes when in salinity stress situations to maintain the intracellular volume (Yancey, 2005).

Thus, organisms living in the lower and upper part of the intertidal face divergent selective pressures that can contribute to divergence evolution at a local scale. Nonetheless, some of the abiotic (e.g., temperature) and biotic factors (e.g., presence or abundance of predators) also vary with latitude at a macrogeographic scale (e.g., across European shores), making the marine rocky intertidal a natural laboratory for the study of adaptation and ecological speciation at different scales.

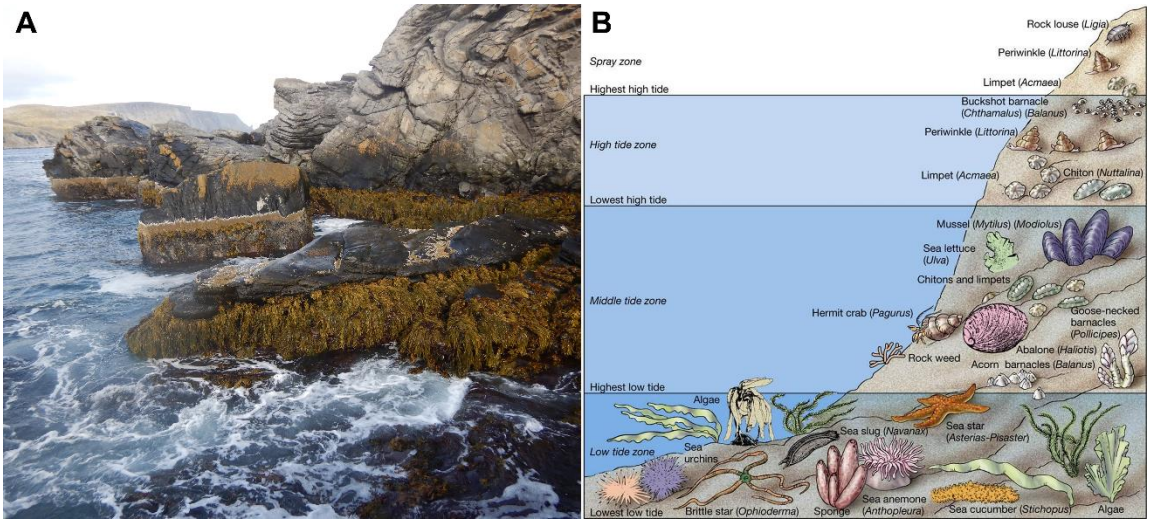

Figure 1. Marine rocky intertidal. (A) Example of a sampled marine rocky seashore (Norway). (B) Drawing scheme of the marine intertidal zones (Source: Copyright © 2005 Pearson Prentice Hall, Inc).

1.2. Species of the genus *Littorina* as evolutionary models to study the marine intertidal

Marine gastropods species of the *Littorina* genus (periwinkles) comprise 18 dioecious species that usually occupy a broad range of the shore habitats, representing a vast portion of all the species in these habitats, distributed across both horizontal and vertical gradients in the intertidal realm. Some of these species present frequent phenotypic polymorphisms (e.g. shell shape and size) associated different habitats in the intertidal (often referred as ecotypes), which make them particularly informative to study the evolution of traits as a response to divergent environmental conditions (Rolán-Alvarez *et al*., 2015). The poor dispersal capacity of some *Littorina* species (subgenus Neritrema, Figure 2), which do not have larval phase (i.e., have direct development) and present internal fertilization have often been suggested to be a key factor explaining their capacity to adapt to different habitats across environmental gradients in the intertidal (Johannesson, 2003). Thus, these species (mainly *L. saxatilis*) have been increasingly recognized as a model system for evolutionary studies in the marine rocky intertidal, namely to understand the mechanisms of adaptation and ecological speciation.

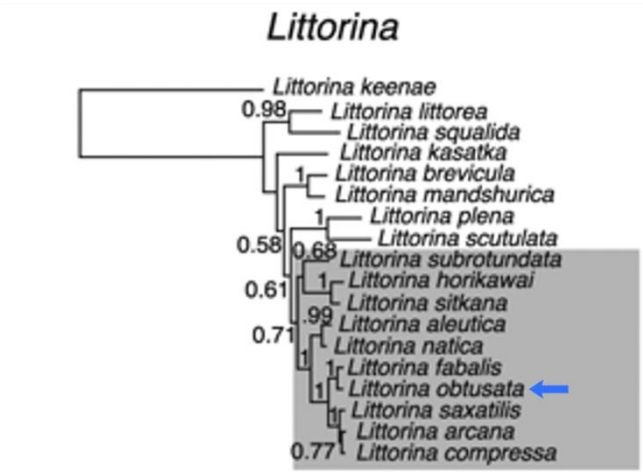

Figure 2. Phylogeny of 17 *Littorina species,* including the subgenus Neritrema (grey box), based on sequences of the 28S rRNA, 12S rRNA, COI, 16S rRNA and Cytb genes using *L. keenae* as outgroup from Reid *et al.* (2012).. Only posterior probabilities > 0.5 of support are shown. The target species (*L. obtusata*) of this work is indicated by the blue arrow.

Species of the genus *Littorina* have been the target of numerous research projects, making this genus the most studied among all marine gastropods (Reid, 1996). The initial focus of these studies was mainly on morphological descriptions of the shells, conchology and the geographical distribution of species (Reid 1996, and references therein). With the developments in evolutionary biology, a focus in intraspecific variation observed in certain *Littorina* species started to emerge at the end of the 19th century (Reid 1996, and references therein). More recently, ecology-based studies became more frequent, increasing the potential of this genus for understanding eco-evolutionary processes in marine rocky intertidal shores, which last until present day (Rolán-Alvarez *et al.,* 2015).

During this last period, phenotypic studies in *L. saxatilis* revealed variation between populations inhabiting different habitats, which was shown to be at least partially heritable (Johannesson *et al.,* 2008). Namely, individuals with smaller shell thicknesses and wider aperture in wave-exposed (named ‘wave’ ecotype) when compared with sheltered habitats, where individuals demonstrate the opposite trend (named ‘crab’ ecotype) (Johannesson *et al.,* 2010). Although plasticity was shown to significantly impact fitness, this was shown to be relatively small when compared to the adaptive component of the differences between ecotypes (Hollander & Butlin, 2010).

More recent studies using genetic data revealed that the crab and wave *L. saxatilis* ecotypes found in multiple European shores across the species distribution range (in United Kingdom, Spain and Sweden) evolved in parallel as a response to similar selective pressures (Figure 3) (Butlin et al. 2014). Benefiting from the assembly of the

first genome reference in the genus (for *L. saxatilis*) a study of hybrid zones in Sweden allowed to characterize for the first time how loci involved in ecotype divergence are distributed across the genome (Westram *et al.,* 2018; Westram *et al.,* 2021). The use of a capture-sequencing approach showed that many of these loci are clustered in specific regions, possibly consisting of chromosomal inversion (Faria *et al.,* 2019), which were further suggested to play a crucial role in rapid parallel ecotype divergence *L. saxatilis* across the species distribution (Morales *et al.,* 2019).

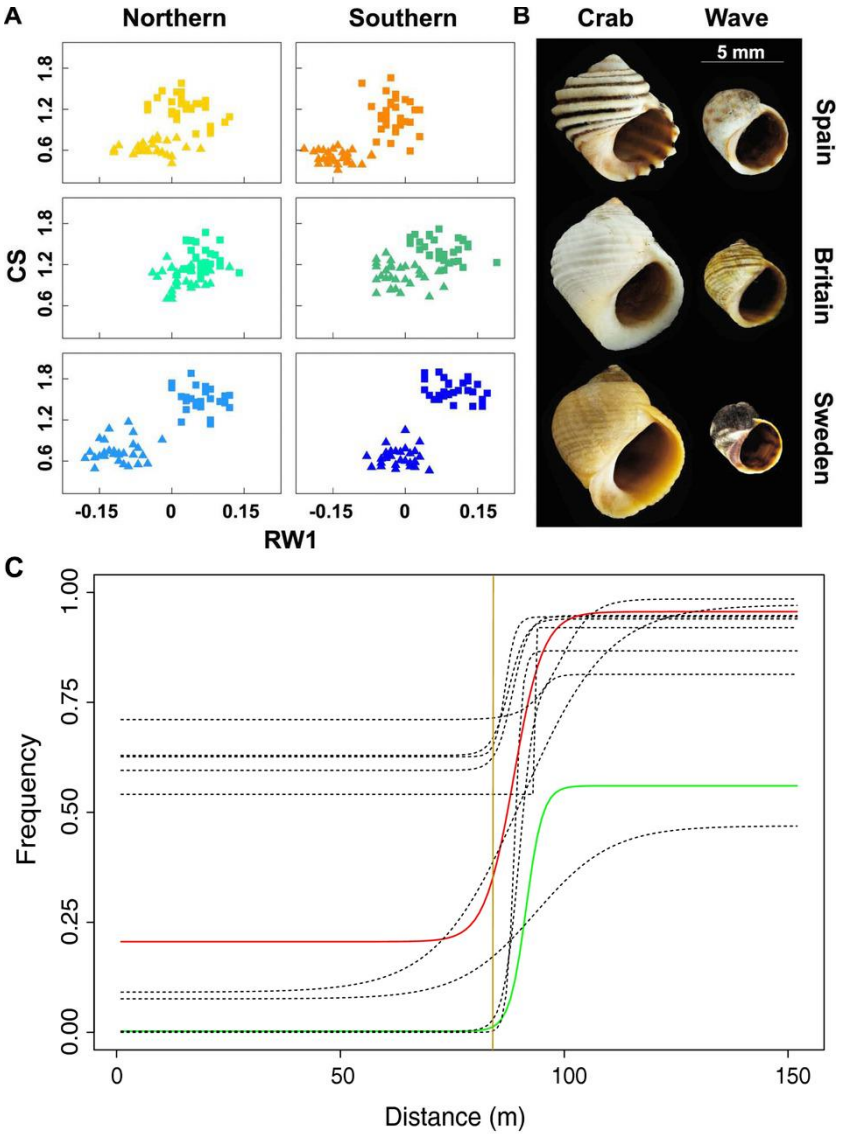

Figure 3. *Littorina saxatilis* phenotypic variation in three different countries and clinal changes in frequency of the genetic variation involved in ecotype divergence in Sweden. (A) Plot of individuals according to centroid size (CS) and the main axis of shape variation (RW1) values for 'wave' (triangles) and 'crab' (squares) individuals. (B) Typical shells of the ecotypes found in Spain, United Kingdom, and Sweden. (C) Inversion frequencies (lines) across an environmental transect in Sweden (yellow vertical line indicating the habitat transition), with the clines for two inversions that contain more outliers highlighted in red and green (Source: Butlin *et al.*, 2014; Faria *et al.,* 2018).

Phenotypic variation across latitudinal gradients have also been described in *Littorina* species (Reid, 1996). For example, the solubility of calcium carbonate is reduced at lower temperatures more typical of Northern Europe, resulting in individuals with thinner shells. Individuals in northernmost locations where temperature is lower tend to present larger sizes due to larger cell size, lower cell division rate and shorter reproductive season, and/or increased nutrient supply related to higher algal productivity and increased underwater feeding time (Reid, 1996 and references therein). Finally, individuals at high latitudes also tend to present taller-spired shells (Reid, 1996). Nonetheless, the phenotypic variation and the underlying genetic basis at this macrogeographic scale have been less studied than those at local scales. Filling this gap is urgent in order to improve our predictions on how species respond to climate change.

1.3. Latitudinal phenotypic variation of the flat periwinkle *L. obtusata*

Flat periwinkles comprise two species, *L. obtusata* and *L. fabalis*, characterized by a low-spire, as well as a globular and smooth shell with circular aperture. Both species can be found throughout the Northern Atlantic shores, from the Portugal shore up to northern Norway, Iceland, Greenland, and the White Sea. However, *L. obtusata* is also present in the southeast of the United States of America, from New Jersey to Quebec and Labrador (Reid, 1996). The two species present direct development and are highly polymorphic in terms shell colour, size and shape.

Although adults *L. obtusata* tend to be larger, there are no diagnostic shell traits between the two species (Figure 4). Thus, the two species are usually distinguished based on the genitalia morphology (see below in section 2.2.1).

Figure 4. Representatives of the two flat periwinkles species with graph paper for size reference. Shell of *L. fabalis* collected in Galiza, Spain (left) and of *L. obtusata* collected in Tromsø, Norway (right).

Both species are found on seaweeds (mainly *Fucus vesiculosus* and *Ascophyllum nodosum*) but whereas *L. obtusata* grazes on macroalgae, *L. fabalis* feeds on epiphytes (de Kluijver *et al*., 2000). Another main difference between the two species is that *L. obtusata* is usually found in the mid-upper intertidal, in more sheltered habitats, while *L. fabalis* inhabits the lower intertidal.

Like for other species in the genus, besides ecotypic variation associated with specific habitats, flat periwinkles present a remarkable variation in shell morphology across latitudinal gradients. In the case of *L. obtusata*, the focal system of this study, this resulted in the classification of two main geographical varieties by Reid (1996): *retusa* (flat), generally presenting low-spired and thick-walled shells; and *palliata*, with shells exhibit higher spirals and thinner walls.

The *retusa* variety occurs southern of the Lofoten islands (Norway) in continental Europe, in the south and western shores of Iceland, and in the Western Atlantic shores from Maine in the North until New Jersey in the South (Figure 5). The *palliata* variety range includes the continental European shore from the Lofoten Islands until to the White Sea, the north and East shores of Iceland, Greenland, and Western Atlantic shores from Maine in the South to Quebec and Labrador, Canada (Figure 5). Intermediate forms were also found in Bodø and from Inhavet to Bogen (near Lofoten Islands), where the shell phenotypic shift occurs (Reid 1996). However, a detailed phenotypic characterization of individuals across the transition between these varieties, enabling a more precise understanding on how the different traits vary (and co-vary) with latitude, is still lacking.

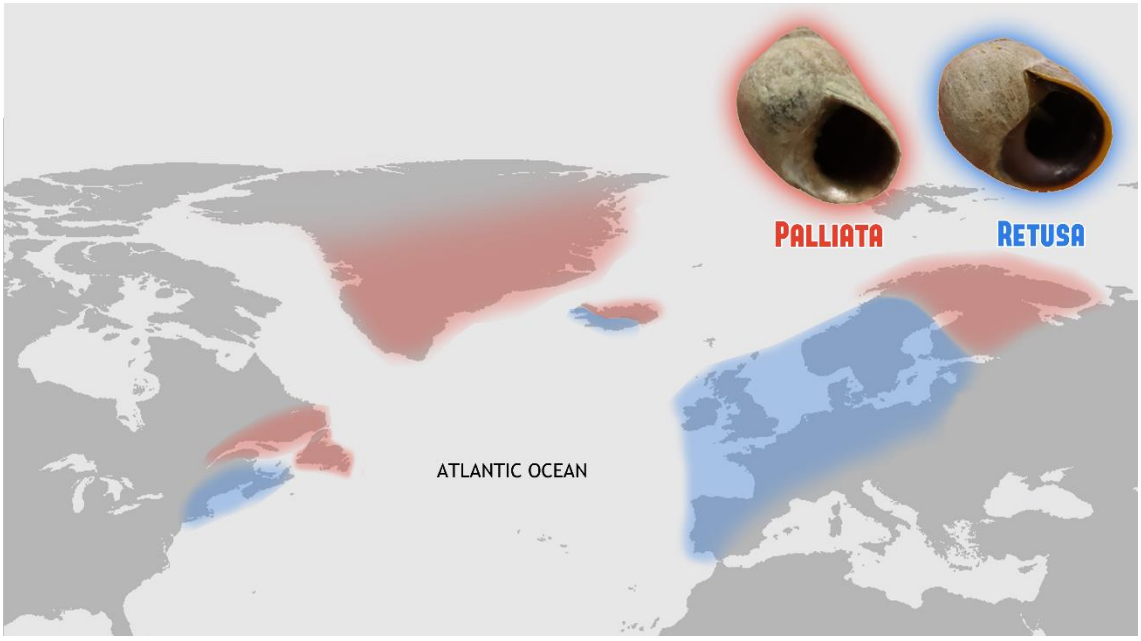

Figure 5. Approximate geographical distribution of *L. obtusata* varieties according to Reid (1996). *Retusa* variety in blue and *palliata* variety in red.

1.4. Factors influencing *L. obtusata* phenotypic variation with latitude

Several explanations exist for the sift in *L. obtusata* shell morphology. First the geographic distribution of the different varieties of this species could reflect population history, with the changes occurring as the populations expanded from North to South or vice-versa. However, the phenotypic trend observed in the two sides of the Atlantic makes this a less plausible scenario.

One of the main explanations for the observed trends is related with predation. The European green crab (*Carcinus maenas*) is one of the major predators of *L. obtusata*. This omnivorous species feeds on the most opportune prey according to the environmental conditions they are exposed to. The impact of *C. maenas* on ecosystems is largely related to the selective pressure it imposes on its preys. This species is native of Europe, ranging from Mauritania (north of Africa) to Norway, including some regions of the United Kingdom and Iceland. However, it expanded its range as an invasive species mainly towards the northwest of the Atlantic Ocean and the northeast of the Pacific Ocean (Young & Elliott, 2020). Records from 1817 show that this species was introduced in north-western coast of the United States of America, arriving at the coastline that comprises the states of New Jersey and New York. From then onwards, its expansion was progressive and mainly in direction to the north, reaching the regions of Massachusetts and Maine around the 1900s, and the Canadian provinces of Nova Scotia and Newfoundland and Labrador in mid-20th century and 2007, respectively (Young & Elliott, 2020).

A genetic and morphological characterization of *L. obtusata* conducted in northern New England populations (United States of America) revealed a shell shape change from typical *palliata* characteristics (i.e., thin walls and high spires) to *retusa* (namely, thick walls and low spires) following the geographic expansion (1980's) of the European green crab after its introduction (Seeley, 1986). Field and laboratory experiments showed that the survival rates between the two varieties in the presence-absence of green crabs differed significantly, with the low-spired shells being less vulnerable to predation, which could result from an adaptation to crab predation via a greater whorl overlap and larger shell thickness (Seeley, 1986).

An alternative, although non-mutually exclusive, explanation was proposed by Trussel *et al*. (2000), after combining transplant with experiments in the laboratory. This study revealed larger shell thickness (and reduced body mass as a trade-off) when snails during their development were exposed to water containing European green crabs (but not directly in contact with them), suggesting the role of plasticity, i.e. the ability of

organisms of the same genotype to produce different phenotypes according to the environmental conditions they are exposed to (Trussel *et al.* 2000). However, it is possible that phenotypic plasticity in this system is adaptive, and that selection could have acted in genetic variation underlying plastic traits.

Since the distribution of *C. maenas* in its native range (Europe) roughly coincides with the distribution of the *retusa* variety (Figures 5 and 6), it could be hypothesised that the phenotypic differences between the two *L. obtutasa* geographic varieties could be caused by differential predation by the European Green crab. However, other predators of *Littorina* snails exist besides crabs (e.g., fishes and birds), making it difficult to explain the observed phenotypic trends solely based on the influence of predators.

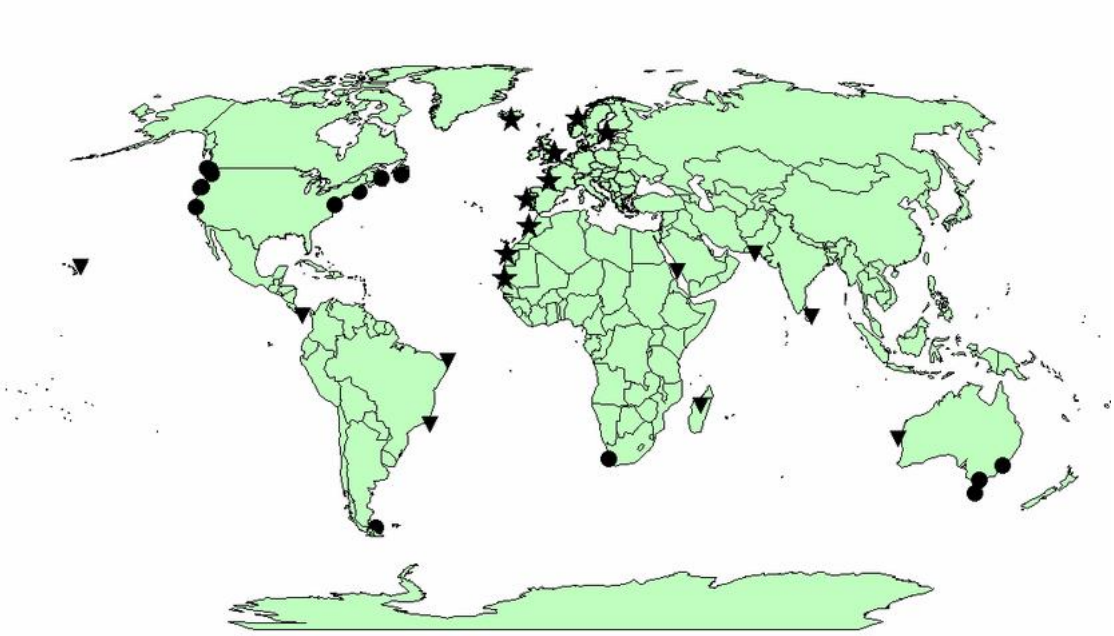

Figure 6. Geographical distribution of *Carcinus maenas*. Indications of the native range (stars), introduced or invasive range (circles) and failed invasions (triangles). (Source: Klassen & Locke, 2007)

Finally, as previously explained, latitudinal variation of temperature could influence changes in *L. obtusata* shells, mainly shell thickness (Reid 1996). Indeed, the study by Trussel *et al*. (2000) showed that predator-induced shell changes were of the same magnitude as those related with temperature effects associated with the different latitudes of the studied populations. Although temperature variation related with latitude is expected to result changes in European *L. obtusata* populations consistent with the distribution of these two varieties, it is not easy to decouple temperature from the predation effects, as the distribution and abundance of green crabs is also associated

and with temperature, both decreasing towards North. Indeed, the study conducted by Trussel *et al.* (2000) revealed a complex interaction between water temperature and presence of green crabs.

As a consequence, the contribution of each of these factors to latitudinal variation in shell morphology in *L. obtusata* across European shores, as well as their interaction, are still poorly understood. Moreover, the genetic basis underlying the observed phenotypic changes remains to be characterized (Seeley, 1986).

1.5. Population genomics tools and the genetic basis of phenotypic variation

The advances in sequencing technologies that occurred during this century contributed to revolutionize the field of evolutionary biology. In particular, ultra-high throughput sequencing allows to obtain whole genome information in fast and cost-effective manner (Yohe, & Thyagarajan, 2017), which can be used to address many questions in the field, including the characterization of genomic regions, genes and nucleotide position influencing phenotypes of interest.

Although sequencing entire genomes, including those of non-model species, is becoming generally affordable, the need to sequence multiple individuals per population remains prohibitive for many research groups. A cost-effective alternative is to sequence pools of individuals (Pool-seq) (Schlotterer, 2014). This approach involves mixing the DNA from multiple individuals in equimolar proportions, and the construction if a single library for the entire pool, instead of one per individual. Thus, Pool-seq has a significant cost advantage compared with individual sequencing, while allowing to obtain relatively accurate allele frequencies (using pools of >50 individuals with ~1x of coverage each) (Schlotterer, 2014).

Although Pool-seq is not so well suited for inferring individual haplotypes hindering certain analyses (Fuentes-Pardo & Ruzzante, 2017), it provides relatively accurate allele frequencies per pool that are still useful to address important evolutionary genomic questions. For example, Pool-seq can be used to characterize the genetic basis/genomic architecture of traits that segregate within a population. By sequencing pools of individuals with extreme phenotypes from the same (panmictic) population we should be able to identify differentiated genomic regions (i.e., presenting larger frequency differences) between the two pools relative to the background differentiation across the

genome. This would result in a list of candidate regions involved in the phenotype of interest (Schlotterer, 2014).

Given the significant cost advantage and the informativeness of this approach to identify possible gene candidates involved in phenotypes with evolutionary significance, its implementation to study the genetic basis of the shell traits that vary latitudinally (and between the two varieties) in *L. obtusata* could improve our understanding on the mechanisms of adaptation and diversification across environmental gradients.

1.6. Motivation

The phenotypic differences between *L. obtusata* varieties are known to be influenced by environmental factors such as historical contingency, temperature, salinity, and predators. However, a detailed and systematic characterization of the different phenotypes in natural populations of this species across a latitudinal gradient encompassing the transitions between varieties was not yet performed. Moreover, the genetic basis underlying the observed phenotypic changes remains to be determined.

Different studies on western Atlantic *L. obtusata* populations after the green crab invasion suggested that changes in shell thickness and body size could have evolved by changes in genetic variation influenced by selection (Seeley, 1986) or be the result of a plastic (adaptive) response (Trussel *et al.,* 2000). However, the contribution of each of these mechanisms (and of their interaction) was not yet quantified. Although the phenotypic gradient observed in *L. obtusata* could be the result of a response to crab predation (via plasticity and/or adaptation), because the crab distribution changes in the same axis as temperature, the contribution of each of these factors (as well as others) have not been yet properly measured.

Aiming to fill these gaps, we designed a research project to characterize phenotypically five European *L. obtusata* populations distributed across the shift in shell variation associated with the two varieties, *retusa* and *palliata*. Together with an environmental characterization across the study area (Northern Norway) and sequencing of extreme phenotypes within a polymorphic population, we hope to improve our understanding of the processes driving intraspecific variation, adaptation, and diversification in the marine intertidal, one of the most biodiversity-rich ecosystems on Earth.

1.7. Main objectives

Although *L. obtusata* morphological variation across latitude has been described since a while ago, a detailed characterization of the varying traits across populations near the phenotypic shift of the varieties *retusa* and *palliata*, as well as its genetic basis remains to be described. As a result, knowledge about the main mechanisms and evolutionary processes involved remain limited. Here, we combine phenotypic, environmental, and genetic analysis of *L. obtusata* populations with the following goals:

I. Quantify the main phenotypic differences between populations across the environmental gradient at high latitudes encompassing the geographic region where the transition between varieties occurs.
II. Identify and characterize the genomic regions involved in phenotypic differences.
III. Gain insights about the main forces and environmental factors responsible for the evolution of different phenotypic varieties.

Ultimately, by understanding and taking into account the adaptive potential of populations or species we hope to contribute to improve the predictions of the impact of climate change on biodiversity, enabling the implementation of more effective management and conservation measures.

2. Methods

2.1. Sample collection and processing

Littorina obtusata individuals were collected from 20 locations along a latitudinal gradient across the North Atlantic coast of Norway, from Seines in the South until Kirkeporten in the North. Five of these locations, spanning the geographic region where the shift in shell spire was described to occur (Lofoten islands, Norway; Reid, 1996), were selected as focal sites of this study based on their even latitudinal distribution (Figure 7).

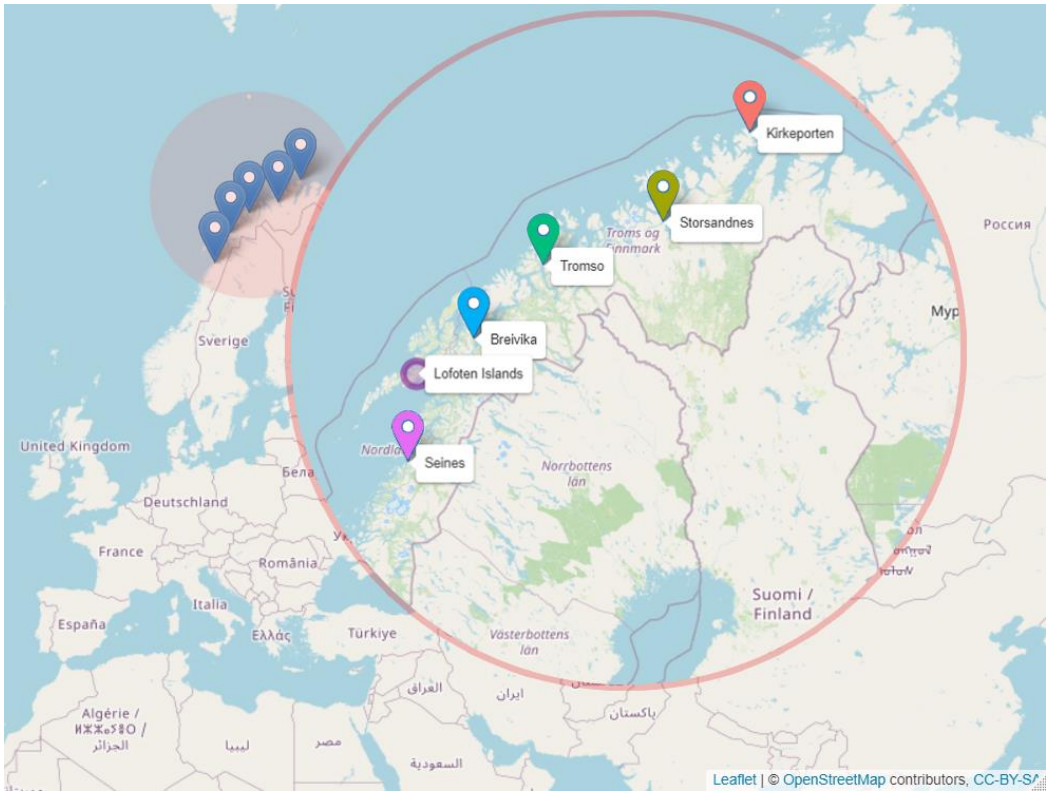

Figure 7. Geographical location of the 5 sampling sites of *L. obtusata* individuals (blue pinpoint markers) with a zoom in within the red circle on the right. Region of shell spire shift described by Reid (1996) (purple circle marker). The map was produced using the 'Leaflet' JavaScript library in RStudio (version 2022.07.0).

Most samples (N>50 from each site) were collected during a field trip in 2021, except in Seines, where snails were also collected in 2020 and 2022 by different researchers. In each location, we spent 15 to 30 min randomly collecting flat periwinkles in macroalgae (mainly *Fucus* spp. And *Ascophyllum nodosum*). The only exception happened in Tromsø, where samples were sent by collaborators (Joost Raeymaekers, Norway). All individuals were first frozen at -5°C to -20°C and then put in 95% ethanol for preservation.

Once in the laboratory, the 50 largest individuals from each sampling location were selected for subsequent phenotypic characterization, to ensure that only adult individuals

were analysed. The only exception was in Breivika, where all collected individuals (100) were analysed, to generate enough samples for the genetic characterization (see details below).

2.2. Phenotypic characterization

Samples were characterized for several traits, including total weight, sex, shell height, spiral height and angle, shell shape, thickness (Figure 8), and strength/resistance using the procedures subsequently described. Although shell colour and presence of scars were also recorded, these were not analysed and therefore are not here presented.

2.2.1. Traits measurement

- Total weight

The excess of ethanol was first removed with paper. The full body (including the shell) of each snail was then measured (mg) using an analytical balance (Ohaus AP210) with a resolution uncertainty of 0.00005 g.

- Sexing and species identification

Whenever possible, the soft tissue was initially removed from the shell and kept in 95% ethanol. The sex of each sample was then assessed using a stereoscopic magnifier (Olympus SZX2-ILLT) and individuals were classified either as male or female. Given that is not possible to fully discriminate between *L. fabalis* and *L. obtusata* individuals solely based on the shell morphology, male genitalia appearance (diagnostic between flat periwinkles' species) was used to classify individuals into species using a criteria described by Reid (1996). Specifically, whereas *L. obtusata* individuals present a short and triangular penial filament, comprising 10-25% of the total penis length, *L. fabalis'* filament is long (30-60% of the total penis length) and vermiform.

Whenever the soft tissue was closed inside the operculum (all samples from Storsandnes and 25 samples from Tromsø), individuals were sexed after breaking the shell once all other measurements were completed.

- Shell thickness

Shell thickness (mm) was measured ~1mm inside the aperture using a digital thickness gauge with resolution uncertainty of 0.0005 mm, (Figure 8). Because shell thickness varies in different shell points, three measurements in three different points of the aperture were taken for each snail.

- Shell height

Total shell height (cm) was measured for each snail using a digital calliper (Biltema, Art. 16-105) with a resolution uncertainty of 0.005 cm (Figure 8).

- Shell spiral height

The spiral height (mm) (Figure 8) was measured with ImageJ (version 1.53t) using the photographs taken for shell shape analysis. The graph paper was used for scaling to real size. Shell spiral height was then divided by total shell height and the values of this ratio for each individual were recorded.

- Spire Angle

Shell spiral angle (º) was also measured with ImageJ (version 1.53t) also resorting to the photographs taken for the shell shape analysis.

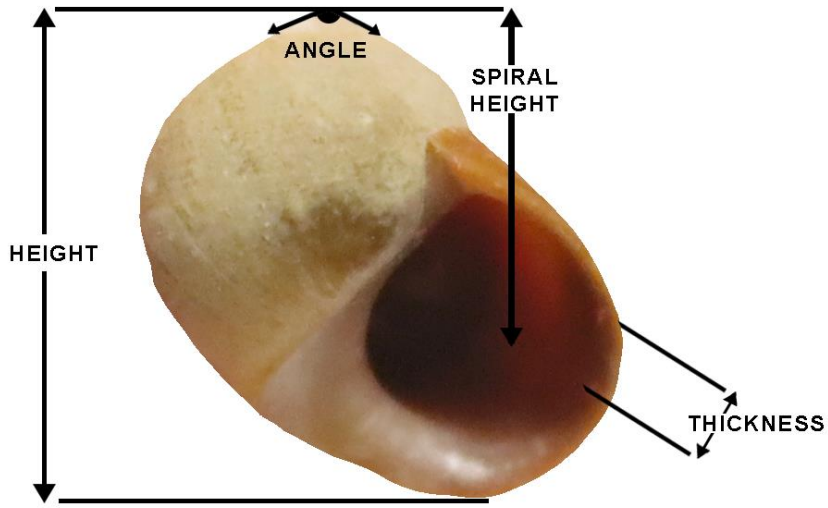

Figure 8. Photograph of a *L. obtusata* shell with a representation of some of the measured traits: shell height, spiral height, thickness, and spiral angle. Shown in is a shell from an individual from Tromsø.

- Shell strength

A measure of shell strength was taken by applying a mechanical force into an adapted nutcracker device until the shell broke. The maximum force (N) applied during this procedure was registered by a force transducer (type 9331B, Kistler Inc., Winterthur, Switzerland) connected to a charge amplifier (type 5995A, Kistler Inc) (Figure 9).

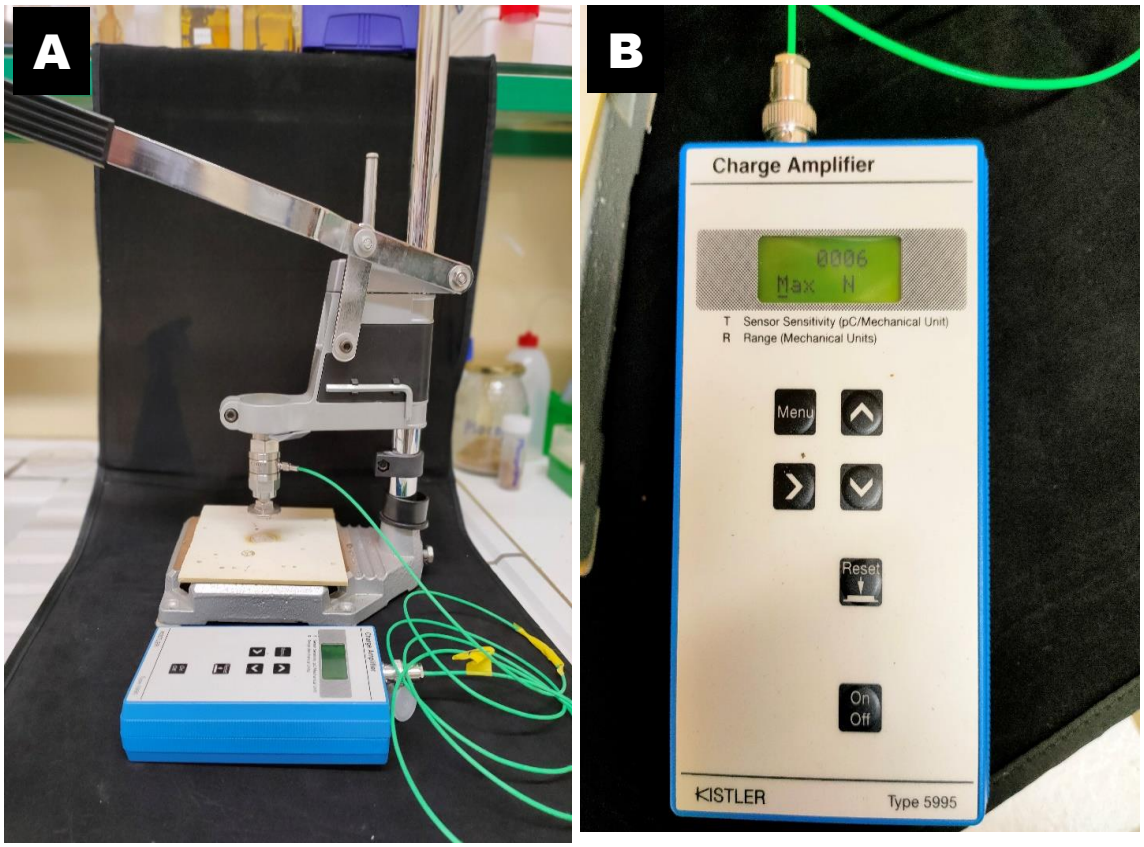

Figure 9. Equipment used to measure shell strength. Adapted nutcracker device with a Kistler force transducer (A) connected to the charge amplifier (B).

- Shell shape

Each snail shell was photographed in a standard position using a digital camara (Canon EOS 250D). The shell was first positioned with its longitudinal and lateral axes on the horizontal plane of the camara, following the protocol from Carvajal-Rodriguez *et al.* (2005) for *L. saxatilis*. However, the shell was later tilt so that the apex became visible (Figure 9).

The resulting pictures were cropped using Adobe Photoshop (version CS6) to remove the scale and colour reference. The cropped pictures were used as input for running a MATLAB (version R2022b) shell outlining script (Jenny Larsson, unpublished). The resulting output consists of a tps file of shell landmarks that was imported into an outline analysis R script (Jenny Larsson, unpublished) ran in RStudio (version 2022.07.0). Within this script, PCA plots are produced with individuals displayed and grouped by population.

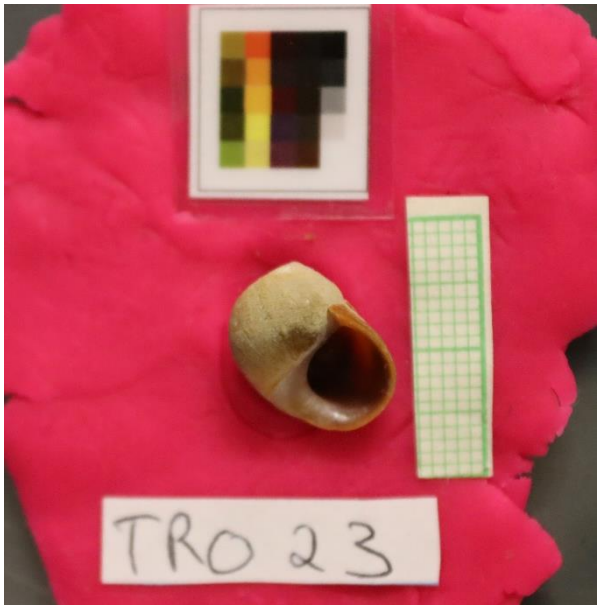

Figure 10. Photograph of a shell from *L. obtusata* in a standardized position for morphological analysis. Shown in is a shell from an individual from Tromsø, as well as the scale and colour standard.

2.2.2. Statistical analysis of phenotypic traits

After the phenotypic characterization, all individuals that were not adults, that presented shell deformations or that could belong to another species than *L. obtusata* were removed from subsequent analysis.

The significance level was set at 0.05, as usual.

A one-way ANOVA (ANalysis Of VAriance) model was used to evaluate the existence of significant mean differences between all five populations, for each phenotypic trait. The tested null hypothesis was the equality of means across locations. When a statistically significant result (p-value < 0.05) was obtained the null hypothesis was rejected, supporting significant mean differences between at least a pair of populations. This is a parametric approach, with three assumptions: i) the data was obtained from populations following a normal distribution, ii) the data was obtained from populations that present equal variances, and iii) the observations are independent from each other, and were sampled randomly. These hypotheses were evaluated graphically, and no serious violations of the model assumptions were identified (Appendix 1).

To determine which specific pairs of populations, exhibit significant differences for each phenotypic trait, pairwise T-tests (Student, 1908) comparisons were used. The null hypothesis tested was that the mean of each trait was the same in each population pair. T-tests were used with pooled standard deviation and correction for multiple tests was

implemented using the Bonferroni adjustment (Jean Dunn, 1961). A Principal Component Analysis (PCA) was implemented using all phenotypic data to visualise how individuals differ from each other.

Multiple pairwise correlation analyses (using a Pearson coefficient) between phenotypic traits were also undertaken to assess the to which extent the phenotypic traits were correlated (Freedman *et al*., 2007).

2.3. Crab presence and environmental data collection

In order to identify possible causes of the observed latitudinal phenotypic changes of *L. obtusata* shell variation, four variables were studied: crab (*C. maenas*) occurrence/presence, sea surface temperature, air temperature and sea salinity. Data from the last three variables were collected for each (or near) each sampling location every 10 days (3 times per month) between 2017 and 2021. For crab occurrence, the total amount of observations during the five years was considered.

The sea surface temperature data was obtained from The National Oceanic and Atmospheric Administration (NOAA) CoastWatch data portal (https://coastwatch.noaa.gov/cwn/cw_b/) within a 5km grid including each location. Air temperature and sea salinity data was collected using NASA's (National Aeronautics and Space Administration) Earth Science Data Systems (https://worldview.earthdata.nasa.gov) from the nearest distances (maximum radius of ~100km) from each sampling location. Information regarding the occurrence of *C. maenas* was obtained from the Norwegian Biodiversity Information Centre (NBIC) (https://www.biodiversity.no) for a radius of 10km from each sampling location. This was complemented by crab presence information during sampling collection. The distances from sampling sites at which the data for each variable was collected are the minimum available by each database.

In order to obtain a general overview of the trends and patterns (monthly and yearly) present in the environmental variables, time series analyses were performed using moving metrics. These consisted of the average, the maximum and the minimum that were estimated from the raw data collected for the sea salinity, sea surface temperature and air temperature in RStudio (version 2022.07.0) using the “zoo” package (Zeileis, & Grothendieck, 2005). The moving metrics model considered a window size of nine points, corresponding to 90 days (Appendix 2).

The time series were then decomposed into three components by the Seasonal and Trend decomposition using Loess (STL) with a periodic window (Cleveland et al., 1990) in RStudio package “xts” (Ryan *et al.,* 2022). This method decomposes the original data into seasonal, trend and remainder components (Appendix 3), which allows an individual analysis of each component, while performing the smoothing of the seasonal and trend components with a minimization of the outliers’ effects. The seasonal component consists of a repetitive pattern by using STL with yearly seasonality. The trend is the result of the main series with the seasonal component subtracted and provides the overall direction of the data. The remainder is obtained by removing the other two components from the main time series and shows the quantity of noise in the collected data.

2.4. Relation between phenotypic traits and environmental variables

In order to understand the effect of each environmental factor on the *L. obtusata* phenotypes, linear model analyses on the mean value, per location, for each factor were carried out. This exploratory approach was conducted in RStudio (version 2022.07.0) using the *lm()* function. The summary statistics for each linear model included the intercept and the slope coefficients with their respective p-values. The standardized slope, reflecting the impact that an increase of one standard deviation in the mean of an environmental variable has on a phenotypic trait, was also used to assess which environmental variable mostly affected each phenotypic trait.

2.5. Genetic characterization

2.5.1. Laboratorial procedures

In order to identify the genomic regions involved in one of the phenotypic traits analysed (shell strength) we selected the location (Breivika) closer to the zone of the transition between the two varieties (Lofoten Islands, Figure 7), under the assumption that it could show higher phenotypic variance. By sequencing the entire genome of individuals from two groups of phenotypes (low shell strength vs high shell strength) we aimed to identify regions in the genome that are more divergent between these two groups. Because we randomly sampled individuals from a putative panmictic population, we expected that genomic regions involved in the trait differences (and other associated traits) would stand out over the rest of the genome, which should show low differentiation due to gene flow.

In order to implement this, we initially characterized 100 individuals from this population for the different traits. After eliminating juveniles, as well as putative *L. fabalis* individuals based on their shell and genitalia morphology, we kept 68 samples for subsequent analysis (Figure 10).

Genomic DNA was extracted from the soft tissue of each sample using a saline-based protocol adapted from Enbody et al. (2021), which started with the digestion of the cleaned tissue, followed by the RNA digestion using RNase, precipitation and removal of proteins, and precipitation of DNA. After elution, DNA integrity and purity were evaluated visually after electrophoresis in agarose gel, and the absorbance ratios (260/280 and 260/230 to assess DNA purity) were obtained using NanoDrop™ 2000 spectrophotometer (Thermo Fisher Scientific).

Furthermore, double stranded DNA quantification was performed for each sample using Qubit 1.0 Fluorometer (Invitrogen, Thermo Fisher Scientific) with the broad range assay kit. The DNA extract was then stored at ~4°C until further use. The DNA from each group of samples (low versus high shell strength) was pooled using equimolar concentrations of DNA from each of the 34 individuals from each group, making a final volume of 200µl and DNA concentration of 50ng/µl for each pool. The pools were then cleaned up using AMPure XP beads from Bioline (2016), which bind double-stranded DNA sample (at a ratio of 1.8x).

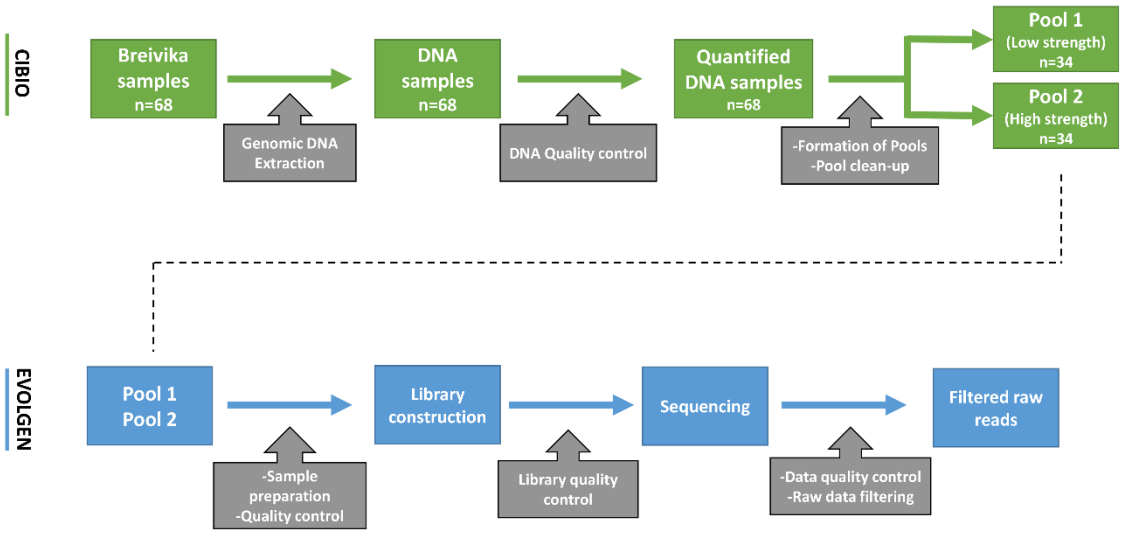

Figure 11. Flow chart representing the workflow applied in the pool sequencing of the Breivika samples.

Cleaned pools were then sent to Novogene (https://en.novogene.com) in Cambridge (UK). There, a quality control of the received extracts was first performed, followed by a PCR-free library preparation. Briefly, genomic DNA was sheared randomly into small fragments that were subsequently filtered by size using purification beads. The resulting fragments were then end-repaired, A-tailed and ligated to Illumina adapters. At the end, the fragments were selected using beads. Quality control of the libraries was done with Qubit and real-time PCR, and the size distribution assessed using bioanalyzer. Finally, the quantified libraries were pooled and sequenced (paired-end 150bp) on an Illumina platform (NovaSeq 6000 system) using sequencing by synthesis.

2.5.2 Genetic Data analyses

The sequenced raw reads were further filtered by removing adapters and removing reads with unidentifiable bases or with bases of poor quality in > 50% of their size using the Novogene raw data filtering pipeline. The filtered raw reads were downloaded to CIBIO (Centro de Investigação em Biodiversidade e Recursos Genéticos) server, where all subsequent analyses were implemented.

Trimmomatic (version 0.36) tool was used to trim the sequences by removing remaining adapter sequences and low-quality bases (Bolger *et al.*, 2014). Trimmed reads were then mapped into reference genome resorting to the Burrows-Wheeler alignment tool (BWA) with the algorithm BWA-MEM (Li, 2013), which is the recommended for high-quality alignments of short reads, resulting in bam file for each pool. Mapping quality was evaluated using SAMtools with the "flagstat" option, originating two flagstat files with statistics of the mapping results. The data coverage was inferred with the SAMtools "depth" option. Bam files were converted to a single mpileup file, with each line representing a pileup of all reads at a certain position in the genome.

The remaining data analysis was done through two specific software for pool-seq data analysis PoPoolation (version: 1.2.2) (Kofler *et al*., January 2011) and PoPoolation2 (version: 1201) (Kofler *et al.*, October 2011). The mpileup was converted into a sync file using mpileup2sync.jar and the script Fst-sliding.pl was used to quantify genetic differentiation (FST) between pools using PoPoolation2. Nucleotide diversity (pi), genetic diversity (theta, θ) and Tajima's D were estimated for each pool using the script Variance-sliding.pl in PoPoolation. However, for these specific estimators, the bam files of each pool had been converted into pileup files using SAMtools. For all analyses, we considered a window size of 10000, a step size of 2500 and minimum and maximum

coverages of 10 and 100, respectively. For the assessment of the genetic differentiation (FST), the minimum fraction of a window with enough coverage was 0.2 and the minimum count of the minor allele considered was 3, whereas for the remaining estimations a minimum count of 2 for the minor allele was used.

Subsequent data analysis and visualisation was done in RStudio (version 2022.07.0) using the "qqman" package. To aid visualization of the nucleotide diversity, 5000 windows from the distribution of D, pi and θ were randomly subsampled from both pools.

3. Results

3.1. Phenotypic traits

- Shell weight

The highest mean weight was observed in Breivika (1273.0 mg) and the lowest in Storsandnes (620.5) (Figure 12, Table 1). Mean weight is significantly higher in the Southern populations (Breivika and Seines) when compared to the three other populations located further north (Kirkeporten, Storsandnes and Tromsø) (Figure 12, Table 2). Within these groups no significant pairwise differences in mean weight were found except for Storsandnes and Tromsø (Table 2). The widest range of values was observed in the southernmost population (Seines: 1277.0 mg), whereas the smallest range was observed in northernmost population (Kirkeporten 502.0 mg) (Figure 12).

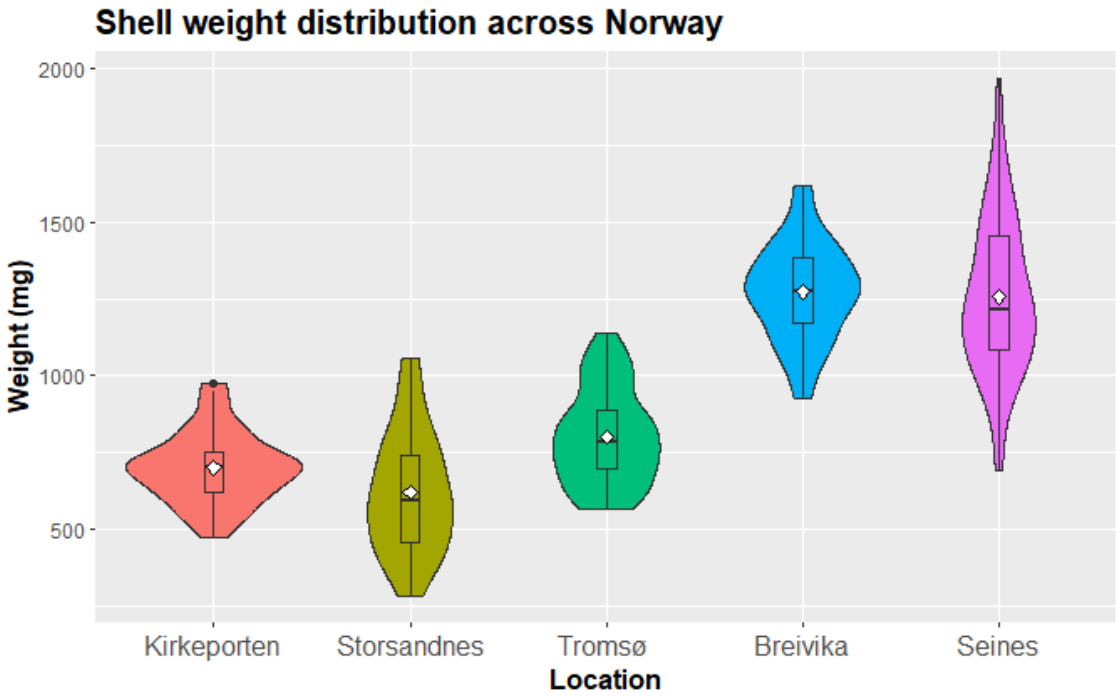

Figure 12. Violin plots of the *L. obtusata* weight distribution for each sampling location ordered from north to south. Box plots are also presented in the middle of the violin plots with average values displayed in white and outliers in black. Population colours are the same as in Figure 7.

Table 1. Summary statistics (sample size, mean and standard deviation) for weight (mg) per population. Population colours are the same as in Figure 7.

Population n= number of individuals	Kirkeporten n=44	Storsandnes n=49	Tromsø n=50	Breivika n=47	Seines n=47
Mean (Standard deviation)	700.9 (113.65)	620.5 (195.43)	802.9 (154.02)	1273.0 (159.09)	1256.0 (256.73)

Table 2. P-values of pairwise t-tests for mean weight. Statistically significant differences between populations are highlighted in bold considering an α of 0.05 and a Bonferroni correction for multiple tests. Population colours are the same as in Figure 7.

Weight	Kirkeporten	Storsandnes	Tromsø	Breivika
Storsandnes	0.353	-	-	-
Tromsø	0.074	**< 0.001**	-	-
Breivika	**< 0.001**	**< 0.001**	**< 0.001**	-
Seines	**< 0.001**	**< 0.001**	**< 0.001**	1.000

- Shell thickness

Whereas average shell thickness was highest in Seines (1.084 mm), the lowest average was observed in Tromsø (0.558 mm), with the Breivika population showing an intermediate value (0.835 mm) (Figure 13, Table 3). Mean thickness is significantly higher in the southern populations (Breivika and Seines) when compared to the three other populations located further north (Kirkeporten, Storsandnes and Tromsø) (Figure 13, Table 3). However, contrary to weight, Seines shows thicker shells on average than Breivika (Table 4). As observed for weight, within the northern group, significant pairwise differences in shell thickness were also observed between Storsandnes and Tromsø, although in this case, differences between Kirkeporten and Tromsø were also significant (Table 4). The widest range of thickness values was observed in the southernmost population (Seines: 0.799 mm), whereas the smallest range was observed in Breivika (0.394 mm) (Figure 13).

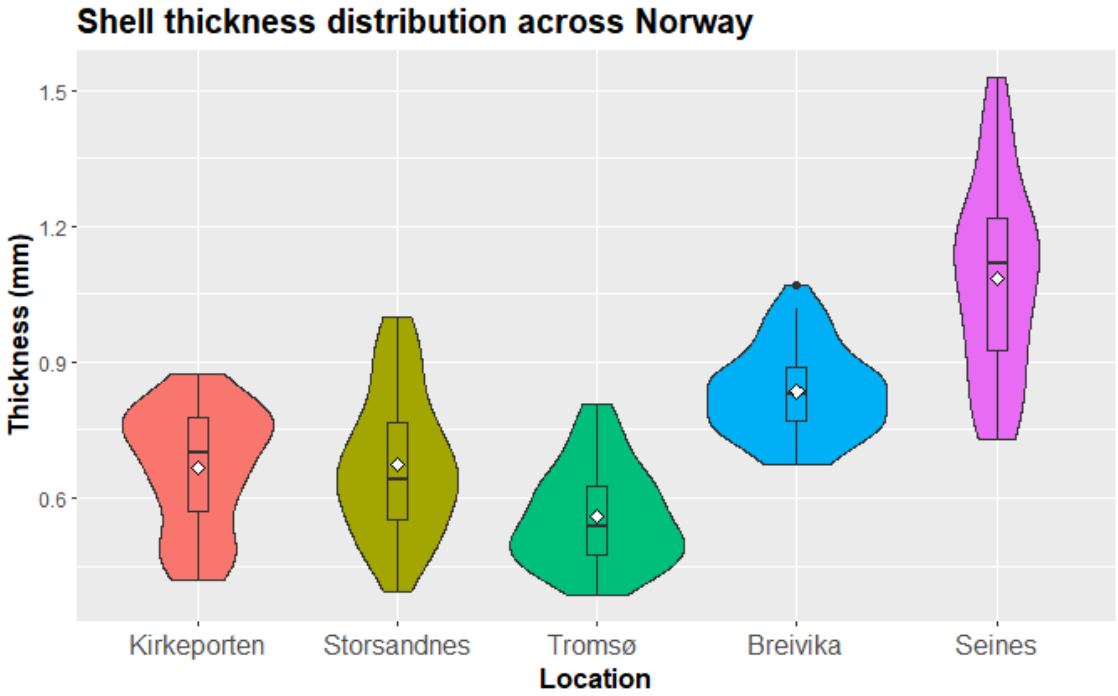

Figure 13. Violin plots of the *L. obtusata* thickness distribution for each sampling location ordered from north to south. Box plots are also presented in the middle of the violin plots with average values displayed in white and outliers in black. Population colours are the same as in Figure 7.

Table 3. Summary statistics (sample size, mean and standard deviation) for thickness (mm) per population. Population colours are the same as in Figure 7.

Population n= number of individuals	Kirkeporten n=44	Storsandnes n=49	Tromsø n=50	Breivika n=47	Seines n=47
Mean (Standard deviation)	0.67 (0.133)	0.67 (0.154)	0.56 (0.107)	0.84 (0.098)	1.08 (0.213)

Table 4. P-values of pairwise t-tests for mean thickness. Statistically significant differences between populations are highlighted in bold considering an α of 0.05 and a Bonferroni correction for multiple tests. Population colours are the same as in Figure 7.

Thickness	Kirkeporten	Storsandnes	Tromsø	Breivika
Storsandnes	1.000	-	-	-
Tromsø	**0.004**	**< 0.001**	-	-
Breivika	**< 0.001**	**< 0.001**	**< 0.001**	-
Seines	**< 0.001**	**< 0.001**	**< 0.001**	**< 0.001**

- Shell height and shell spiral height

The trends of total and spiral shell lengths are very similar (Figures 14 and 15), with significantly higher values observed in the Southern populations (Breivika and Seines) than in the two northernmost populations, Kirkeporten and Storsandnes, with these two presenting the lowest spire and total heights (8.61 and 10.89 mm, respectively) (Figures 14 and 15, Tables 5 and 6). Breivika was the population with higher spire and total heights (13.71 and 10.23 mm, respectively). However, contrary to the other phenotypic traits, Tromsø has a similar mean total and spiral shell length as those observed for the southernmost populations rather than those found in populations further north (Tables 5 and 6). Within the three most southern populations, no significant pairwise differences were found between Tromsø and Seines for shell height, as well as between Tromsø and Breivika for spiral height. Whereas within the northernmost populations no significant differences were observed for the spiral height, Storsandnes presents a significantly smaller mean total shell height than Kirkeporten (Tables 7 and 8). In both, total shell height and spiral height, the widest range was observed in the Storsandnes (4.77 and 3.79 mm, respectively), and the smallest in Kirkeporten (2.95 and 2.98 mm, respectively) (Figure 14 and Figure 15).

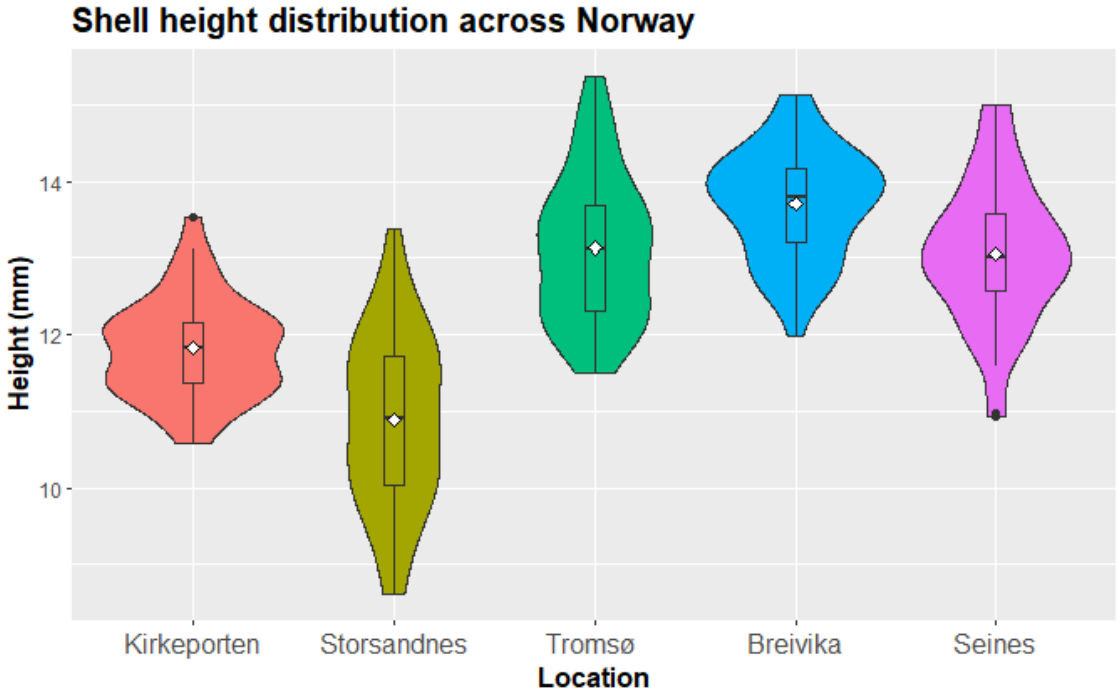

Figure 14. Violin plots of the L. obtusata shell height distribution for each sampling locations ordered from north to south. Box plots are also presented in the middle of the violin plots with average values displayed in white and outliers in black. Population colours are the same as in Figure 7.

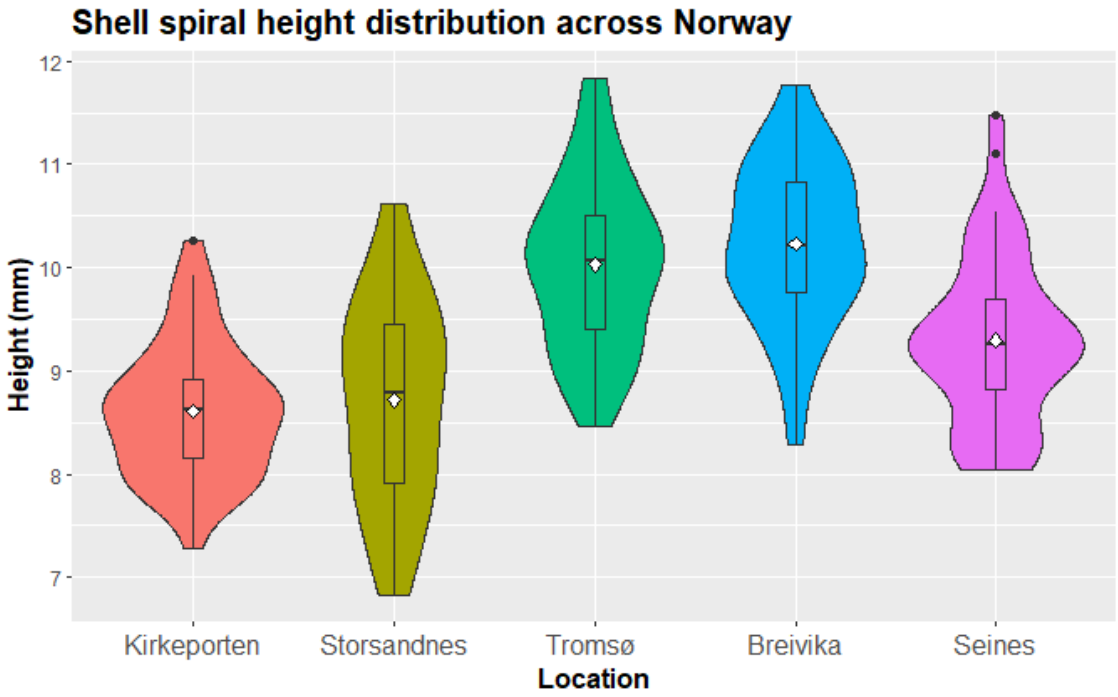

Figure 15. Violin plots of the *L. obtusata* shell spiral height distribution for each sampling location ordered from north to south. Box plots are also presented in the middle of the violin plots with average values displayed in white and outliers in black. Population colours are the same as in Figure 7.

Table 5. Summary statistics (sample size, mean and standard deviation) for shell height (mm) per population. Population colours are the same as in Figure 7.

Population n= number of individuals	Kirkeporten n=44	Storsandnes n=49	Tromsø n=50	Breivika n=47	Seines n=47
Mean (Standard deviation)	11.8 (0.65)	10.9 (1.13)	13.1 (0.96)	13.7 (0.72)	13.1 (0.93)

Table 6. Summary statistics (sample size, mean and standard deviation) for shell spiral height (mm) per population. Population colours are the same as in Figure 7.

Population n= number of individuals	Kirkeporten n=44	Storsandnes n=49	Tromsø n=50	Breivika n=47	Seines n=47
Mean (Standard deviation)	8.6 (0.65)	8.7 (0.99)	10.0 (0.82)	10.2 (0.78)	9.3 (0.81)

Table 7. P-values of pairwise t-tests for mean shell height. Statistically significant differences between populations are highlighted in bold considering an α of 0.05 and a Bonferroni correction for multiple tests. Population colours are the same as in Figure 7.

Height	Kirkeporten	Storsandnes	Tromsø	Breivika
Storsandnes	**< 0.001**	-	-	-
Tromsø	**< 0.001**	**< 0.001**	-	-
Breivika	**< 0.001**	**< 0.001**	**0.019**	-
Seines	**< 0.001**	**< 0.001**	1.000	**0.006**

Table 8. P-values of pairwise t-tests for mean shell spiral height. Statistically significant differences between populations are highlighted in bold considering an and a Bonferroni correction for multiple tests. Population colours are the same as in Figure 7.

Spiral Height	Kirkeporten	Storsandnes	Tromsø	Breivika
Storsandnes	1.000	-	-	-
Tromsø	**< 0.001**	**< 0.001**	-	-
Breivika	**< 0.001**	**< 0.001**	1.000	-
Seines	**< 0.001**	**0.006**	**< 0.001**	**< 0.001**

- Ratio shell spiral height/shell height

The mean ratio between shell spiral and total shell height decreases from Storsandnes to Seines, with these two populations presenting the highest and lowest mean values for this ratio, 0.80 and 0.71 respectively (Figure 16 and Table 9). Kirkeporten is the only exception in this trend of successive lower mean ratio values towards the south, being the population with the second lowest mean value (0.73). Statistically significant pairwise differences between Storsandnes and every other. There was lack of statistical significance for differences between Kirkeporten and both Breivika and Seines, and same applies for Tromsø and Breivika (Table 10). Similarly, to the total shell height and spiral height, the widest range of values was verified in Storsandes (0.19), although the smallest was found in Breivika (0.13).

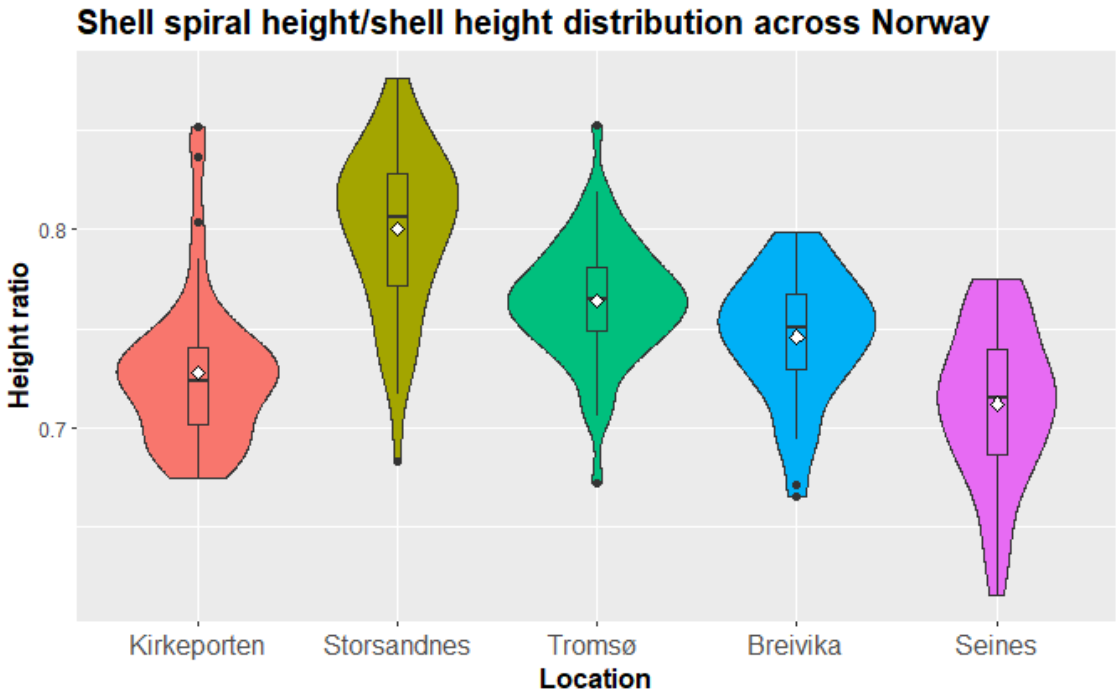

Figure 16. Violin plots of the *L. obtusata* shell spiral height/shell height ratio distribution for each sampling location ordered from north to south. Box plots are also presented in the middle of the violin plots with average values displayed in white and outliers in black. Population colours are the same as in Figure 7.

Table 9. Summary statistics (sample size, mean and standard deviation) for shell spiral height/shell height ratio per population. Population colours are the same as in Figure 7.

Population n= number of individuals	Kirkeporten n=44	Storsandnes n=49	Tromsø n=50	Breivika n=47	Seines n=47
Mean (Standard deviation)	0.73 (0.038)	0.80 (0.041)	0.76 (0.031)	0.75 (0.032)	0.71 (0.039)

Table 10. P-values of pairwise t-tests for mean shell spiral height/shell height ratio. Statistically significant differences between populations are highlighted in bold considering an α of 0.05 and a Bonferroni correction for multiple tests. Population colours are the same as in Figure 7.

Spiral Height/Height	Kirkeporten	Storsandnes	Tromsø	Breivika
Storsandnes	**< 0.001**	-	-	-
Tromsø	**< 0.001**	**< 0.001**	-	-
Breivika	0.182	**< 0.001**	0.156	-
Seines	0.414	**< 0.001**	**< 0.001**	**< 0.001**

- Shell spiral angle

The mean values for shell spiral angle in the northernmost populations (Kirkeporten, Storsandnes and Tromsø) are significantly lower in comparison to the obtained values for the Seines and Breivika populations (Figure 17 and Table 11). The highest overall spiral angle mean value and the widest amplitude were observed in the southernmost populations (Seines, 150.8º; and Breivika, 49.1 º, respectively). The lowest overall mean value was observed in Tromsø (123.5º) and the smallest range in Storsandnes (25.5º). Absence of significant pairwise difference in mean spiral angle was only observed between Kirkeporten and Storsandnes (Table 12).

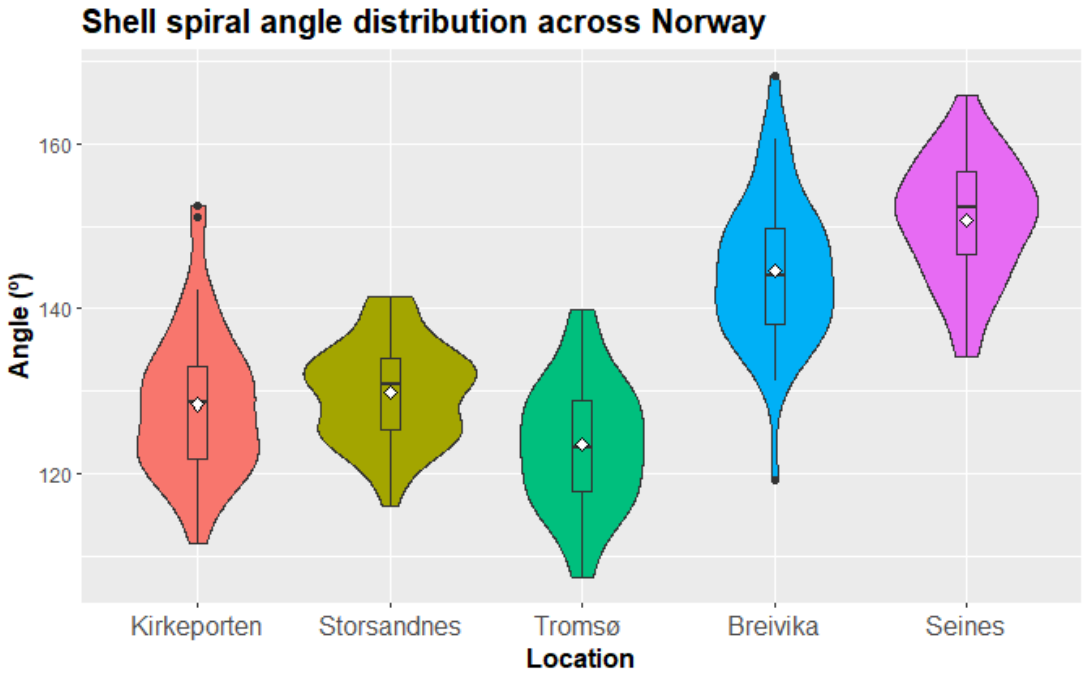

Figure 17. Violin plots of the *L. obtusata* shell spiral angle distribution for each sampling location ordered from north to south. Box plots are also presented in the middle of the violin plots with average values displayed in white and outliers in black. Population colours are the same as in Figure 7.

Table 11. Summary statistics (sample size, mean and standard deviation) for shell spiral angle per population. Population colours are the same as in Figure 7.

Population n= number of individuals	Kirkeporten n=44	Storsandnes n=49	Tromsø n=50	Breivika n=47	Seines n=47
Mean (Standard deviation)	128.4 (8.79)	129.8 (5.96)	123.5 (7.68)	144.6 (9.06)	150.8 (5.33)

Table 12. P-values of pairwise t-tests for mean shell spiral angle. Statistically significant differences between populations are highlighted in bold considering an α of 0.05 and a Bonferroni correction for multiple tests. Population colours are the same as in Figure 7.

Spiral Angle	Kirkeporten	Storsandnes	Tromsø	Breivika
Storsandnes	1.000	-	-	-
Tromsø	**0.027**	**< 0.001**	-	-
Breivika	**< 0.001**	**< 0.001**	**< 0.001**	-
Seines	**< 0.001**	**< 0.001**	**< 0.001**	**0.002**

- Shell strength

Shell strength varied in a very similar way to thickness. However, while the highest mean was observed in Seines (522.9 N) for both traits, the weakest shells are from Kirkeporten (198.5 N) (Figure 18). Additionally, mean shell strength is significantly higher in the Southern populations (Breivika and Seines) when compared to the three other populations located further north (Kirkeporten, Storsandnes and Tromsø) (Figure 18, Table 13). Within the northernmost group, no significant pairwise differences in shell strength were found (Table 14). This was not the case in the southern populations where Seines showed significantly stronger shells on average than those in Breivika (Table 10). As for wet weight, the widest range of values was observed in the southernmost population (Seines: 527 N), whereas the smallest range was observed in northernmost population (Kirkeporten: 182 N) (Figure 18).

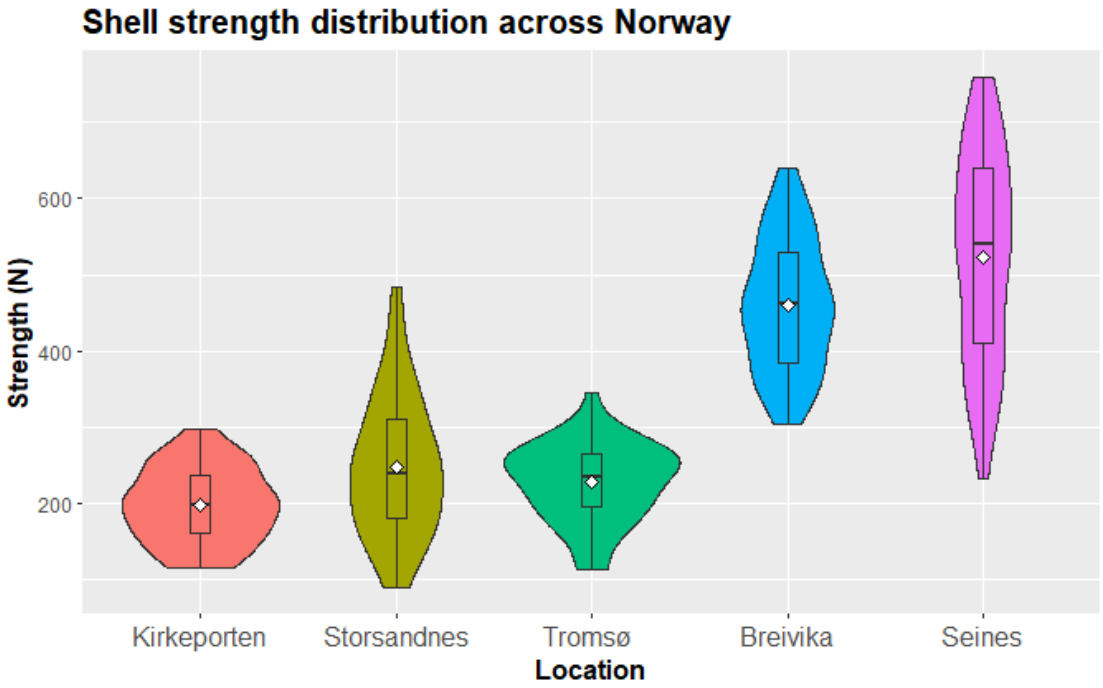

Figure 18. Violin plots of the *L. obtusata* strength distribution for each sampling location ordered from north to south. Box plots are also presented in the middle of the violin plots with average values displayed in white and outliers in black. Population colours are the same as in Figure 7.

Table 13. Summary statistics (sample size, mean and standard deviation) for the strength (in Newtons - N) per population. Population colours are the same as in Figure 7.

Population n= number of individuals	Kirkeporten n=44	Storsandnes n=49	Tromsø n=50	Breivika n=47	Seines n=47
Mean (Standard deviation)	198.5 (48.41)	248.1 (90.48)	228.6 (51.39)	459.7 (85.55)	522.9 (135.93)

Table 14. P-values of pairwise t-tests for mean shell strength. Statistically significant differences between populations are highlighted in bold considering an α of 0.05 and a Bonferroni correction for multiple tests. Population colours are the same as in Figure 7.

Strength	Kirkeporten	Storsandnes	Tromsø	Breivika
Storsandnes	0.071	-	-	-
Tromsø	1.000	1.000	-	-
Breivika	**< 0.001**	**< 0.001**	**< 0.001**	-
Seines	**< 0.001**	**< 0.001**	**< 0.001**	**0.007**

- Shell shape

The first two principal components explain 39.6% and 25.7% of the variance in shell shape, respectively. However, the shells from different populations largely overlap, with the exception of some individual outliers (Figure 19). Despite some overlap, shells from Kirkeporten are more abundant in the upper half of PC2 values, whereas those from Seines in the lower half of the PC2 axis.

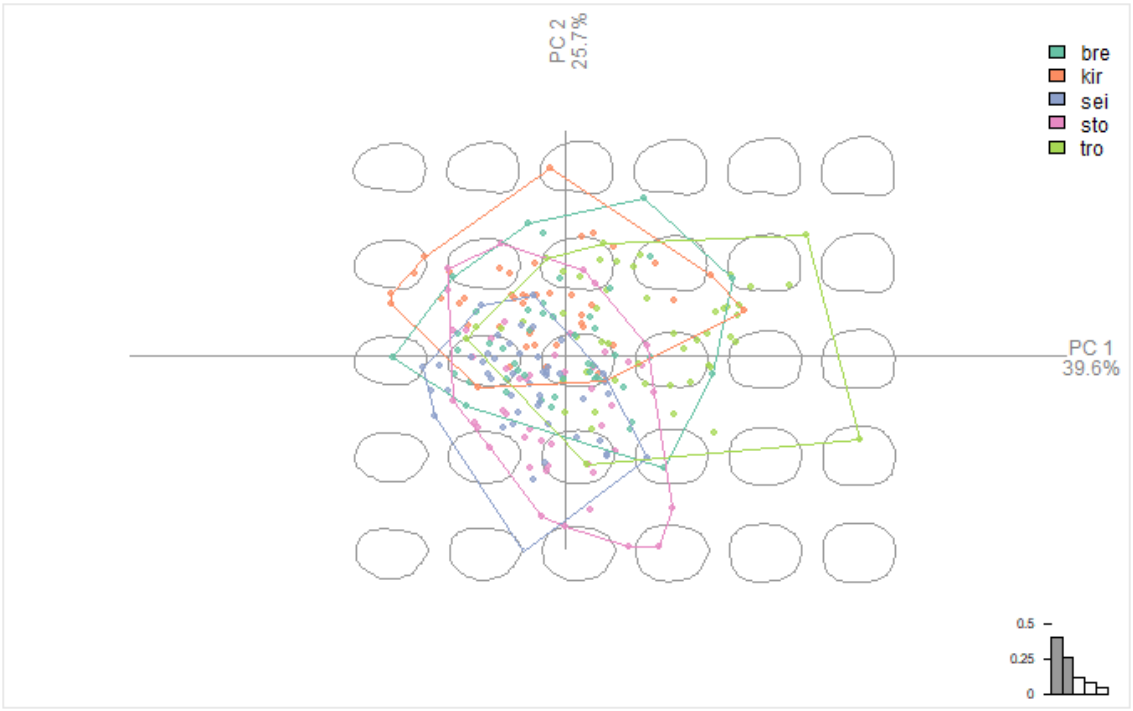

Figure 19. Principal component analysis (PCA) analysis results regarding the shell shape differences between individuals. Individuals from each population have the same colour and are grouped by polygons.

- Combined analysis of all traits

The first two principal components for all the phenotypic traits combined explained 58.2% and 22.9% of the variance (Figure 20). PC1 shows a clear separation between the two southernmost (on the right) and the three northernmost populations (on the left), although shells from Tromsø have a more central position. Seines and Tromsø tend to be positioned in the opposite sides of the PC2 axis.

Whereas weight is the variable that most contributes to the PC1, followed by strength and thickness, variation across the PC2 axis is more influenced by the ratio between the spiral and total height, as well as the spiral angle.

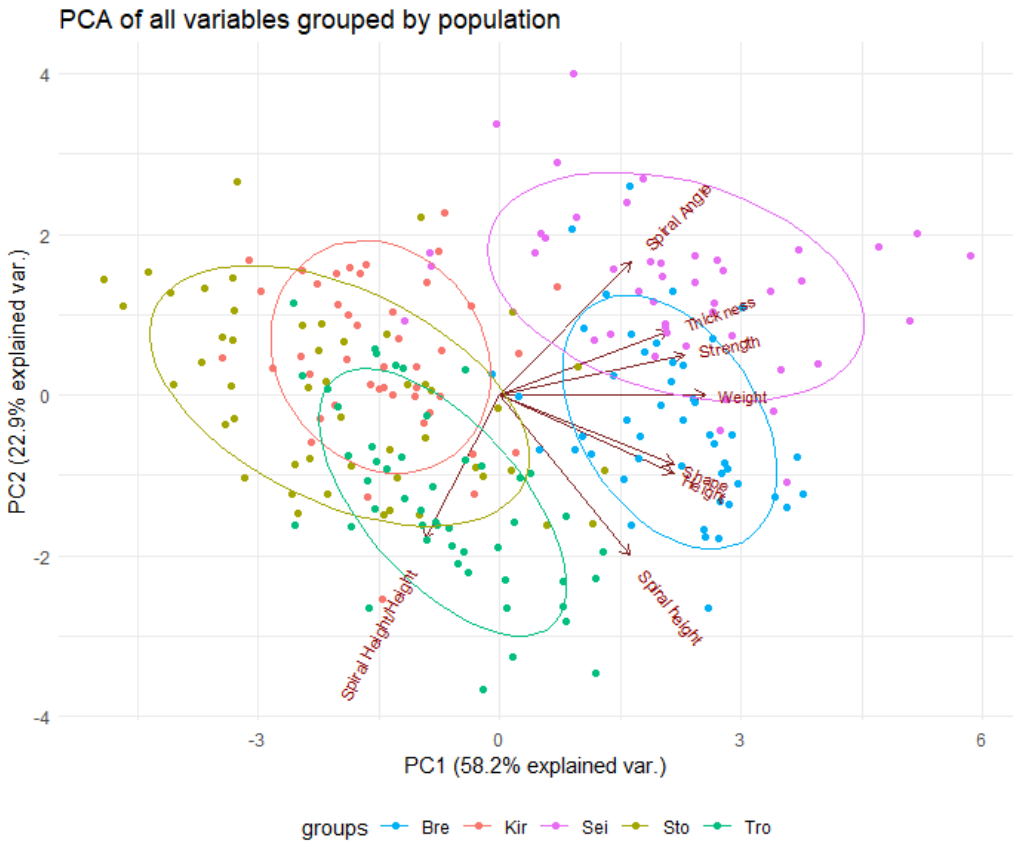

Figure 20. Principal component analysis (PCA) analysis regarding the variation of the phenotypic traits between individuals. Eigenvectors (red arrows) are presented showing the direction of each phenotypic traits in the parameter space. Individuals from each population have the same colour and are grouped by ellipses (95% confidence). Population colours are the same as in Figure 7.

- Correlation between phenotypic traits

Kirkeporten was the location with the largest number of non-significant correlations, with 12 pairs of traits out of 28 (Figures 21 to 25), although this number was similar in the other locations. In contrast, Storsandnes was the population with the largest values of correlation coefficients, presenting values as high as 0.96 between weight and both shell height and shape, and also 0.96 between shell shape and height (Figure 22).

Considering all locations, the phenotypic traits that showed the highest consistency of high correlation coefficients between them were weight and shell height, followed by spiral height and total height, and weight and shell shape (Figures 21 to 25). On the other end, the highest negative correlation coefficients between traits were found between spiral height/height ratio and spiral angle.

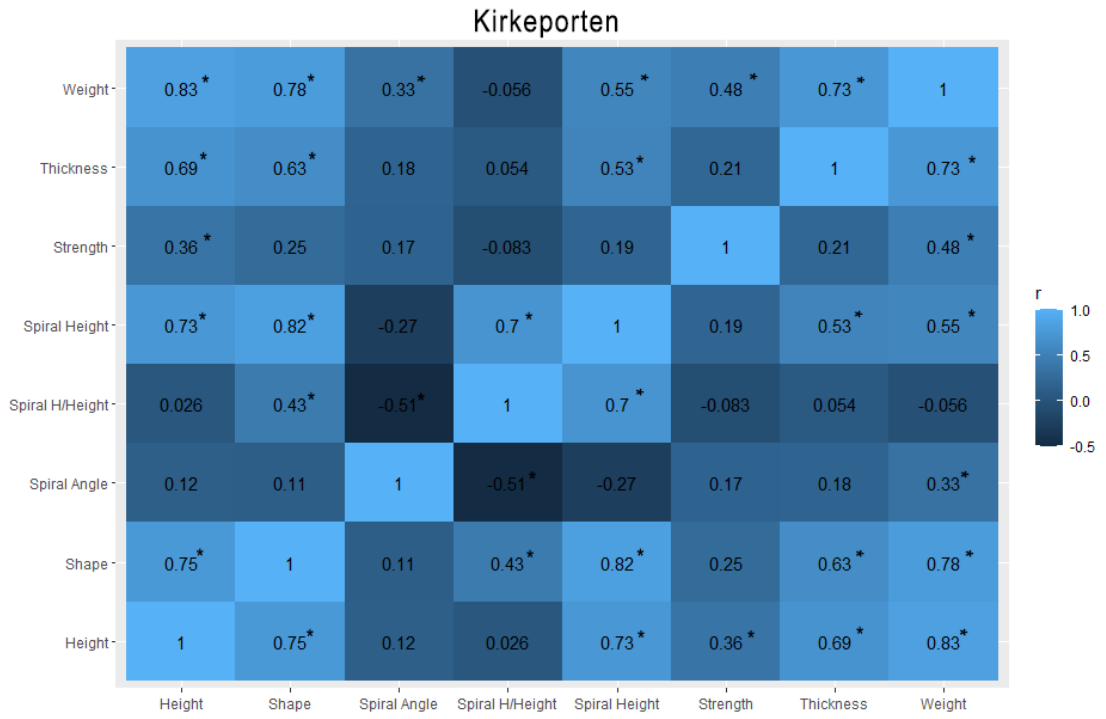

Figure 21. Correlation matrix with coefficients (r) for the measured phenotypic traits in the Kirkeporten population. Statistically significant correlations between traits are indicated by asterisks considering an α of 0.05.

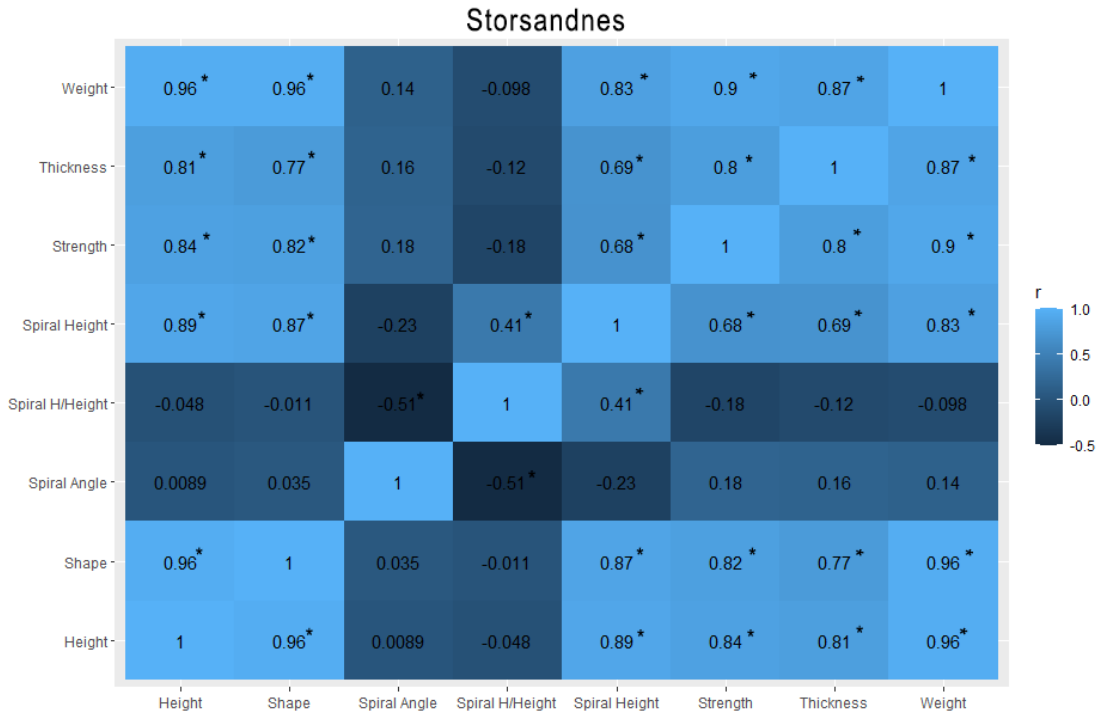

Figure 22. Correlation matrix with coefficients (r) for the measured phenotypic traits in the Storsandnes population. Statistically significant correlations between traits are indicated by asterisks considering an α of 0.05.

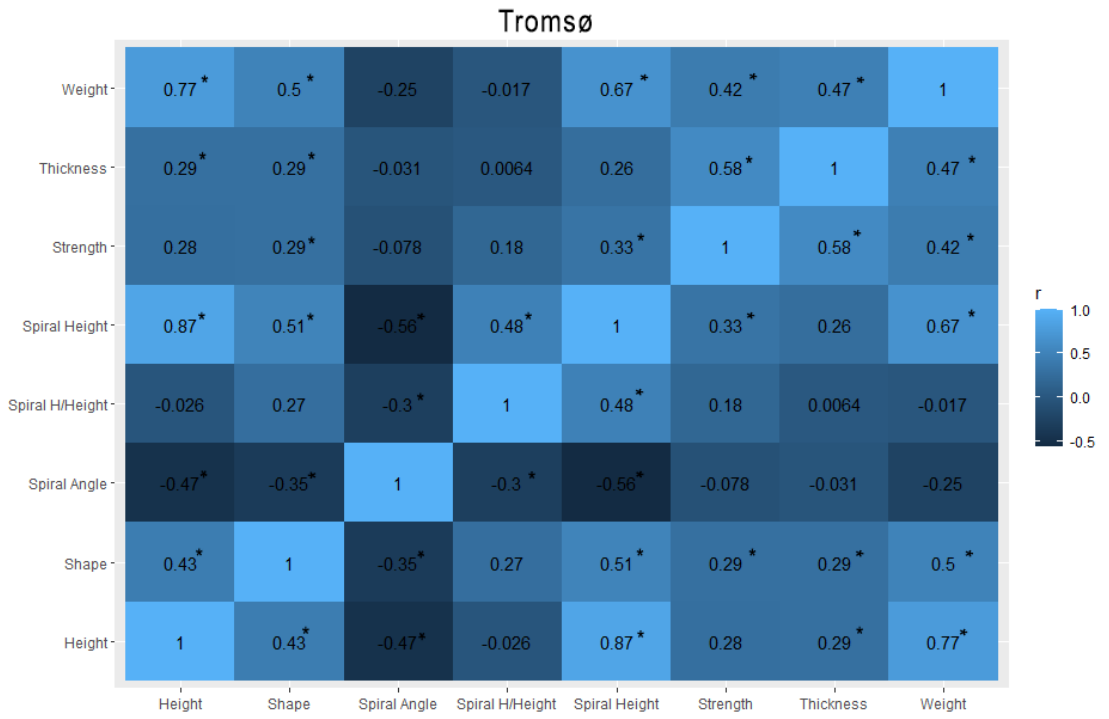

Figure 23. Correlation matrix with coefficients (r) for the measured phenotypic traits in the Tromsø population. Statistically significant correlations between traits are indicated by asterisks considering an α of 0.05.

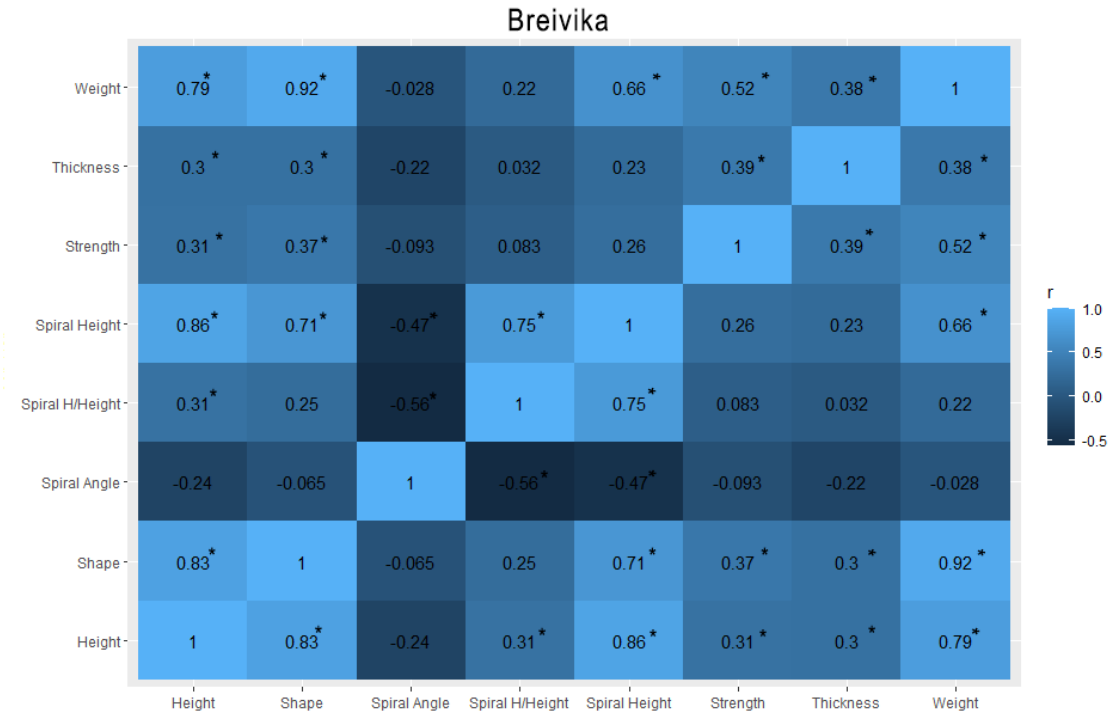

Figure 24. Correlation matrix with coefficients (r) for the measured phenotypic traits in the Breivika population. Statistically significant correlations between traits are indicated by asterisks considering an α of 0.05.

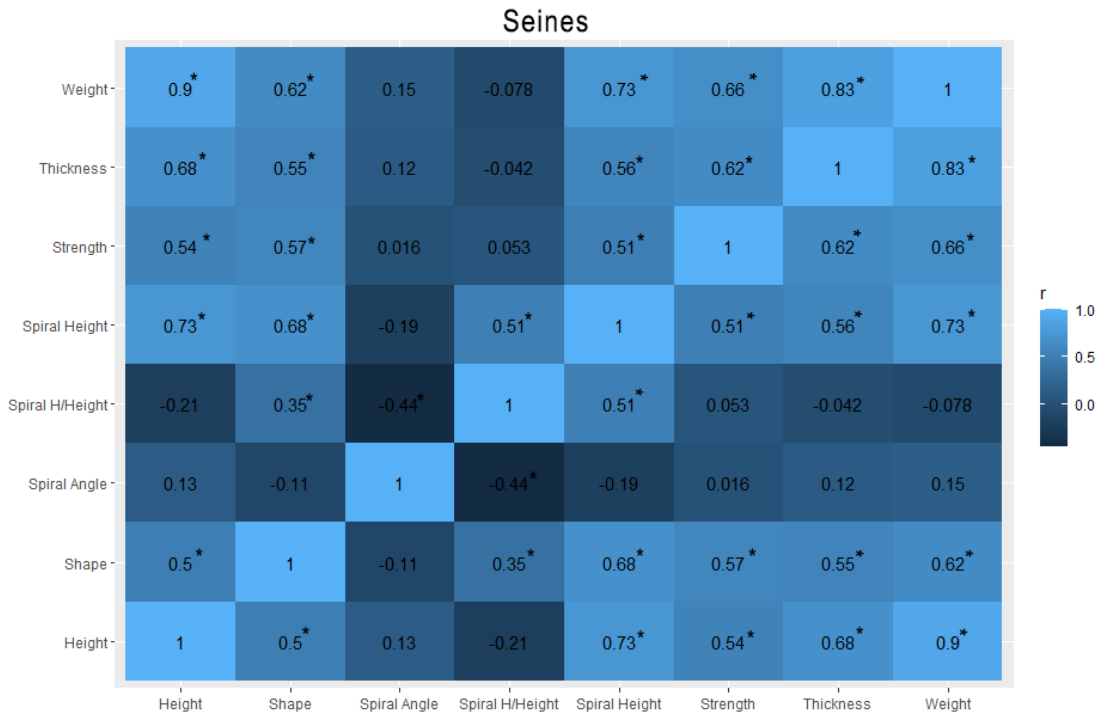

Figure 25. Correlation matrix with coefficients (r) for the measured phenotypic traits in the Seines population. Statistically significant correlations between traits are indicated by asterisks considering an α of 0.05.

3.2. Environmental variables

- Salinity

The variation of sea salinity during the years of 2017 to 2021 reveals lower salinity during the summer, and higher salinity during winter (Figures 26 and 27). This pattern is more evident in the southern locations, mainly in Seines (Figure 26) where the standard deviation is higher (1.32) (Table 15). A tendency for an overall increase in the maximum and minimum annual salinity during the time frame considered was observed in the northern locations (Kirkeporten and Tromsø) (Figure 27, Supplementary Figure 6).

Salinity increases from north to south (mainly during winter), the only exception being in Tromsø (mean salinity of 35.6 PSU), which presents higher salinity than Breivika (mean of 35.2 PSU) (Figure 27 and Table 15). Kirkeporten and Storsandnes, the two northernmost locations display almost identical salinity and variations, with standard deviations of 0.45 and 0.43 PSU, respectively (Supplementary Figure 6). In the other locations, higher salinity (and fluctuations) is observed, with Seines overall showing higher salinity (mean of 36.1 PSU) and higher amplitudes (6 PSU) (Table 15), which is particularly evident between the colder and hotter months (Figures 26 and 27).

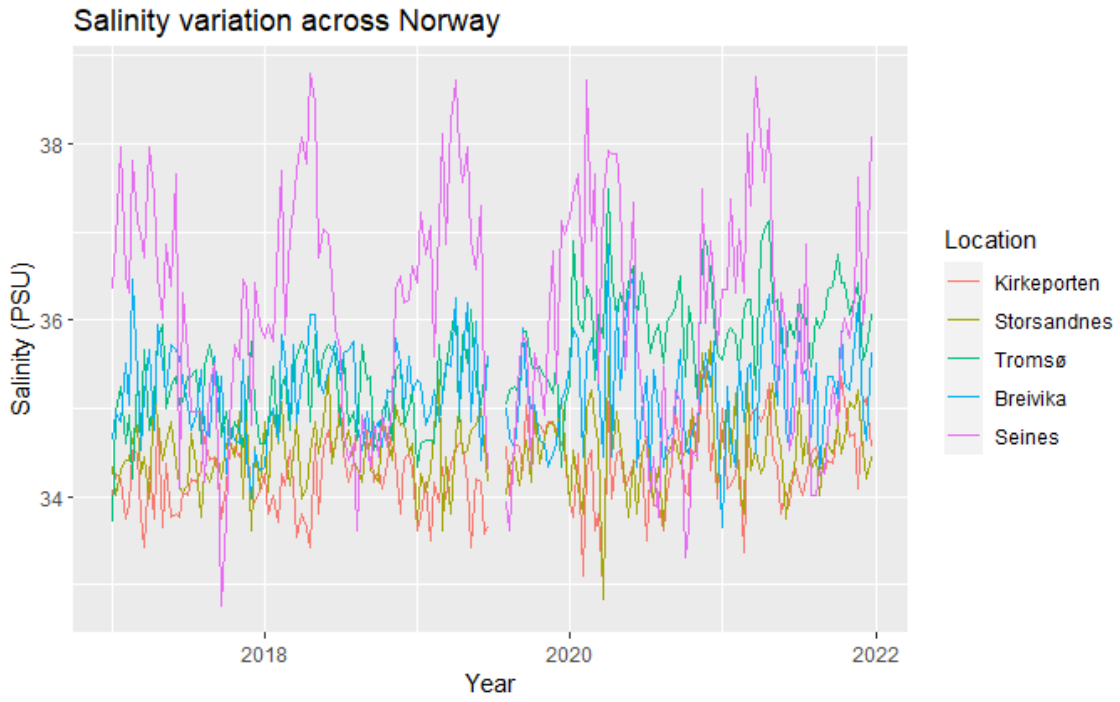

Figure 26. Combined line charts of sea salinity variation (PSU) for each sampling location between 2017 and 2021.

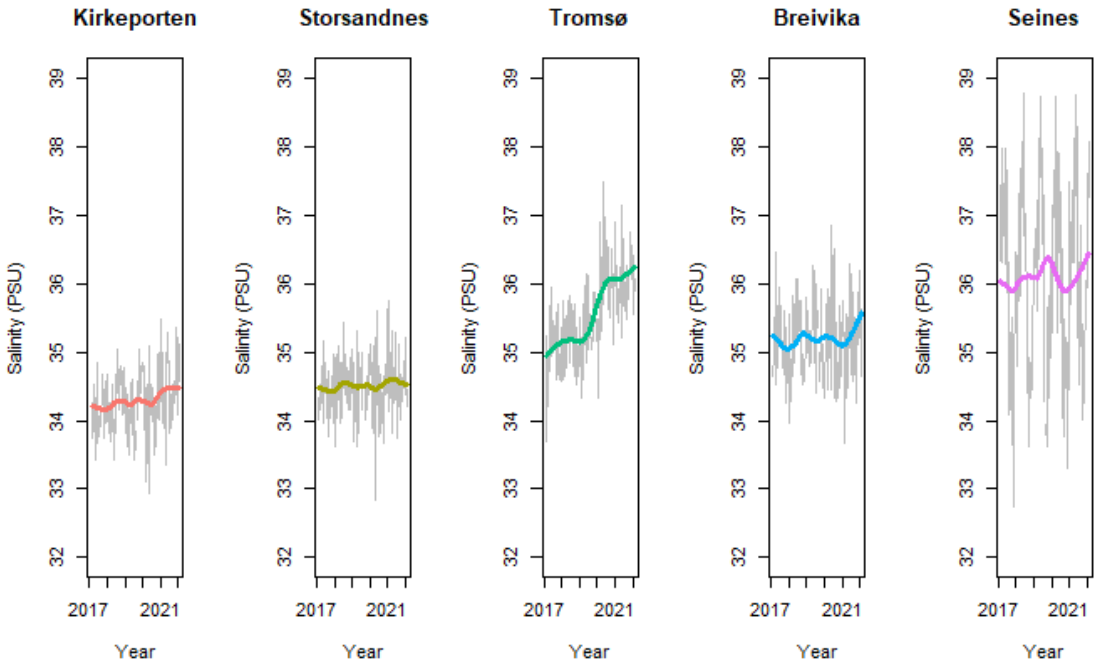

Figure 27. Charts of sea salinity variation (PSU) with overlayed trend in each sampling location, ordered from North to South, between 2017 and 2021. Trend lines, obtained from STL decomposition (Appendix 3), colored for each location the same way as in Figure 7.

Table 15. Summary statistics (maximum, minimum, average, median and standard deviation) for the sea salinity data (in Practical Salinity Unit - PSU), collected between 2017 and 2021, per population. Population colours are the same as in Figure 7.

Salinity	Kirkeporten	Storsandnes	Tromsø	Breivika	Seines
Minimum	32.9	32.8	33.7	33.7	32.8
Maximum	35.5	35.8	37.5	36.9	38.8
Mean	34.3	34.5	35.6	35.2	36.1
Median	34.3	34.5	35.5	35.2	36.3
Standard deviation	0.45	0.43	0.65	0.55	1.32

- Sea surface temperature

Sea surface temperature variation along seasons shows the opposite pattern in comparison to salinity, with higher temperatures during summer and lower during winter (Figures 28 and 29). Greater temperature amplitude between seasons is observed in Breivika and Seines, with Kirkeporten showing the lowest amplitude of sea temperature between seasons (overall amplitude of 8.5 ºC). An increasing trend in the annual minimum sea surface temperature over the five years here analysed was observed in Storsandnes, Tromsø, and in Kirkeporten to a lesser extent, although the overall trend is relatively stable (Figure 29, Supplementary Figure 10).

The southernmost locations (Seines and Breivika) present sea surface temperature variations with similar curve patterns (standard deviations of 3.08 and 3.23 ºC, respectively) and ranges (overall amplitudes of 11.6 and 12 ºC, respectively), although with slightly lower temperatures in Breivika (mean of 7.7 ºC). Tromsø and Storsandnes also present similar curve patterns (standard deviations of 2.87 and 3.03 ºC, respectively) and ranges (12.1 and 12.6 ºC, respectively) between them (Table 16, Supplementary Figure 7). A general trend of increasing mean sea surface temperatures is observed towards the south, as expected (Figure 29 and Table 16). Although Kirkeporten presents a higher mean sea surface temperature than Storsandnes and Tromsø (Table 16).

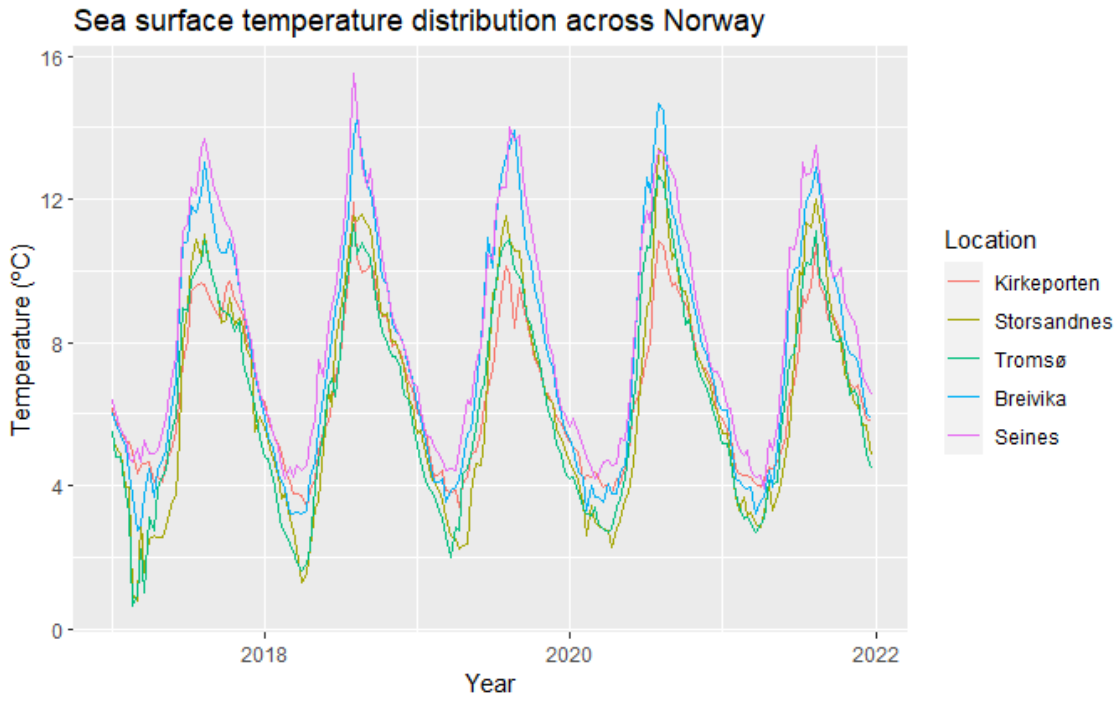

Figure 28. Combined line charts of the sea surface temperature variation (°C) for each sampling location between 2017 and 2021.

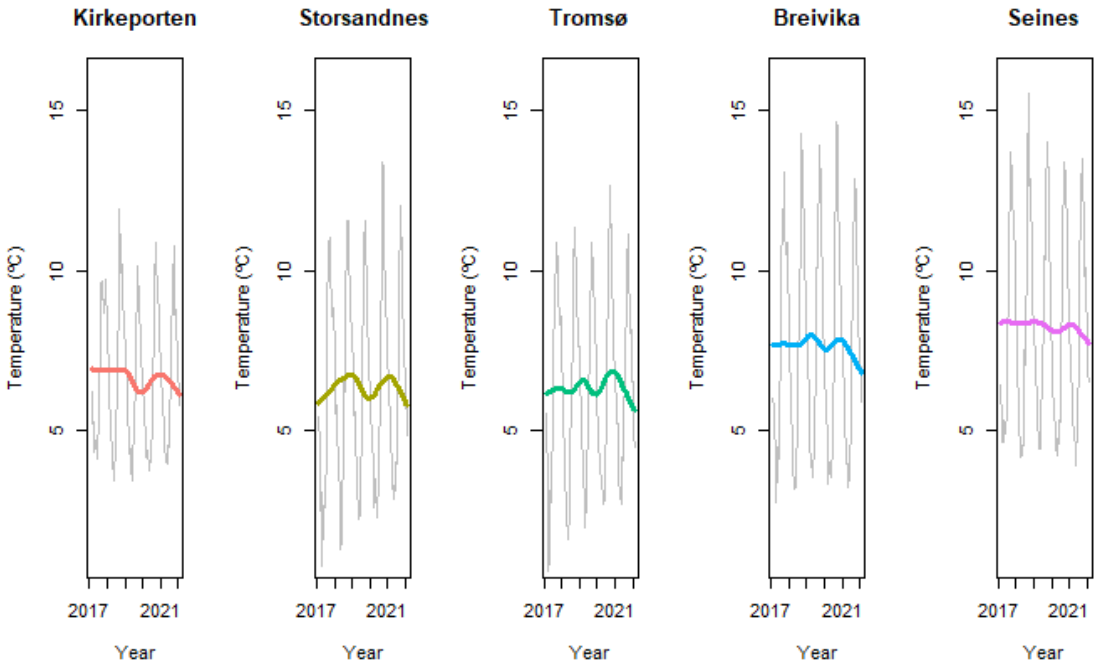

Figure 29. Charts of the sea surface temperature variation (°C) with overlayed trend for each sampling location separately, ordered from North to South, between 2017 and 2021. Trend lines, obtained from STL decomposition (Appendix 3), colored for each location the same way as in Figure 7.

Table 16. Summary statistics (maximum, minimum, average, median and standard deviation) for the sea surface temperature data (in degrees Celsius - ºC), collected between 2017 and 2021, per population. Population colours are the same as in Figure 7.

Sea surface temperature	Kirkeporten	Storsandnes	Tromsø	Breivika	Seines
Minimum	3.4	0.8	0.6	2.7	3,9
Maximum	11.9	13.4	12.7	14.7	15,5
Mean	6.7	6.4	6.4	7.7	8.3
Median	6.3	5.8	6.4	7.4	7.8
Standard deviation	2.11	3.03	2.87	3.23	3.08

- Air temperature

As expected, air temperature presents a similar variation across season as the sea surface temperature (Figures 30 and 31). A clear trend of increasing air temperatures across the five years of study was observed in Kirkeporten, Tromsø and Seines (Figure 31, Supplementary Figure 8).

Differences in air temperature variation among locations is not so obvious as observed for sea surface temperature, with Storsandnes, Tromsø and Breivika showing similar patterns of higher amplitudes (43, 40.1 and 37.7 ºC, respectively), with also similar standard deviations (Figure 31 and Table 17). As for sea temperature, Kirkeporten presents the smallest overall amplitude (31.3 ºC) and Seines presents the highest mean temperature (2.9 ºC) (Table 17).

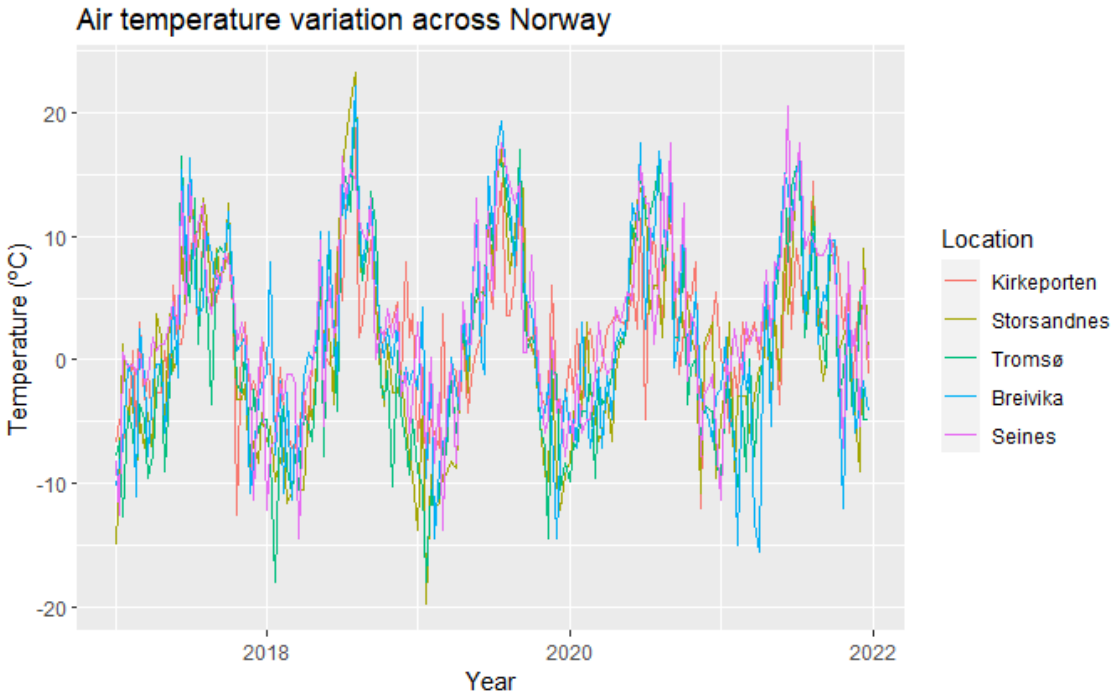

Figure 30. Combined line charts of the air temperature variation (°C) for each sampling location between 2017 and 2021.

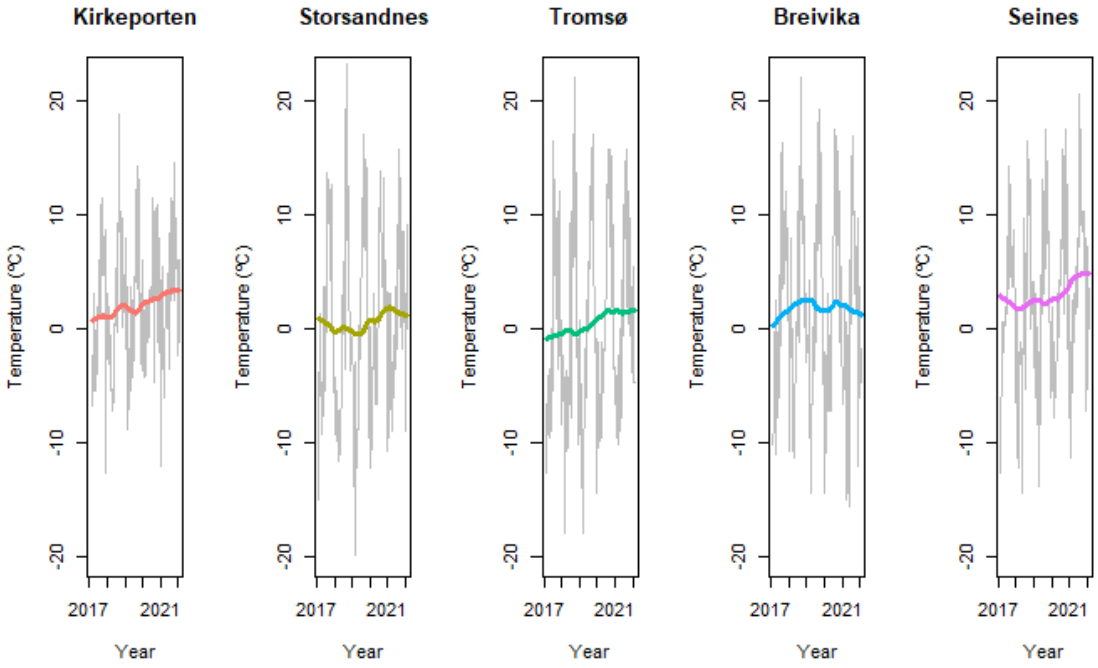

Figure 31. Charts of the air temperature variation (°C) for each sampling location separately, ordered from North to South, between 2017 and 2021. Trend lines, obtained from STL decomposition (Appendix 3), colored for each location the same way as in Figure 7.

Table 17. Summary statistics (maximum, minimum, average, median and standard deviation) for the air temperature data (in degrees Celsius - ºC), collected between 2017 and 2021, per population. Population colours are the same as in Figure 7.

Air temperature	Kirkeporten	Storsandnes	Tromsø	Breivika	Seines
Minimum	-12.6	-19.8	-18.0	-15.6	-14.4
Maximum	18.7	23.2	22.1	22.1	20.5
Mean	2.0	0.6	0.5	1.8	2.9
Median	2.5	0.2	0.5	0.4	2.2
Standard deviation	5.38	7.94	8.17	7.84	7.04

- Crab occurrence/presence

The presence of *C. maenas* crabs was reported across the geographical range from the Seines to Storsandnes area, with a decreasing trend towards north, as expected (Figure 32, Table 18). However, when we consider only the reports near our sampling sites, crabs seem absent from the two northernmost locations, Storsandnes and Kirkporten (Table 18). The single exception to this overall trend is observed near Tromsø, perhaps due to an observation bias related with a higher human population density in one of the largest cities in northern Norway (Figure 32). In general, these reports are concordant with the presence of crabs observed during sampling, with Tromsø being the only exception (Table 18).

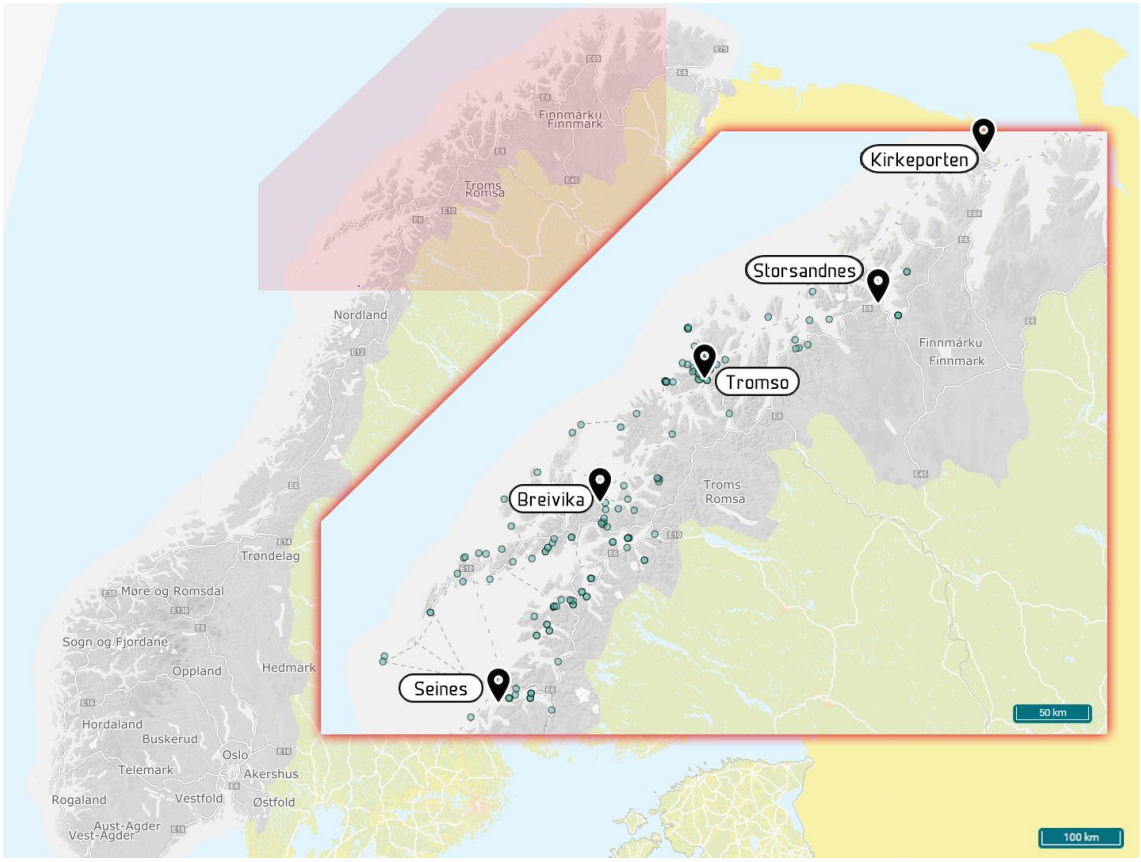

Figure 32. Geographical occurrence of the crab *C. maenas* (dark green circles) around sampling regions (black pinpoint markers) in Norway from 2017 until 2021. (Source: Norwegian Biodiversity Information Centre).

Table 18. Information regarding *C. maenas* presence (1) or absence (0) in each sampling location. Data obtained from occurrences reported in the Norwegian Biodiversity Information Center and direct observations recorded by researchers during sampling.

Location	Norwegian Biodiversity Information Centre	Direct observations during sampling
Kirkeporten	0	0
Storsandnes	0	0
Tromsø	1	0
Breivika	1	1
Seines	1	1

3.3. Relation between phenotypic traits and environmental variables

The linear regression models used to fit the collected phenotypic and environmental data exhibited statistically significant slopes (p-value < 0.05) in all cases, with the solely exception of spiral height and air temperature. Plots from which the linear models were obtained are shown in figure 33, this being the specific example for the shell strength trait with the three environmental variables used.

The standardized slope reflects the impact that an increase of one standard deviation in the mean of the environmental variables has on the respective phenotypic trait, also in terms of standard deviations. For the weight, thickness, spiral angle, strength and shape traits, sea surface temperature was the environmental variable that presented the largest effects, with overall high standardized slopes of 0.78, 0.74, 0.79, 0.80 and 0.50, respectively (Tables 19, 20, 24, 25 and 26). The phenotypic traits of height, spiral height and spiral height/height ratio were the only ones in which the largest effect is induced by sea salinity, with standardized coefficients of 0.55, 0.37 and -0.29, respectively (Tables 21, 22 and 23).

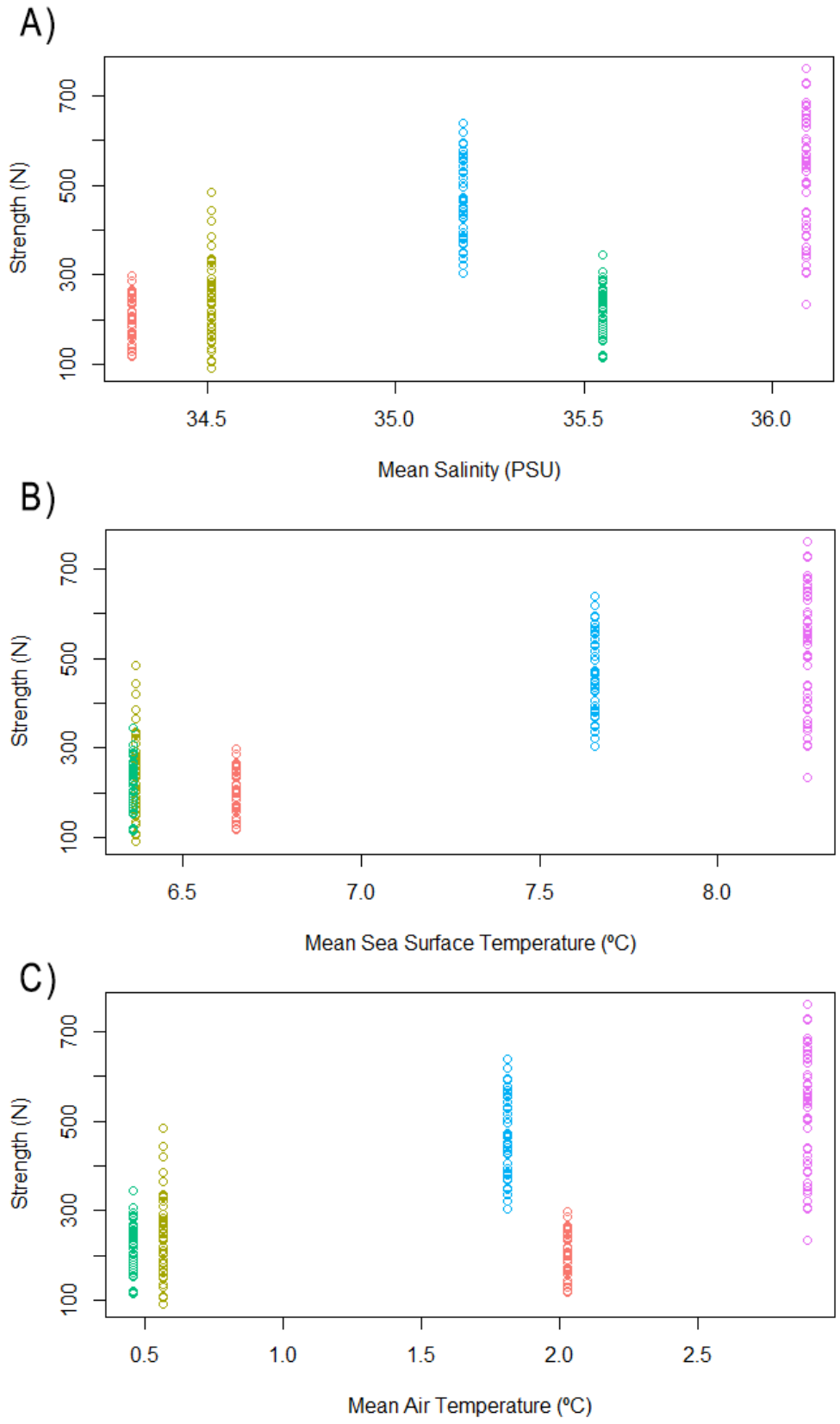

Figure 33. Dot plots demonstrating the variation of the shell strength (N) according to the different mean values of sea salinity (A), sea surface temperature (B) and air temperature (C) verified across the sampling locations which are colored in the same way as in Figure 7.

Table 19. Summary coefficients of intercept, slope, and standardized slope for the environmental variables of sea salinity, sea surface temperature and air temperature, according to the weight values across all sampling locations. The standardized slope of the environmental variable that has a greater effect on weight is highlighted in bold.

Weight						
Linear model	Salinity		Sea surface temperature		Air temperature	
	Estimate	P-value	Estimate	P-value	Estimate	P-value
Intercept	-9677.05	<0.001	1452.80	<0.001	618.55	<0.001
Slope	312.19	<0.001	337.97	<0.001	203.69	<0.001
Standardized Slope	0.60	-	**0.78**	-	0.57	-

Table 20. Summary coefficients of intercept, slope, and standardized slope for the environmental variables of sea salinity, sea surface temperature and air temperature, according to the thickness values across all sampling locations. The standardized slope of the environmental variable that has a greater effect on thickness is highlighted in bold.

Thickness						
Linear model	Salinity		Sea surface temperature		Air temperature	
	Estimate	P-value	Estimate	P-value	Estimate	P-value
Intercept	-4.10	<0.001	-0.72	<0.001	0.52	<0.001
Slope	0.14	<0.001	0.21	<0.001	0.15	<0.001
Standardized Slope	0.42	-	**0.74**	-	0.66	-

Table 21. Summary coefficients of intercept, slope, and standardized slope for the environmental variables of sea salinity, sea surface temperature and air temperature, according to the height values across all sampling locations. The standardized slope of the environmental variable that has a greater effect on height is highlighted in bold.

Height						
Linear model	Salinity		Sea surface temperature		Air temperature	
	Estimate	P-value	Estimate	P-value	Estimate	P-value
Intercept	-27.29	<0.001	6.95	<0.001	11.94	<0.001
Slope	1.13	<0.001	0.79	<0.001	0.38	<0.001
Standardized Slope	**0.55**	-	0.45	-	0.26	-

Table 22. Summary coefficients of intercept, slope, and standardized slope for the environmental variables of sea salinity, sea surface temperature and air temperature, according to the spiral height values across all sampling locations. The standardized slope of the environmental variable that has a greater effect on spiral height is highlighted in bold.

Spiral Height						
Linear model	Salinity		Sea surface temperature		Air temperature	
	Estimate	P-value	Estimate	P-value	Estimate	P-value
Intercept	-11.53	<0.001	7.72	<0.001	9.50	<0.001
Slope	0.60	<0.001	0.24	<0.001	-0.07	0.335
Standardized Slope	**0.37**	-	0.17	-	-0.06	-

Table 23. Summary coefficients of intercept, slope, and standardized slope for the environmental variables of sea salinity, sea surface temperature and air temperature, according to the shell spiral height/shell height ratio values across all sampling locations. The standardized slope of the environmental variable that has a greater effect on spiral height is highlighted in bold.

Spiral Height/Height Ratio						
Linear model	Salinity		Sea surface temperature		Air temperature	
	Estimate	P-value	Estimate	P-value	Estimate	P-value
Intercept	1.49	<0.001	0.96	<0.001	0.80	<0.001
Slope	-0.02	<0.001	-0.03	<0.001	-0.03	<0.001
Standardized Slope	**-0.29**	-	-0.47	-	-0.58	-

Table 24. Summary coefficients of intercept, slope, and standardized slope for the environmental variables of sea salinity, sea surface temperature and air temperature, according to the spiral angle values across all sampling locations. The standardized slope of the environmental variable that has a greater effect on spiral height is highlighted in bold.

Spiral Angle						
Linear model	Salinity		Sea surface temperature		Air temperature	
	Estimate	P-value	Estimate	P-value	Estimate	P-value
Intercept	-173.59	<0.001	41.18	<0.001	121.52	<0.001
Slope	8.79	<0.001	13.36	<0.001	9.05	<0.001
Standardized Slope	0.44	-	**0.79**	-	0.65	-

Table 25. Summary coefficients of intercept, slope, and standardized slope for the environmental variables of sea salinity, sea surface temperature and air temperature, according to the spiral height values across all sampling locations. The standardized slope of the environmental variable that has a greater effect on spiral height is highlighted in bold.

Strength						
Linear model	Salinity		Sea surface temperature		Air temperature	
	Estimate	P-value	Estimate	P-value	Estimate	P-value
Intercept	-4562.24	<0.001	-845.71	<0.001	179.42	<0.001
Slope	139.27	<0.001	166.99	<0.001	99.21	<0.001
Standardized Slope	0.58	-	**0.80**	-	0.58	-

Table 26. Summary coefficients of intercept, slope, and standardized slope for the environmental variables of sea salinity, sea surface temperature and air temperature, according to the shape values across all sampling locations. The standardized slope of the environmental variable that has a greater effect on shape is highlighted in bold.

Shape						
Linear model	Salinity		Sea surface temperature		Air temperature	
	Estimate	P-value	Estimate	P-value	Estimate	P-value
Intercept	-11.17	<0.001	2.85	<0.001	5.98	<0.001
Slope	0.50	<0.001	0.50	<0.001	0.27	<0.001
Standardized Slope	0.43	-	**0.50**	-	0.32	-

3.4. Genetic basis of shell strength

Pool 1 is formed by the set of individuals from the Breivika population where the lowest values of strength were recorded, while pool 2 is composed by the individuals that presented the highest strength values in this population.

Although the two pools were prepared using the same protocol, more data (number of reads) was obtained for Pool 1, which contains the individuals from Breivika with lower shell strength. Although we targeted a coverage of at least 34x, the real coverage was lower, with 26.78x and 21.36x for the first pool and second pool, respectively (Table 27). The percentage of mapping reads is high (>98%), although the percentage of correctly

paired reads is much lower, being slightly higher for the second pool (~63% vs 65% for the first and second pool, respectively).

Pool 1 presents a mean nucleotide diversity of 0.0071, which is higher than that in pool 2 (mean π= 0.0060) (Figure 34). In contrast, Tajima's D is very similar among the two pools (mean Tajima's D= -0.8729 and -0.8399 for Pool 1 and Pool 2, respectively), and in both pools the distribution is mainly composed by native values (Figure 35). Theta (θ) mean values for both pools are also very similar and similarly to the previous values, the pool 1 presents a slightly higher mean (mean θ = 0.0094) than pool 2 (mean θ = 0.0088) (Figure 36).

Table 27. Descriptive summary of the data mapping quality in Pool 1 and Pool 2. Information regarding the total number of reads, its average coverage, percentage of reads mapped to the reference genome and of properly reads are paired.

	Average coverage	Number of reads	Percentage of mapping reads	Percentage of properly paired reads
Pool 1	26.78	419544317	98.53%	62.68%
Pool 2	21.36	335997108	98.49%	65.00%

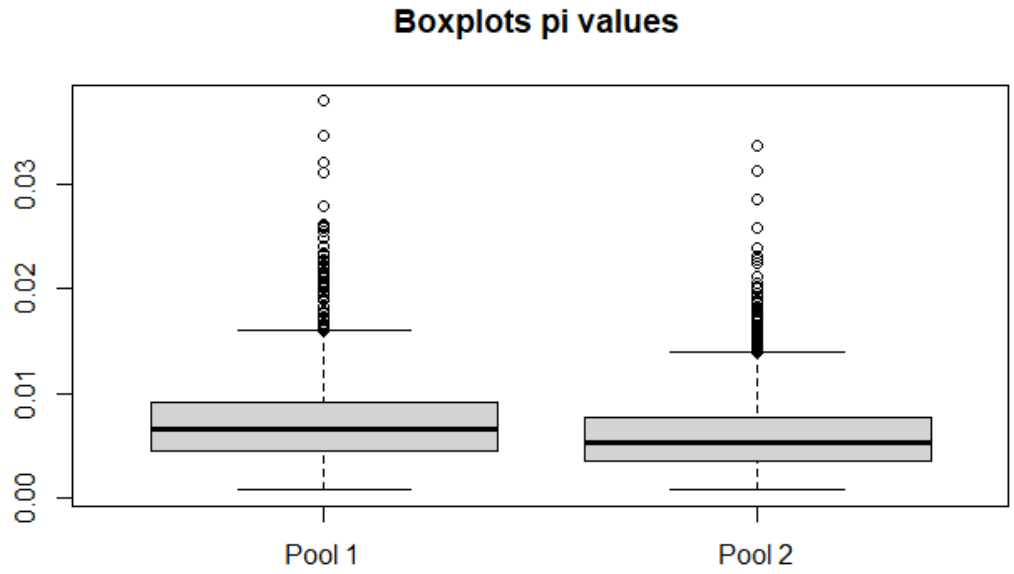

Figure 34. Boxplots of pairwise nucleotide diversity (pi) values obtained for Pool 1 (low shell strength) and Pool 2 (high shell strength) in Breivika.

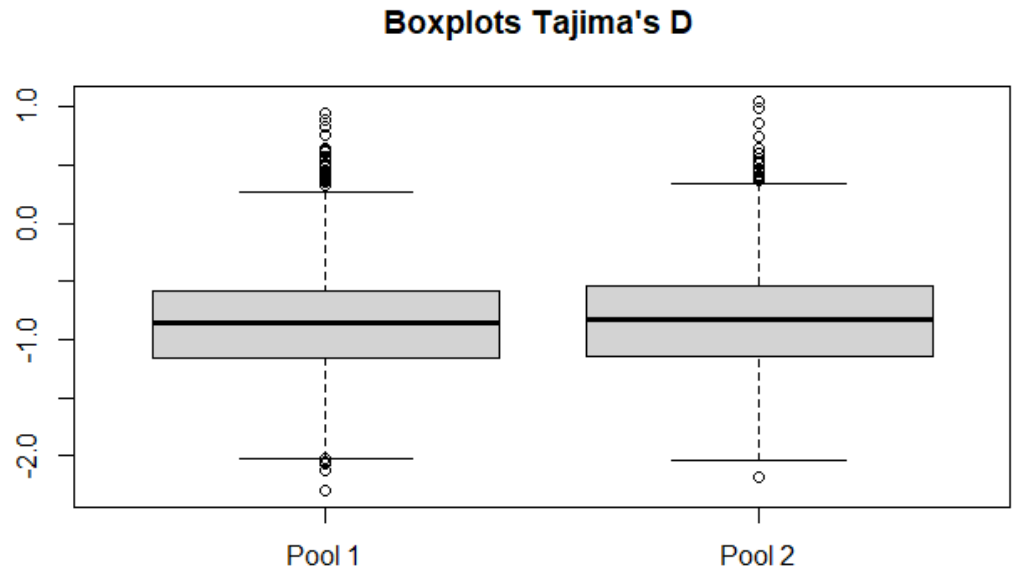

Figure 35. Boxplots of Tajima's D values obtained for Pool 1 (low shell strength) and Pool 2 (high shell strength) in Breivika.

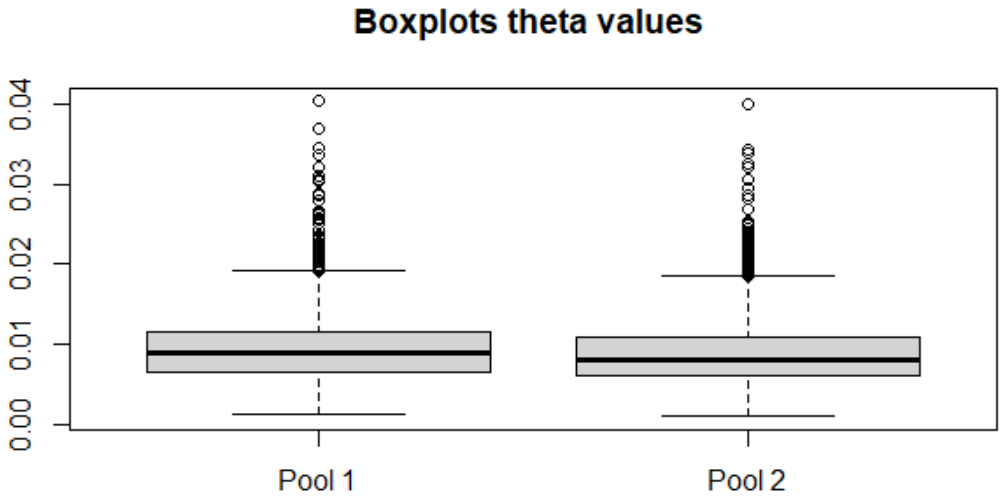

Figure 36. Boxplots of theta (θ) values obtained for Pool 1 (low shell strength) and Pool 2 (high shell strength) in Breivika.

Genetic differentiation measured as FST (fixation index) across the genome revealed a relatively low baseline across the genome (average FST= 0.036), as expected for two pools composed by individuals from a panmictic populations (Figure 37). Concordantly, the highest density of FST values is below 0.095 (99.5% quantile). Above this threshold (red line in Figure 37) several outlier windows can be observed, with the highest FST (~0.27) window located in chromosome 1. Although some of these outliers represent isolated windows (e.g., in chromosomes 1 and 2), which could represent artefacts, several outlier windows are clustered around the same position in other parts of the genome (e.g., chromosomes 6, 14 and 17) (Figure 37).

A zoom in of the distribution of FST across these three chromosomes shows one region with several windows of high FST in chromosome 6 (Figure 38A), at least two regions in chromosome 14 (Figure 38B) and at least one region in chromosome 17 (Figure 38C). Although further tests are needed, these comprise promising candidate regions to contain genetic variation associated to shell strength.

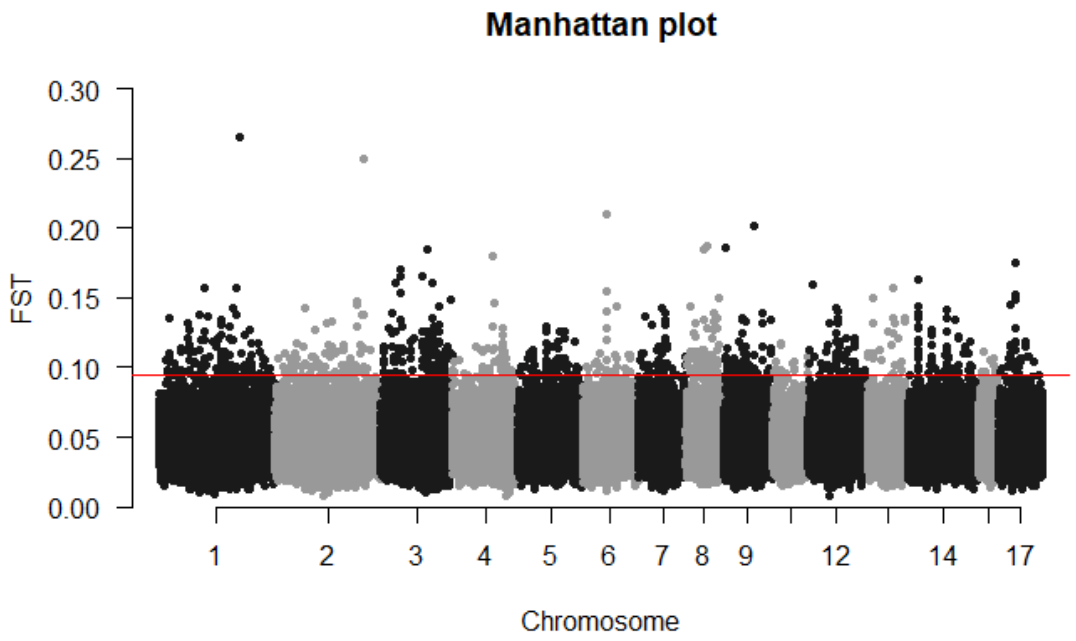

Figure 37. Manhattan plot of FST values between pools of low shell strength and high shell strength in the Breivika population across 17 linkage groups (reference genome of *L. saxatilis*). Percentile 99.5% (FST =0.095) is indicated by the red line. Dots represent average FST per windows of 10kb.

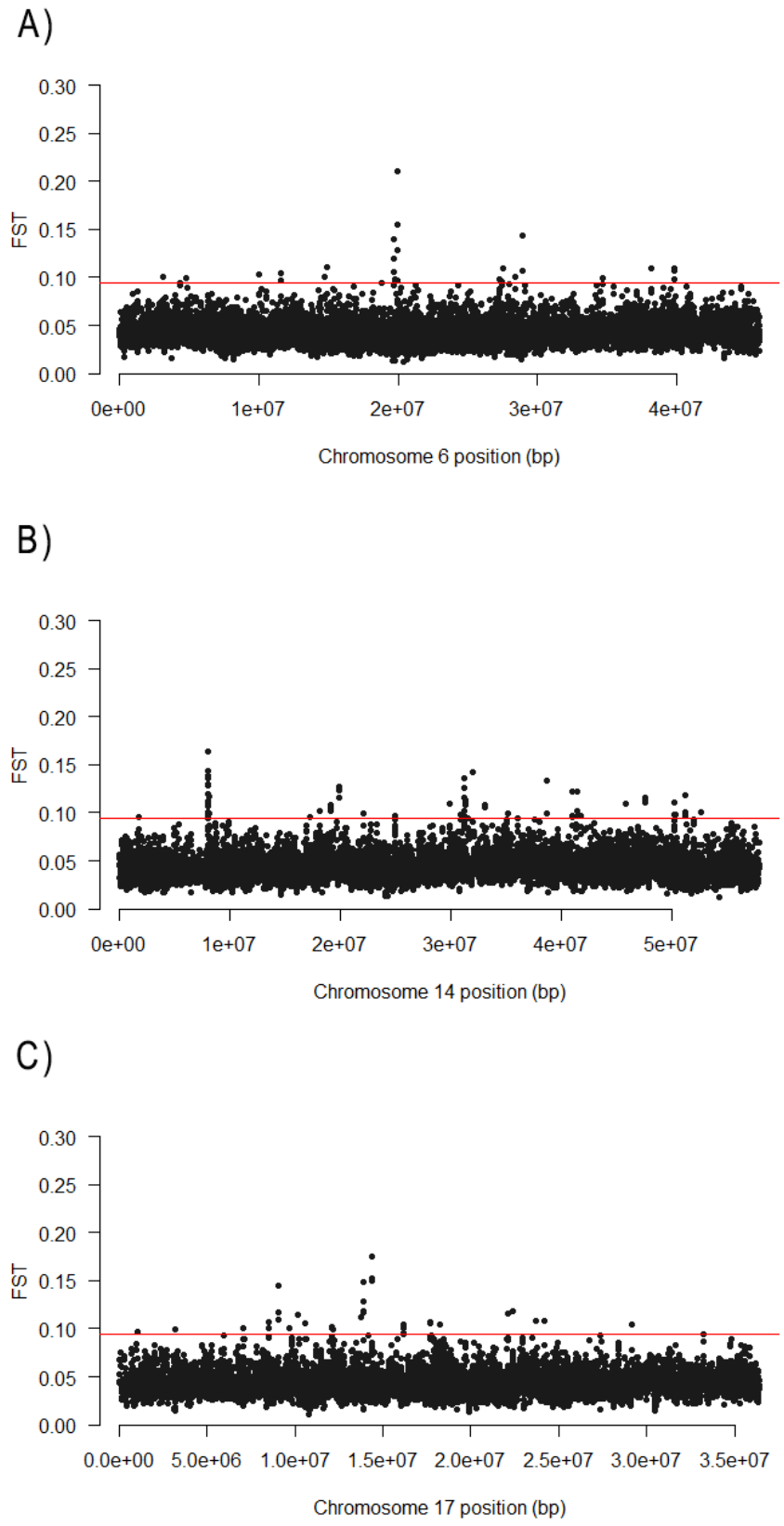

Figure 38. Distribution of FST between pools of low shell strength and high shell strength in Breivika along chromosomes 6 (A), 14 (B) and 17 (C) (using the genome of *L. saxatilis* as reference). Percentile 99% (FST =0.095) for the entire genome is indicated by the red line. Dots represent average FST per windows of 10kb.

4. Discussion

The first proposed objective of this work was to quantify the main phenotypic differences between populations across the environmental gradients at high latitudes encompassing the geographic region where the transition between *L. obtusata* varieties occur.

The results obtained across a latitudinal gradient in northern Norway (Seines, Breivika, Tromsø, Storsandnes and Kirkeporten) spanning the shift between *retusa* and *palliata* varieties of *L. obtusata* not only confirmed but added substantial information concerning how phenotypes, many of which were never characterized before, vary across this gradient.

The phenotypic traits that showed more differences between populations were shell thickness, shell spiral angle, total shell height, shell spiral height, weight, and strength, in that order. Shape differences were not so evident, and their patterns proved to be difficult to interpret, suggesting that shape does not vary with latitude. However, it is possible that our approach failed to capture existing shape variation within and between populations. Noise related with failure to remove individuals from other species (mainly females) could have also contributed for this result, but the trait distribution within each population suggests that this is unlikely. Future characterization of the shell shape, in particular of the aperture shape, using different approaches (e.g Larsson *et al.,* 2020) would be important to understand if these varies with latitude, as this has been suggested to be related with predation pressure (Reid 1996).

In general, the distribution of the phenotypic values showed differences between populations that varied with their latitude, with increased averages for all traits except spiral height/height ratio and shell shape towards the southernmost populations. Most of the differences for each of these phenotypes were always significant between the two southernmost (Seines and Breivika) and the two northernmost populations (Kirkeporten and Storsandnes).

For some phenotypic traits (weight, thickness, spiral angle and strength), Tromsø was more similar to the northernmost populations, while it was closer to the southernmost populations for shell height, spiral height and spiral height/height ratio. Interestingly, Breivika presents somehow an intermediate mean and distribution for thickness, spiral angle and strength between the southernmost population (Seines) the northernmost populations. Altogether, these patterns suggest that the region between Breivika and Tromsø could be a transition area between the two varieties and/or that these populations are exposed to somehow intermediate selective pressures.

The interpretation of the variation for individual traits is corroborated by the PCA analysis with all phenotypic traits, where a clear distinction between the more southerly populations (Seines and Breivika) and the two northernmost populations (Kirkeporten and Storsandnes) was observed. Although Tromsø individuals occupy a more intermediate position on the PC1 axis, they show a clear tendency to be placed closer to the northernmost populations, reinforcing the inconsistent clustering pattern of this with the other populations.

Some of the analysed traits are significantly and highly correlated, as shown by the positive correlation coefficients obtained for shell weight and total height, and shell total height and spiral height. Noteworthy, a significant negative correlation was found between shell spiral height/height ratio and spiral angle, showing that the higher the spiral angle, the lower the normalized spiral height (ratio) and the flatter the shells. Future work is needed to understand the causes of these associations, for instance, to test if they result from pleiotropy, epistasis, or any other causes.

Regardless, our results show that *L. obtusata* individuals are heavier (weight), overall larger (total height and spiral height), present shells with thicker walls, flatter (spiral height/height ratio and spiral angle), and that are more resistant to breakage (strength) towards the south of the studied range. In general, these patterns are in agreement with the varieties reported by Reid (1996), despite only based in spire height and shell thickness. Although Breivika (near Lofoten Islands, close to the previously described latitudinal shift between varieties (Reid, 1996)) is somehow intermediate for some traits, Tromsø does not always cluster with the same (northern or southern) populations for different traits. This could suggest that, regardless of the main selective pressures acting on this location, the transition zone could be larger and/or more northwards than previously thought.

Among the studied environmental parameters, salinity, and *C. maenas* occurrence are those where perturbations were observed in Tromsø, with an increase in salinity during the studied period and/or a more frequent occurrence of *L. obtusata*'s main predator. It is known that these crabs survive better at environments of higher sea temperature (minimum of 10 °C) and salinity (Young & Elliott, 2020). This suggests a shift in the *C. maenas* distribution towards north (even considering a possible observation bias in Tromsø), probably related with an increase of minimum temperature and salinity (but see below).

Importantly, to our knowledge, here we implemented the first genetic characterization of *L. obtusata* using whole genome data aiming to identify regions influencing the analysed

traits. However, due to time constraints, I had to focus on a single population (Breivika) and trait (shell strength). The two pools presented similar levels of polymorphism as measured by nucleotide diversity, theta and Tajima's D (although the difference in average nucleotide diversity was more pronounced), suggesting that the pooling of DNA from different individuals in equimolar proportions worked relatively well in the two pools. Nevertheless, an excess of low frequency polymorphisms was detected in the two pools (negative Tajima's D values), suggesting that this population could have experienced a demographic expansion. Further analyses need to be conducted in order to understand if a similar pattern is observed in the other populations, suggesting a population expansion in the region after the last glacial period.

As expected, the baseline FST values between individuals from the two pools formed by individuals from the same (panmictic population, Breivika) are low, once more suggesting that the pooling worked successfully. Importantly, some FST outliers were identified in different chromosomes. While some of these outliers (mainly the ones comprising single windows) could be spurious, the ones observed in chromosomes 6, 14 and 17 are promising candidates to explain the differences in shell strength. Nevertheless, these results should be interpreted with caution as further analysis applying filters with different stringency are necessary to exclude possible artefacts. Moreover, given the significant correlation between shell strength and other traits (total weight, shell thickness, shell shape and total height), we cannot exclude that the identified regions are actually influencing other (correlated) traits. Because the reference genome is incomplete and fragmented, the existence of other genomic regions influencing this phenotype, beyond the ones detected here, cannot be excluded. Thus, caution is needed when drawing conclusions about the genetic architecture of shell strength based on these results. Resequencing of individuals with variation at this trait is further needed to validate these results, followed by functional studies to establish a direct a link between genotypes and phenotypes.

Since the environmental variables studied here and the *C. maenas* occurrence have a similar trend from North to South, presenting intermediate values or a shift in Breivika and/or Tromsø, it is not easy to disentangle what is the main factor (if any) contributing for *L. obtusata* variation across this latitudinal gradient. Still, the linear regression models suggested that sea surface temperature was associated with all phenotypic traits except size related traits (total shell height, spiral height and spiral height/height ratio), which seem more associated with sea salinity. The lower sea water temperature and salinity is known to increase the solubility of calcium carbonate, resulting in a higher energy cost

of shell calcification (Reid, 1996). Thus, individuals facing these conditions (further north: Storsandes and Kirkeporten) are expected to display thin shell walls, as we observed.

The studies by Seeley (1986) and Trussell *et al*. (2000) also showed that the presence of *C. maenas* (together with temperature) influenced the shell thickness of *L. obtusata* individuals. However, these studies presented different mechanisms to explain their results: adaptation via natural selection versus phenotypic plasticity, respectively.

The results obtained here showed that shells are thicker in individuals from locations where the presence of *C. maenas* is unequivocal (Seines and Breivika). However, we would expect that the presence of *C. maenas* scent in the water would induce a similar response in all individuals from the same population. Thus, although we cannot reject that *L. obtusata* individuals in Breivika are differently influenced by *C. maenas* due to their heterogeneous/structured distribution, and our genetic results need further validation, our findings are compatible with the role of natural selection causing the observed differences in phenotypes. The functional identification of the genes located near the FST outliers could help us in the future to identify the main pathways and factors involved. Nevertheless, our results cannot completely exclude an adaptive response via phenotypic plasticity. Thus, future experimental studies are needed to quantify the contribution of these processes to explain the phenotypic variation of *L. obtusata* across the environmental gradient at high latitudes.

5. Conclusions

Our detailed phenotypic characterization of *L. obtusata* populations distributed across a latitudinal gradient spanning the phenotypic shift between varieties *retusa* and *palliata* revealed a general increase in most traits (weight, shell thickness, total shell height, shell spiral height, shell spiral angle and shell strength) from north to south, where crabs are generally more abundant and sea water and air temperature, as well as salinity, are higher.

Although this is in agreement with previous literature (for shell thickness and spiral variation), our study not only expanded the number of traits that vary with latitude but also revealed a possible shift in the transition between varieties towards the North (Breivika and Tromsø). This is supported by a slight increase in salinity and air temperature, as well as a northward expansion of one of *L. obtusata*'s main predators (*C. maenas*). Nevertheless, given the resolution level of environmental and crab-presence data, and the fact that all these factors overall vary in the same direction across latitude, it was not possible to confidently disentangle their individual contribution the phenotypes.

The use of Pool-seq to obtain genome-wide sequence data from two phenotypic extremes within a population revealed an informative approach that resulted in the identification of several candidate regions involved in shell strength variation. However, further research is needed to test and validate these candidates, as well as to understand how allelic variants within these regions change in frequency across all five studied populations. Finally, although these findings suggest that shell strength variation has, at least partially, a genetic component, we cannot exclude the influence of plasticity.

The observed variation of phenotypic and environmental variables, as well as of the presence of a main *L. obtusata* predator across latitude, particularly suggest the possibility of some environmental shifts occurring towards north. This opens doors for further studies aiming to understand how climate change affects biodiversity at higher latitudes.

References

Behrens Yamada, S. (1977). Geographic range limitation of the intertidal *gastropods Littorina sitkana* and *L. planaxis*. *Marine Biology*, 39(1), 61-65. https://doi.org/10.1007/BF00395594

Benson, K. R. (2002). The Study of Vertical Zonation on Rocky Intertidal Shores—A Historical Perspective1,2. *Integrative and Comparative Biology*, 42(4), 776–779. doi:10.1093/icb/42.4.776

Bioline 2016. Clean-up using AMPure XP beads. *protocols.io*. dx.doi.org/10.17504/protocols.io.f3ebqje

Bland, J. M., & Altman, D. G. (1995). Multiple significance tests: the Bonferroni method. *BMJ, 310(6973)*, 170. doi:10.1136/bmj.310.6973.170

Bolger, A. M., Lohse, M., & Usadel, B. (2014). Trimmomatic: A flexible trimmer for Illumina Sequence Data. *Bioinformatics*, btu170. https://doi.org/10.1093/bioinformatics/btu170

Butlin, R.K., Saura, M., Charrier, G., Jackson, B., André, C., Caballero, A., Coyne, J.A., Galindo, J., Grahame, J.W., Hollander, J., Kemppainen, P., Martínez-Fernández, M., Panova, M., Quesada, H., Johannesson, K. and Rolán-Alvarez, E. (2014). Parallel evolution of local adaptation and reproductive isolation in the face of gene flow. *Evolution, 68*: 935-949. https://doi.org/10.1111/evo.12329

Carvajal-Rodríguez, A., Conde-Padín, P., & Rolán-Alvarez, E. (2005). Decomposing shell form into size and shape by geometric morphometric methods in two sympatric scotypes of *Littorina saxatilis*. *Journal of Molluscan Studies, 71*. doi:10.1093/mollus/eyi037

Carvalho, J., Sotelo, G., Galindo, J., & Faria, R. (2016). Genetic characterization of flat periwinkles (Littorinidae) from the Iberian Peninsula reveals interspecific hybridization and different degrees of differentiation. *Biological Journal of the Linnean Society*, 118(3), 503–519. doi:10.1111/bij.12762

Cleveland, R. B., Cleveland, W. S., McRae, J. E. & Terpenning, I. (1990). STL: A Seasonal-Trend Decomposition Procedure Based on Loess (with Discussion). *Journal of Official Statistics,* 6, 3--73.

Dayton, P. K. (1971). Competition, Disturbance, and Community Organization: The Provision and Subsequent Utilization of Space in a Rocky Intertidal Community. *Ecological Monographs, 41*(4), 351–389. https://doi.org/10.2307/1948498

de Kluijver, M.J., S.S. Ingalsuo and R.H. de Bruyne. (2000). Macrobenthos of the North Sea [CD-ROM]: 1. Keys to Mollusca and Brachiopoda. *World Biodiversity Database CD-ROM Series*. Expert Center for Taxonomic Identification (ETI): Amsterdam, The Neth.

Denny, M. W., & Gaines, S. D. (Eds.). (2007). *Encyclopedia of tidepools and rocky shores* (Vol. 735). Berkeley: University of California Press.

Dunn, Olive Jean (1961). "Multiple Comparisons Among Means" (PDF). *Journal of the American Statistical Association*. 56 (293): 52–64. doi:10.1080/01621459.1961.10482090

Erickson, E., Wakao, S. and Niyogi, K.K. (2015). Light stress and photoprotection in Chlamydomonas reinhardtii. *The Plant Journal* 82: 449–465. https://doi.org/10.1111/tpj.12825

Faria, R, Chaube, P, Morales, HE, et al. (2019). Multiple chromosomal rearrangements in a hybrid zone between *Littorina saxatilis* ecotypes. *Mol Ecol.* 28: 1375– 1393. https://doi.org/10.1111/mec.14972

Feder, M. E. and Hofmann, G. E. (1999). Heat shock proteins, molecular chaperones, and the stress response*: Evolutionary and ecological physiology*. Annu. Rev. Physiol. doi: 10.1146/annurev.physiol.61.1.243. PMID: 10099689.

Fletcher, C. (1995). Microgeographical variation in shell strength in the flat periwinkles *Littorina obtusata* and *Littorina mariae*. *Hydrobiologia*, 309(1), 73-87. https://doi.org/10.1007/BF00014474

Freedman, D., Pisani, R., & Purves, R. (2007). Statistics (international student edition). *Pisani, R. Purves, 4th Edn*. *WW Norton & Company, New York*.

Fuentes-Pardo, A., & Ruzzante, D. (2017). Whole-genome sequencing approaches for conservation biology: Advantages, limitations, and practical recommendations. *Molecular Ecology, 26(20),* 5369-5406. doi: 10.1111/mec.14264. Epub 2017 Sep 5. PMID: 28746784.

Galindo, J, Carvalho, J, Sotelo, G, et al. (2021). Genetic and morphological divergence between *Littorina fabalis* ecotypes in Northern Europe. *J. Evol. Biol*; 34: 97– 113. https://doi.org/10.1111/jeb.13705

Gentleman, R., Carey, V. J., Huber, W., Irizarry, R. A., & Dudoit, S. (Eds.). (2005). *Bioinformatics and computational biology solutions using R and Bioconductor* (Vol. 1, No. 0). New York: Springer. https://doi.org/10.1007/0-387-29362-0

Hollander, J., & Butlin, R. (2010). The adaptive value of phenotypic plasticity in two ecotypes of a marine gastropod. *BMC evolutionary biology*, 10, 333. doi:10.1186/1471-2148-10-333

Johannesson, K. (2003). Evolution in Littorina: ecology matters. *Journal of Sea Research*, 49(2), 107–117. doi:10.1016/S1385-1101(02)00218-6

Johannesson, K., & Tatarenkov, A. (1997). Allozyme Variation in a Snail (*Littorina saxatilis*)-Deconfounding the Effects of Microhabitat and Gene Flow. *Evolution, 51*(2), 402–409. https://doi.org/10.2307/2411112

Klassen, G., & Locke, A. (2007). A Biological Synopsis of the European Green Crab, *Carcinus maenas*. *Canadian Manuscript Report of Fisheries and Aquatic Sciences, 2818*.

Kneib, Ronald T., (2002), Knox, G. A. (2001). The ecology of seashores. CRC Press. 557 p. US$90. ISBN 0-8493-0008-8, *Limnology and Oceanography*, 47(4), 1268–1268. doi:10.4319/lo.2002.47.4.1268

Kofler, R., Orozco-terWengel, P., De Maio, N., Pandey, R. V., Nolte, V., Futschik, A., Schlötterer, C. (2011). PoPoolation: A Toolbox for Population Genetic Analysis of Next Generation Sequencing Data from Pooled Individuals. *PLOS ONE, 6*(1), 1–9. doi:10.1371/journal.pone.0015925

Kofler, R., Pandey, R. V., & Schlötterer, C. (2011). PoPoolation2: identifying differentiation between populations using sequencing of pooled DNA samples (Pool-Seq). *Bioinformatics (Oxford, England)*, 27(24), 3435–3436. https://doi.org/10.1093/bioinformatics/btr589

Larsson, J., Westram, A. M., Bengmark, S., Lundh, T., & Butlin, R. K. (2020). A developmentally descriptive method for quantifying shape in gastropod shells. *Journal of The Royal Society Interface, 17*(163), 20190721. doi:10.1098/rsif.2019.0721

Li, H. (2013). Aligning sequence reads, clone sequences and assembly contigs with BWA-MEM. doi:10.48550/ARXIV.1303.3997

Morales, H. E., Faria, R., Johannesson, K., Larsson, T., Panova, M., Westram, A. M., & Butlin, R. K. (2019). Genomic architecture of parallel ecological divergence: Beyond a single environmental contrast. *Science Advances, 5*(12), eaav9963. doi:10.1126/sciadv.aav9963

Reid D. G. (1996). *Systematics and Evolution of Littorina*. London, UK: Ray Society.

Reid, D. G., Dyal, P., & Williams, S. T. (2012). A global molecular phylogeny of 147 periwinkle species (Gastropoda, Littorininae). *Zoologica Scripta, 41*(2), 125–136. doi:10.1111/j.1463-6409.2011.00505.x

Rolán-Alvarez, Emilio & Austin, Christopher & Boulding, Elizabeth. (2015). The Contribution of the Genus *Littorina* to the Field of Evolutionary Ecology. *Oceanography and Marine Biology: an annual review, 53*, 157-214.

Ropes, J. W. (1968). The feeding habits of the green crab, Carcinus maenas (L.). *Fishery Bulletin, 67*(2), 183-203.

Ryan, A. J., Ulrich, M. J., Bennett, R., Joy, C. (2022). xts: eXtensible Time Series.

Samuels, M., Witmer, J., & Schaffner, A. (2012). *Statistics for the Life Sciences*. Prentice Hall.

Schlotterer, V. (2014). Sequencing pools of individuals – mining genome-wide polymorphism data without big funding. *Nature Reviews Genetics*, *15*(11), 749-763. https://doi.org/10.1038/nrg3803

Seeley R. H. (1986). Intense natural selection caused a rapid morphological transition in a living marine snail. *Proceedings of the National Academy of Sciences of the United States of America, 83*(18), 6897–6901. https://doi.org/10.1073/pnas.83.18.6897

Sokolova, I., Bock, C. & Pörtner, HO. (2000). Resistance to freshwater exposure in White Sea *Littorina* spp. I: Anaerobic metabolism and energetics. *J Comp Physiol B* 170, 91–103. https://doi.org/10.1007/s003600050264

Student. (1908). The Probable Error of a Mean. *Biometrika*, 6(1), 1–25. https://doi.org/10.2307/2331554

Trussell, G. C., & Smith, L. D. (2000). Induced Defenses in Response to an Invading Crab Predator: An Explanation of Historical and Geographic Phenotypic Change. *Proceedings of the National Academy of Sciences of the United States of America*, *97*(5), 2123–2127. http://www.jstor.org/stable/122006

Trussell, G. C., Johnson, A. S., Rudolph, S. G., & Gilfillan, E. S. (1993). Resistance to dislodgement: habitat and size-specific differences in morphology and tenacity in an intertidal snail. *Marine Ecology Progress Series*, 100(1/2), 135–144. http://www.jstor.org/stable/24838058

Westram, A.M., Faria, R., Johannesson, K. and Butlin, R. (2021). Using replicate hybrid zones to understand the genomic basis of adaptive divergence. *Mol Ecol, 30*: 3797-3814. https://doi.org/10.1111/mec.15861

Westram, A.M., Rafajlović, M., Chaube, P., Faria, R., Larsson, T., Panova, M., Ravinet, M., Blomberg, A., Mehlig, B., Johannesson, K. and Butlin, R. (2018). Clines on the seashore: The genomic architecture underlying rapid divergence in the face of gene flow. *Evolution Letters, 2*: 297-309. https://doi.org/10.1002/evl3.74

Yancey P. H. (2005). Organic osmolytes as compatible, metabolic, and counteracting cytoprotectants in high osmolarity and other stresses. *The Journal of experimental biology, 208*(Pt 15), 2819–2830. https://doi.org/10.1242/jeb.01730

Yohe, S., & Thyagarajan, B. (2017). Review of Clinical Next-Generation Sequencing. *Archives of Pathology & Laboratory Medicine, 141*(11), 1544-1557. doi:10.5858/arpa.2016-0501-RA

Young, A. M., & Elliott, J. A. (2020). Life History and Population Dynamics of Green Crabs (*Carcinus maenas*). *Fishes, 5*(1), 4–0. doi:10.3390/fishes5010004

Zeileis, A., & Grothendieck, G. (2005). zoo: S3 Infrastructure for Regular and Irregular Time Series. *Journal of Statistical Software, 14(6)*, 1–27. doi:10.18637/jss.v014.i06

Attachments

1. Graphical assessment of ANOVA assumptions

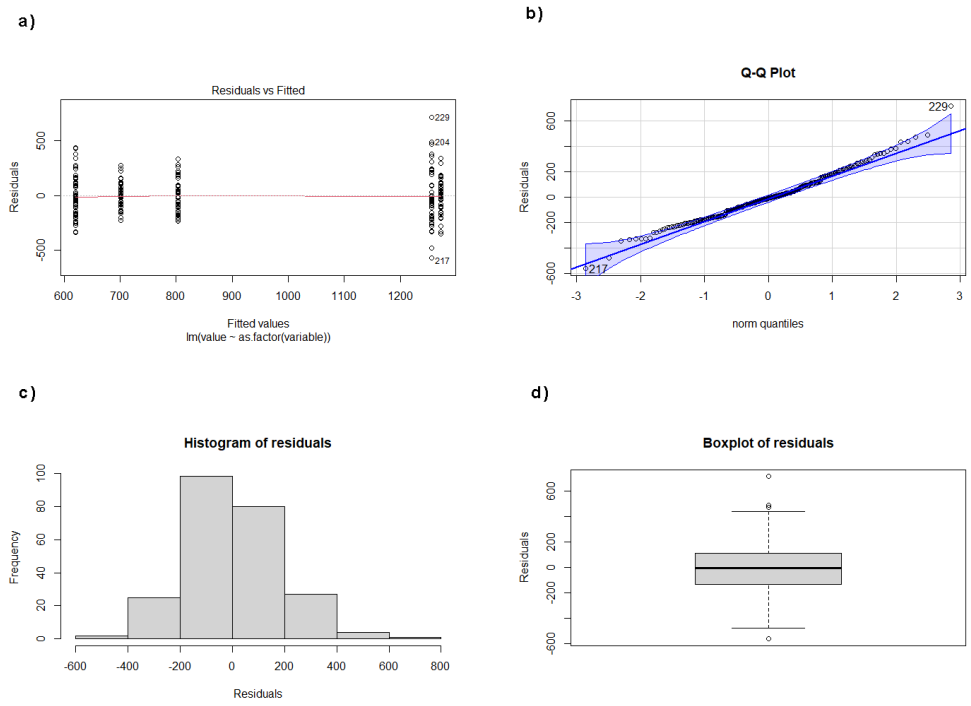

Supplementary Figure 1. Assessment plots for ANOVA assumption for the shell weight values. (a) residuals versus fitted values, (b) normal quantile-quantile plot, (c) histogram of the residuals, and (d) boxplot of the residuals.

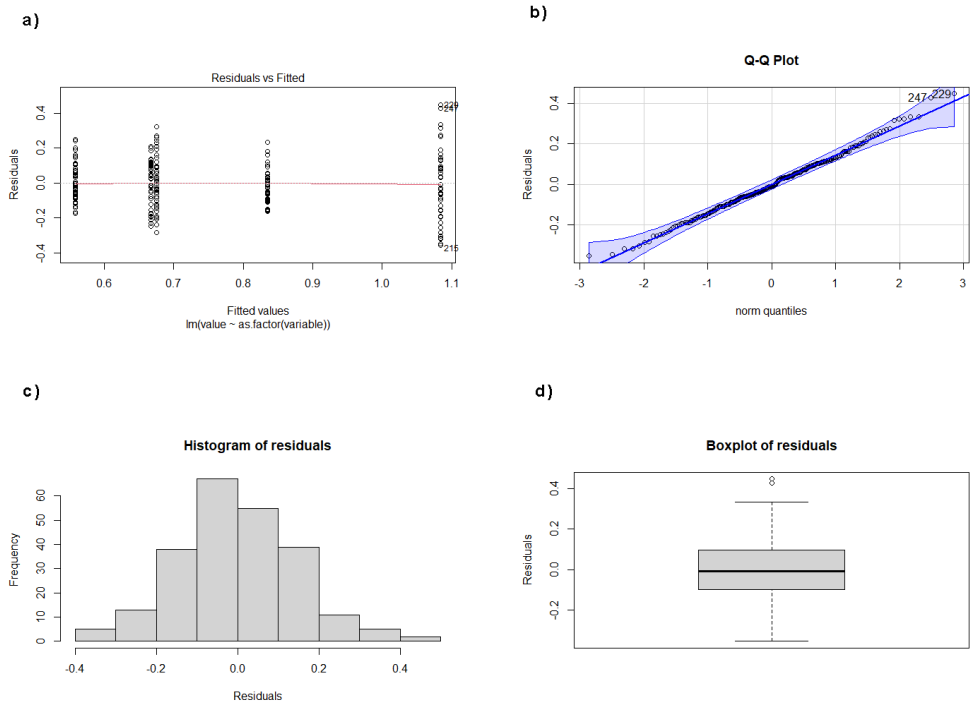

Supplementary Figure 2. Assessment plots for ANOVA assumption for the shell thickness values. (a) residuals versus fitted values, (b) normal quantile-quantile plot, (c) histogram of the residuals, and (d) boxplot of the residuals.

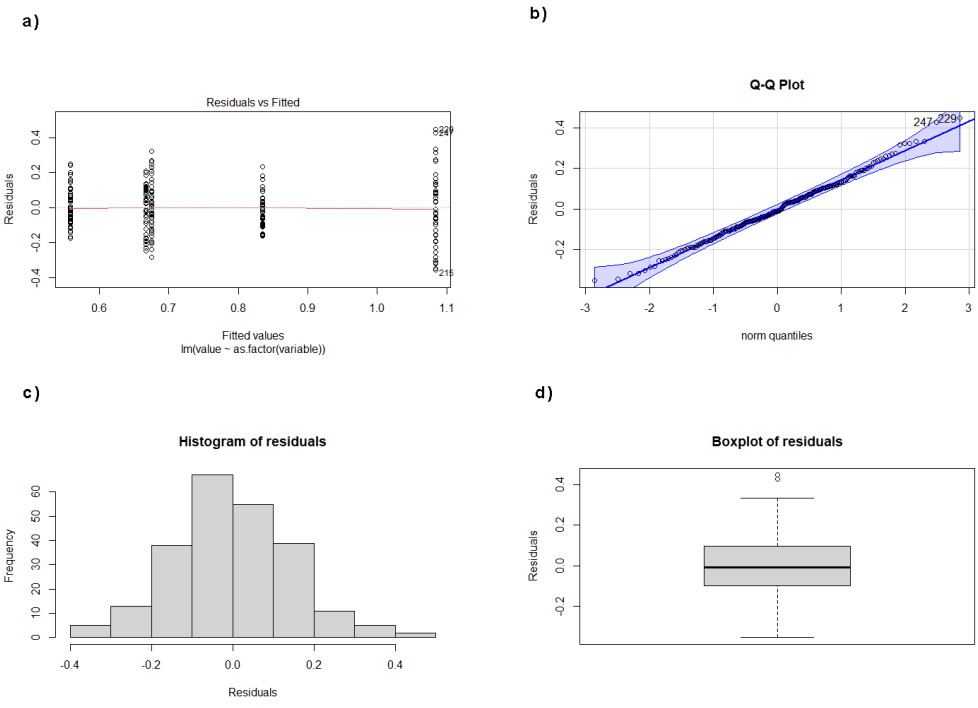

Supplementary Figure 3. Assessment plots for ANOVA assumption for the shell height values. (a) residuals versus fitted values, (b) normal quantile-quantile plot, (c) histogram of the residuals, and (d) boxplot of the residuals.

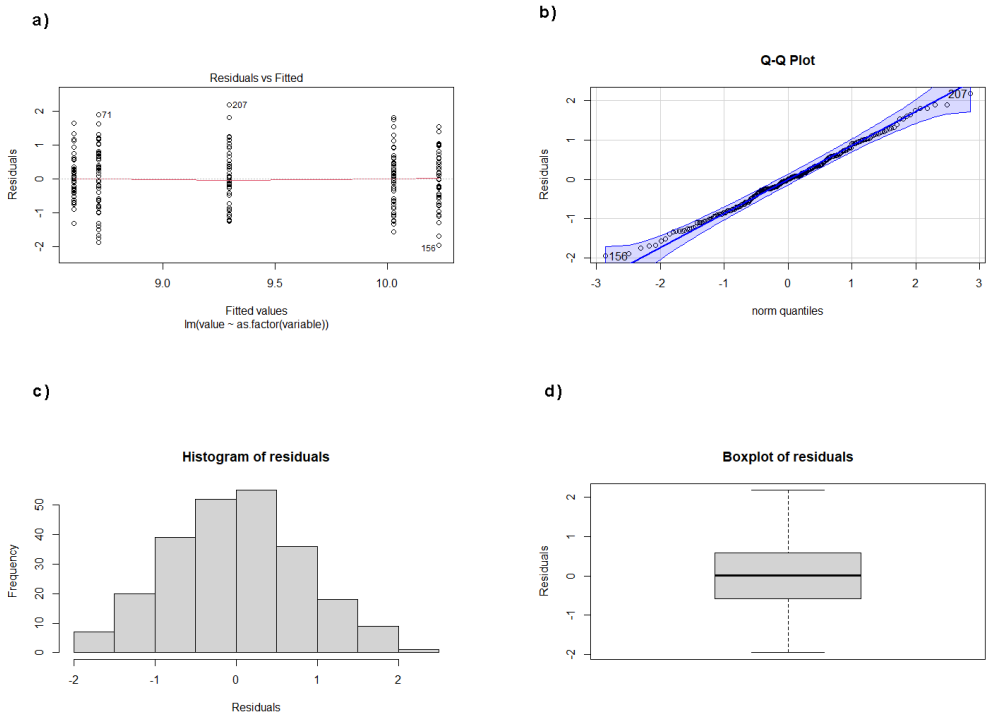

Supplementary Figure 4. Assessment plots for ANOVA assumption for the shell spiral height values. (a) residuals versus fitted values, (b) normal quantile-quantile plot, (c) histogram of the residuals, and (d) boxplot of the residuals.

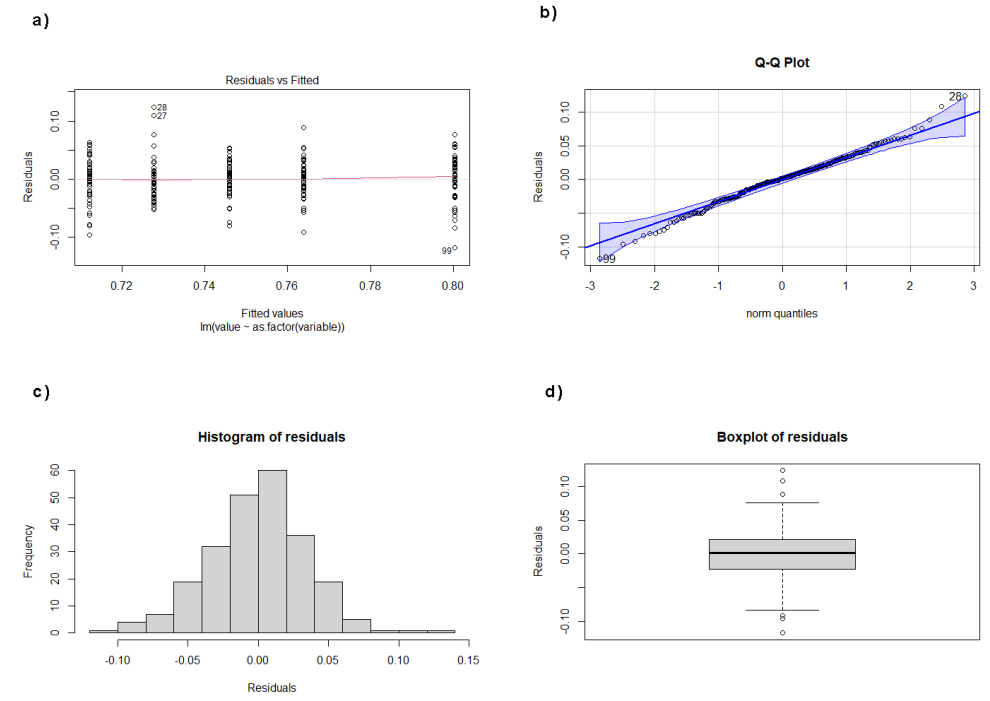

Supplementary Figure 5. Assessment plots for ANOVA assumption for the shell spiral height/height ratio. (a) residuals versus fitted values, (b) normal quantile-quantile plot, (c) histogram of the residuals, and (d) boxplot of the residuals.

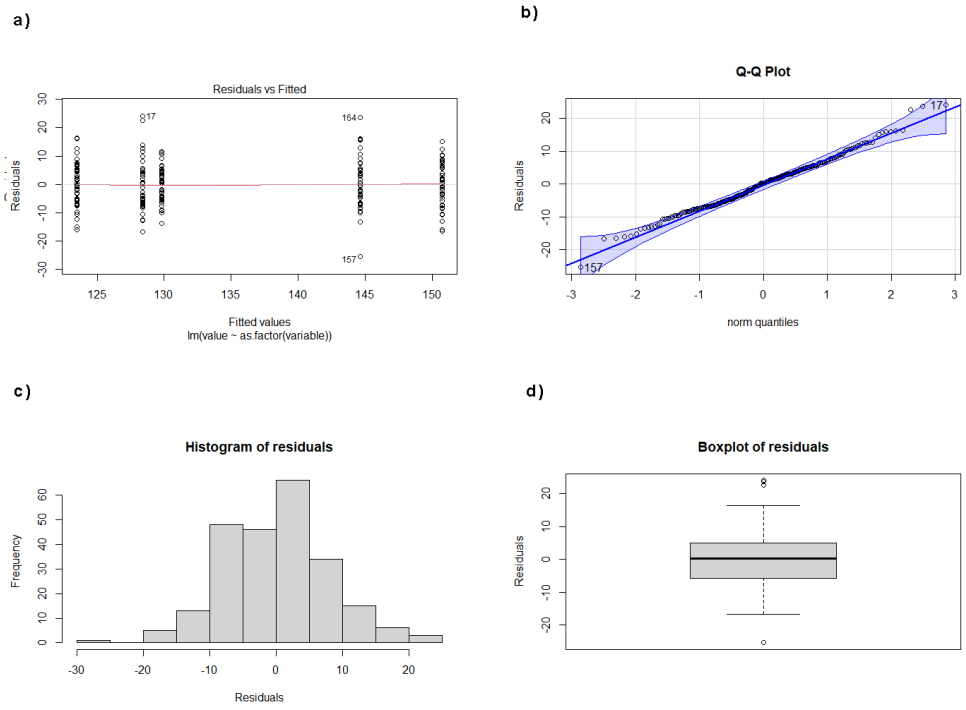

Supplementary Figure 6. Assessment plots for ANOVA assumption for the shell spiral angle. (a) residuals versus fitted values, (b) normal quantile-quantile plot, (c) histogram of the residuals, and (d) boxplot of the residuals.

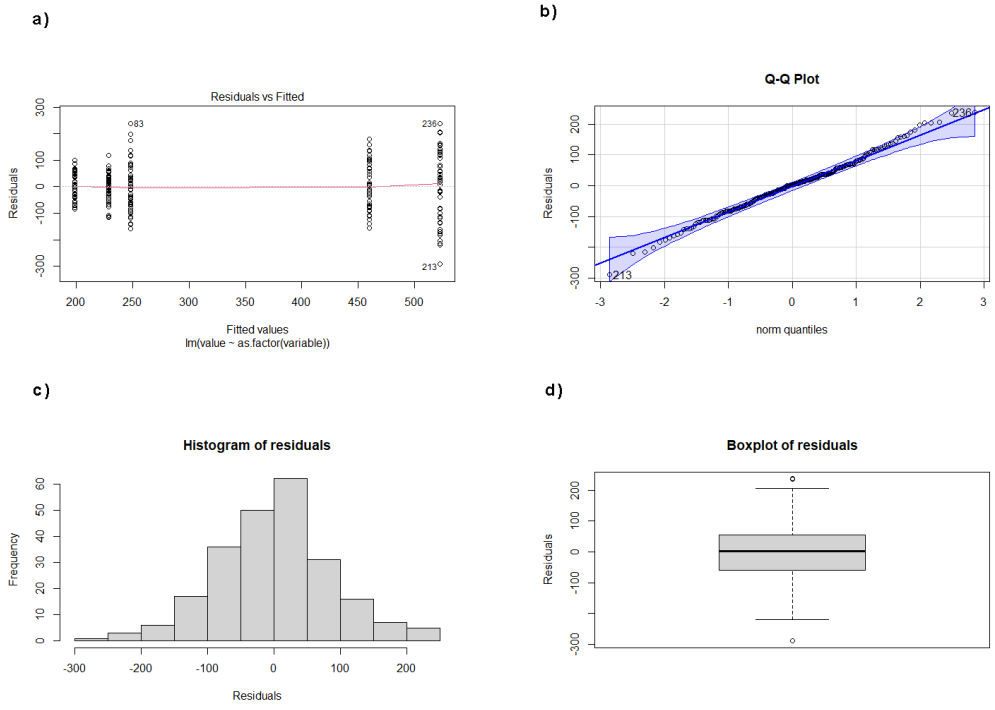

Supplementary Figure 7. Assessment plots for ANOVA assumption for the shell strength. (a) residuals versus fitted values, (b) normal quantile-quantile plot, (c) histogram of the residuals, and (d) boxplot of the residuals.

2. Environmental time series with moving metrics

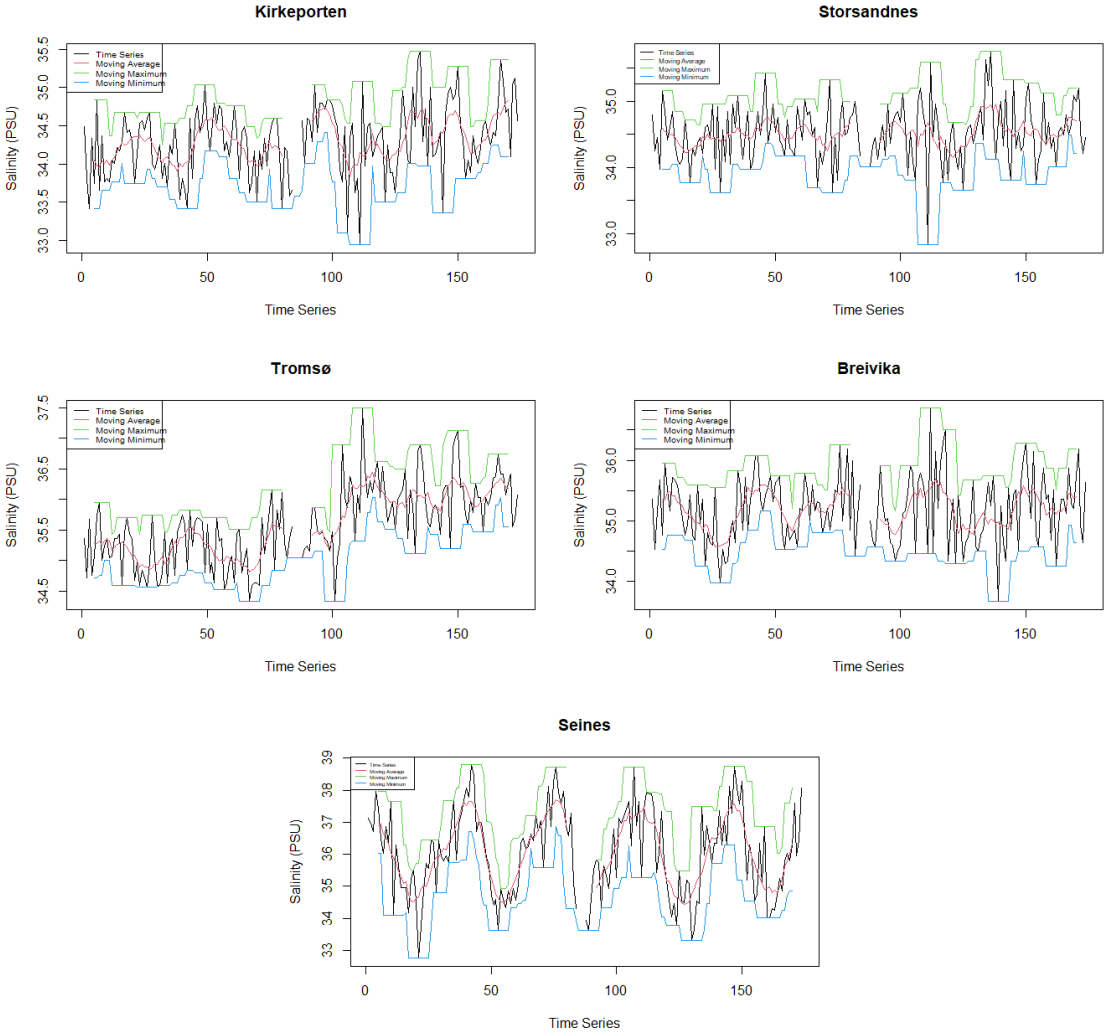

Supplementary Figure 8. Time series plots with moving metrics (window size = 90 days) for the salinity data (PSU) collected between 2017 and 2021 in each sampling location. Time series represented in black, moving metrics presented are moving average (red), moving maximum (green), and moving minimum (blue).

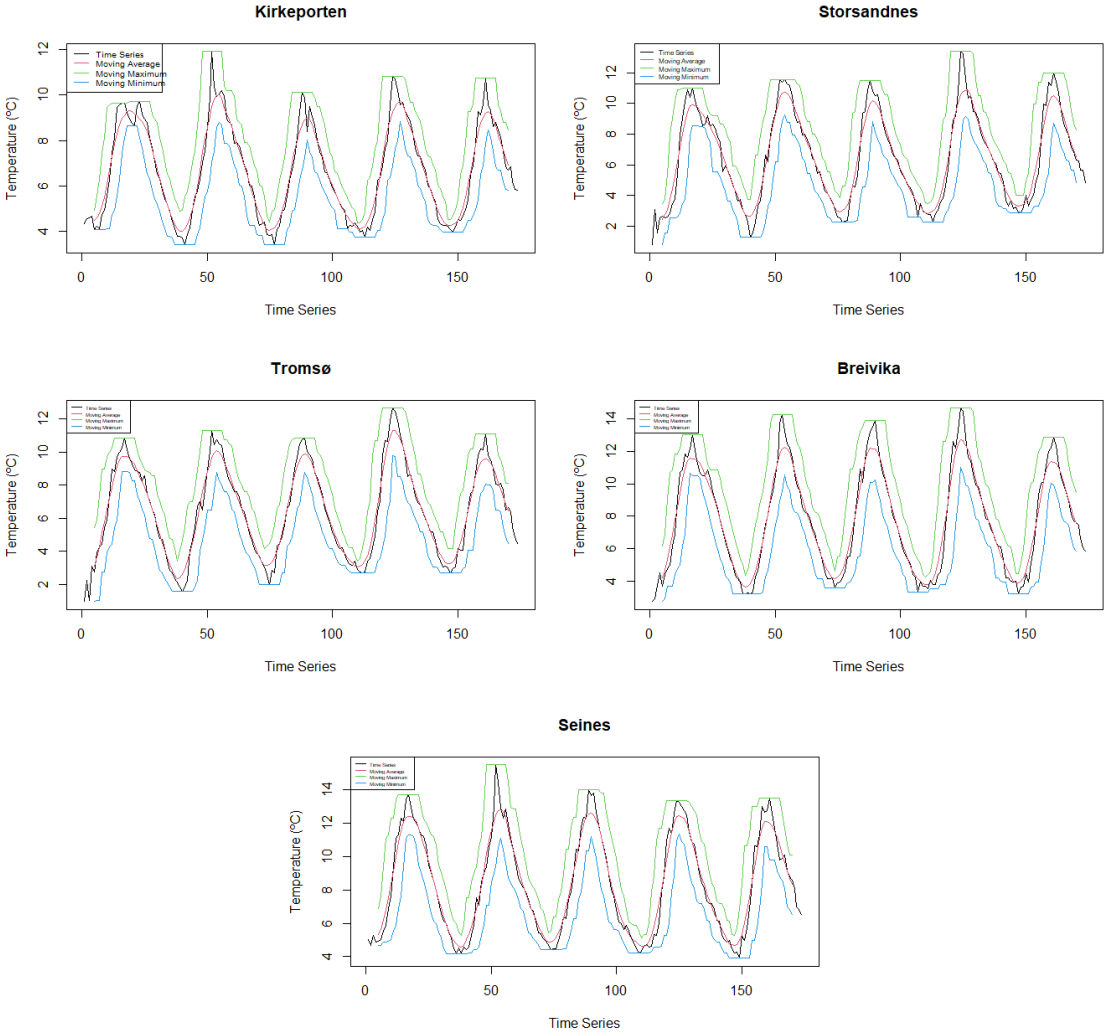

Supplementary Figure 9. Time series plots with moving metrics (window size = 90 days) for the sea surface temperature data (ºC) collected between 2017 and 2021 in each sampling location. Time series represented in black, moving metrics presented are moving average (red), moving maximum (green), and moving minimum (blue).

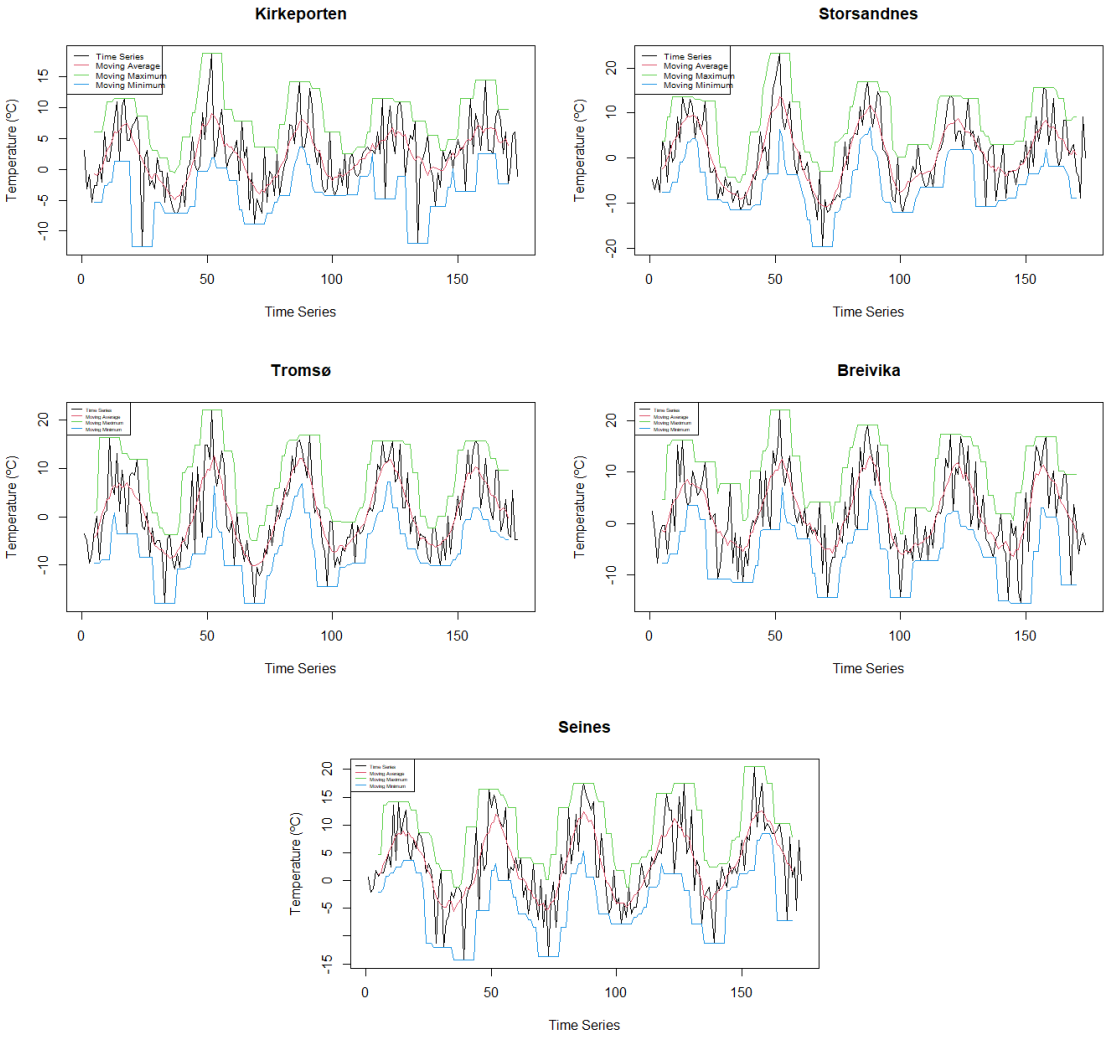

Supplementary Figure 10. Time series plots with moving metrics (window size = 90 days) for the air temperature data (ºC) collected between 2017 and 2021 in each sampling location. Time series represented in black, moving metrics presented are moving average (red), moving maximum (green), and moving minimum (blue).

3. Seasonal and Trend decomposition using loess (STL)

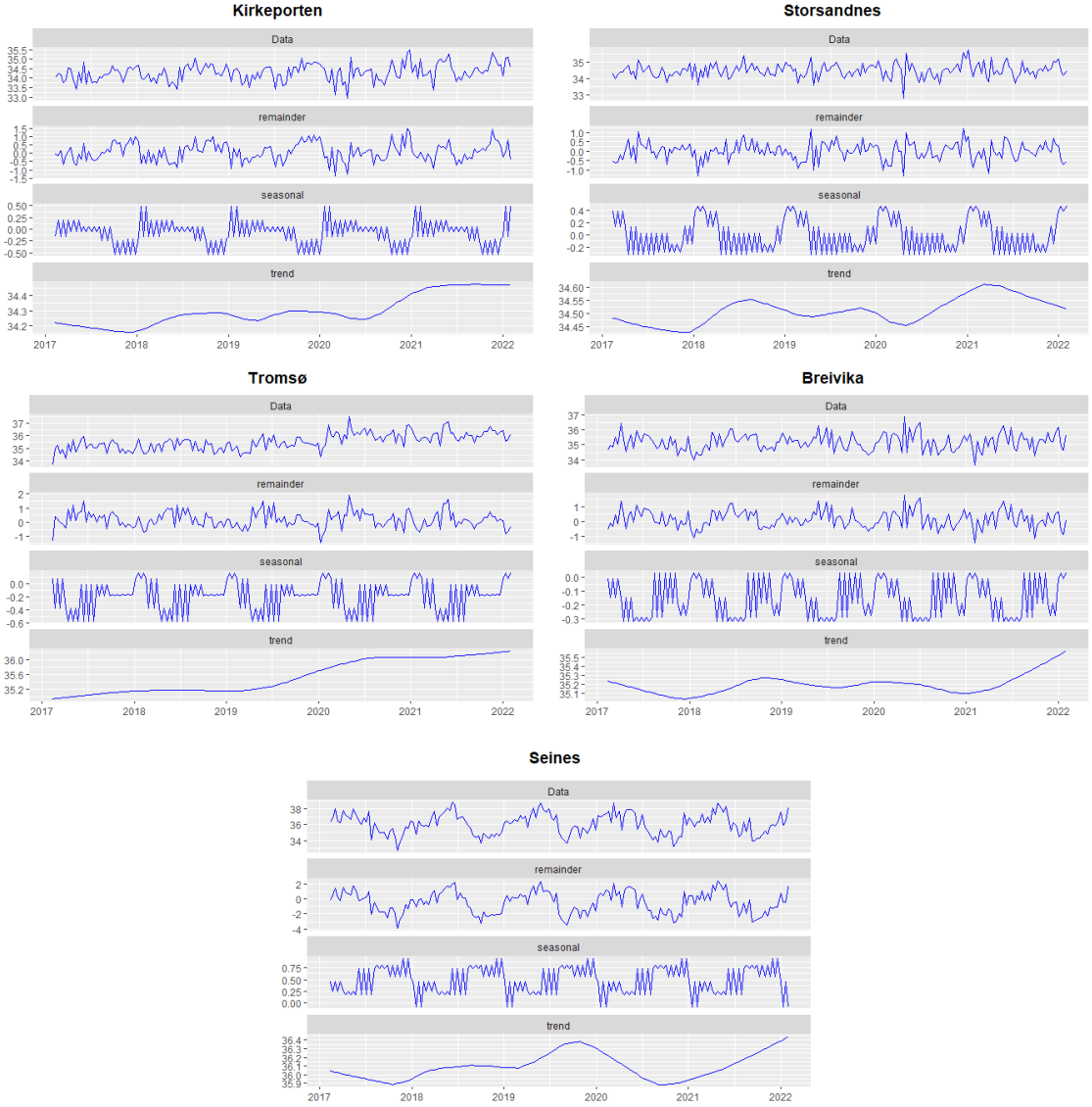

Supplementary Figure 11. Seasonal and trend decomposition plots using loess (STL) for the sea salinity data (PSU) collected between 2017 and 2021 in each sampling location.

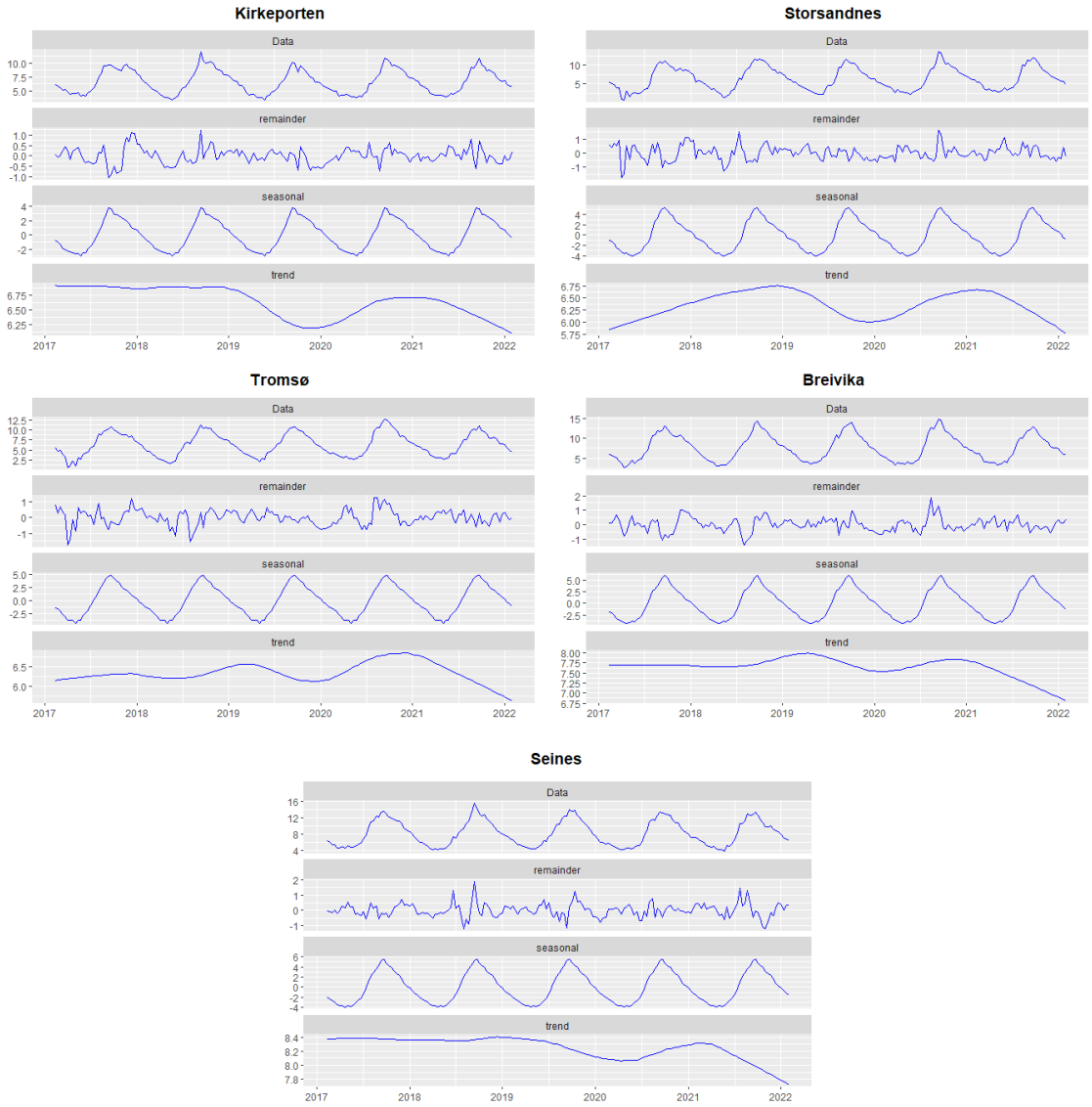

Supplementary Figure 12. Seasonal and trend decomposition plots using loess (STL) for the sea surface temperature data (ºC) collected between 2017 and 2021 in each sampling location.

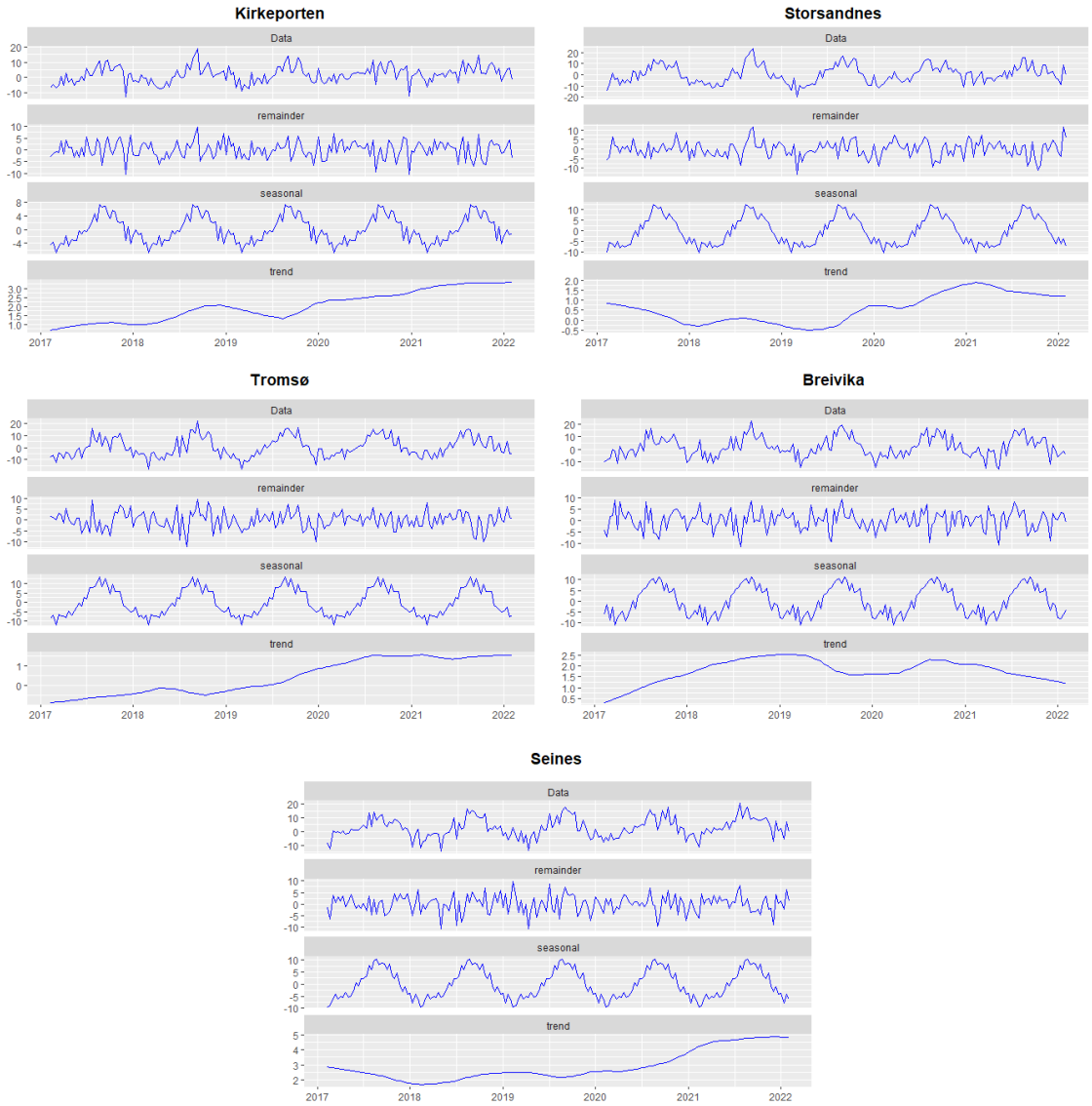

Supplementary Figure 13. Seasonal and trend decomposition plots using loess (STL) for the air temperature data (ºC) collected between 2017 and 2021 in each sampling location.